

Unraveling the Role of Endoplasmic Reticulum Stress in Idiopathic Pulmonary Fibrosis (IPF)

By

Ankita Burman

Dissertation

Submitted to the Faculty of the
Graduate School of Vanderbilt University

in partial fulfillment of the requirements

for the degree of

DOCTOR OF PHILOSOPHY

in

Cell and Developmental Biology

January 31st, 2019

Nashville, Tennessee

Approved:

Timothy S. Blackwell, M.D.

Chin Chiang, Ph.D.

Mark deCaestecker, M.B., B.S., Ph.D.

Volker H. Haase, M.D.

Copyright © January 2019 by Ankita Burman

All Rights Reserved

To my parents, Anil and Rina, for their love, strength, and faith,
and
my husband Jaybee, for being my soulmate.

ACKNOWLEDGEMENTS

This thesis is the culmination of a journey that I have made through my twenties – a journey that has enriched me in ways beyond what I could have ever imagined. I owe the sense of exhilaration that I feel today to multiple individuals and I want to take the space of the next few pages to express my feelings towards them.

Tim, words feel inadequate if I try to pen down my feelings of gratefulness towards you. Every Thursday for seven years that I walked out of your office, I clearly remember feeling a sense of rejuvenation, confidence, enthusiasm, and most of all an urge to find a way, to do better, and to fix things. Thank you for believing in me each time I found it hard to believe in myself. You had high expectations and were yet able to be incredibly supportive and optimistic during the most challenging of times – this is a quality that I have admired and that I want to thank you for. And more so than anything, thank you for being such a warm and thoughtful person – I cannot even enumerate the innumerable little thoughtful gestures that came naturally to you and that you showed over the last seven years, but their impact remains. It's been a privilege knowing you, Tim, and I hope I have been able to convey some of the gratitude, respect, and admiration that I feel towards you. As I leave the nest that your mentorship has been and traverse the world outside, what I have learnt from you both at a professional and personal level will remain with me forever.

Hari, I will miss going to your office and saying good morning to you first thing in the morning, every single day, when I stepped into lab. Thank you for going above and beyond the call of duty for teaching me the ropes of graduate school. When I first started in Tim's lab, your willingness to take me under your wing and help me in every way that you possibly could made navigating the early years of graduate school both easy and enjoyable. You were always there whenever I needed you and whatever I needed you for – with an exceptional level of readiness,

helpfulness, and patience. You were my biggest support when the learning curve was at its steepest. I am very fortunate to have had the opportunity to work so closely with you over all of these years and I hope you know how grateful I am for everything that you have done for me.

I would like to thank both present and past members of the Blackwell laboratory (and the larger pulmonary group) for helping me in various ways. Specifically, I want to thank Jonathan Kropski, Carla Calvi, Ana Serezani, Bruno Pascoalino, Wei Han, Taylor Sherrill, Linda Gleaves, William Lawson, and Lisa Young for their contributions to part of the research described in this thesis. Also, I want to thank other current lab members Bradley Richmond, Rui-Hong-Du, Pierre Hunt and Vasily Polosukhin and former lab members Dong-Sheng Cheng, Allison Perry, Jamie Saxon, Rasul Abdolrasulnia, Rinat Zaynagetdinov, and Mindy McConaha for teaching me one thing or the other. Finally, I would like to thank Deanna Sledge for helping me with numerous little things over the years with willingness and enthusiasm. And even with the plethora of names that I have listed here, I am certain that I am missing out on names of people in the lab (and the department) who have helped me; and perhaps therein lies the beauty of a collaborative work culture, which I was fortunate enough to be a part of.

I would like to thank my thesis committee members Dr. Chin Chiang, Dr. Mark DeCaestecker, Dr. David Bader, and Dr. Volker Haase for providing constructive feedback and helping me shape my project as I moved through graduate school. Mark, in addition to being my committee member, you were also my FOCUS group leader and program director for the Certificate Program for Molecular Medicine (CPMM); my interactions with you accorded me insight into your critical thinking skills and provided me new perspectives towards approaching scientific questions. Also, I would like to thank my CPMM clinical mentor Dr. Lisa Lancaster for letting me shadow her when she cared for patients with IPF, sleep apnea, and other lung diseases.

Watching the suffering, pain, and grief of patients and their loved ones, and the resilience that they would show in the face of adversity was a humbling experience for me – it would shift perspective and also be a reminder of the meaning of my vocation as a scientist. Thank you, Mark, for leading this creative program at the intersection of bench and bedside, and thank you Lisa for being so welcoming, accommodating, and enthusiastic in showing me the clinical side of my work.

I would also like to thank my Vanderbilt International Scholars Program (VISIP) mentors Dr. Roger Colbran, Dr. Kathy Gould, Dr. Mark Denison, Dr. Anne Kenworthy and program coordinator Amanda Connolly for their guidance and support when I first entered graduate school. Roger, I would like to mention here that my interview with you on skype before I came to Vanderbilt had made me feel very positively about coming to graduate school here and I want to especially thank you for your understanding, support, and guidance during my first year in the Interdisciplinary Graduate Program (IGP). Kathy, I want to thank you for your strong support for the VISIP program; this amazing program does not exist anymore, and I was among the fortunate ones who had the opportunity to be a part of it. Amanda, you are not a part of Vanderbilt anymore, but my gratitude to VISIP would remain incomplete without expression of my gratitude towards you – thank you very much for being so helpful to the 2011 batch of VISIP students while they were settling down in graduate school and in Nashville.

‘Friends become our chosen family’ they say, and so it has been. My friends in Nashville – there is no way I could have gotten through graduate school without you guys! Thank you for making me laugh at my own failures, thank you for lifting my spirits up at times when the road ahead seemed unending, thank you for your craziness, and thank you for being there. I would like to thank Sam, my roommate of three years and my best friend, for being the sister I never had. Sam, it was for you that I could call our apartment ‘home’. Sam, Ashish, Xiaohan, Alisha, Satabdi,

Ushashi, Huzefa, Arwa, Kami, and Kousik – we made memories over these years that I will cherish forever; and, the times that we have spent together and an era that we have lived together will probably define parts of who I would be as a person for the rest of my life. As I leave Nashville today, I take with me the long-lasting friendships that I found in this city.

Lastly, I would like to express my gratitude to my family for being the iron pillars of support as life moved forth with ebbs and tides of joy and pain. My father dreamt a dream that I was too scared to dream myself; he gave me wings when I was clinging to my roots. He taught me that love is strong, and that courage is absolutely essential to living life. My mother has embodied selflessness, generosity, and strength to a level that I can only hope to achieve through probably a lifetime of practice, if at all. As I stand at the verge of finishing this journey today, it is to my parents that I owe its very beginning. Finally, I would like to thank Jaybee, my husband, for being the blessing in my life that he is. Our paths crossed three years ago – and for that piece of fortune I will remain forever grateful. You are my biggest strength, Jaybee, and it is your patience, steadfastness, and confidence that has let me keep my head above water every single day. Thank you for being the person that you are.

TABLE OF CONTENTS

ACKNOWLEDGEMENTS	IV
LIST OF FIGURES	XI
LIST OF TABLES	XV
LIST OF ABBREVIATIONS	XVI
I. INTRODUCTION	1
WHAT IS IPF?	1
THE BURDEN OF IPF: AN UNMET MEDICAL NEED	2
PATHOGENESIS OF IPF: DYSFUNCTION OF THE ALVEOLAR EPITHELIUM	2
ENDOPLASMIC RETICULUM STRESS AS A PATHOGENIC MECHANISM IN LUNG FIBROSIS	4
THE UNFOLDED PROTEIN RESPONSE (UPR) PATHWAY: AN OVERVIEW	5
FACTORS INFLUENCING ER STRESS	8
REGULATION OF EFFECTOR PATHWAYS BY ER STRESS	9
PRO-FIBROTIC EFFECTS OF ER STRESS IN INDIVIDUAL LUNG CELL TYPES IN LUNG FIBROSIS	12
C/EBP HOMOLOGOUS PROTEIN (CHOP)	16
HYPOXIA AND FIBROSIS	18
HYPOXIA-INDUCIBLE FACTOR (HIF) SIGNALING	19
II. MATERIALS AND METHODS	22
HUMAN SAMPLES	22
MICE	22
LUNG FIBROSIS MODELS	23
EXPOSURE OF MICE TO HYPOXIA	23
DETECTION OF CELLULAR HYPOXIA	23
MORPHOMETRY	23
IHC AND IMMUNOFLUORESCENCE	24

EVALUATION OF CELL DEATH	25
MEASUREMENT OF COLLAGEN AND FIBRONECTIN	25
QUANTIFICATION OF IMMUNE/INFLAMMATORY CELL TYPES BY FLOW CYTOMETRY	25
M1/M2 MACROPHAGE POLARIZATION	26
CELL CULTURE AND HYPOXIA EXPOSURE	27
HIF REPORTER CELLS	27
SIRNA STUDIES	28
SMALL MOLECULE-MEDIATED INHIBITION OF UPR PATHWAYS	28
WESTERN BLOTTING	28
RNA ISOLATION AND QUANTITATIVE PCR	29
MOUSE APOPTOSIS PCR ARRAY	30
ISOLATION OF EpCAM⁺ CELLS	31
RNA-SEQUENCING	31
STATISTICS	32
STUDY APPROVAL	32
III. HYPOXIA WORSENS LUNG FIBROSIS THROUGH EXPRESSION OF ER STRESS EFFECTOR	
C/EBP HOMOLOGOUS PROTEIN (CHOP)	33
CHOP REGULATES EPITHELIAL CELL SURVIVAL AND MEDIATES LUNG FIBROSIS IN THE PRESENCE OF ER	
STRESS	33
CHOP REGULATES EPITHELIAL CELL RESPONSES AND INFLAMMATION FOLLOWING REPETITIVE BLEOMYCIN	
TREATMENT	38
REPETITIVE BLEOMYCIN INJURY RESULTS IN LOCALIZED TISSUE HYPOXIA	43
EXPOSURE TO HYPOXIA FOLLOWING BLEOMYCIN INJURY INCREASES ER STRESS AND WORSENS LUNG	
FIBROSIS	46
CHOP^{-/-} MICE ARE PROTECTED FROM EXAGGERATED LUNG FIBROSIS INDUCED BY EXPOSURE TO HYPOXIA ...50	
CHOP AND MARKERS OF HYPOXIA ARE PROMINENTLY EXPRESSED IN LUNGS OF IPF PATIENTS	57
DISCUSSION	59

IV. REGULATION AND DOWNSTREAM FUNCTION OF C/EBP HOMOLOGOUS PROTEIN (CHOP) IN ALVEOLAR EPITHELIAL CELLS IN HYPOXIA	62
HYPOXIA INDUCES CHOP EXPRESSION IN AECs THROUGH THE IRE1A/XBP1 AND PERK/ATF4 PATHWAYS	62
CHOP REGULATES HYPOXIA-INDUCED APOPTOSIS OF AECs	66
DISCUSSION.....	71
V. THE ROLE OF HYPOXIA-INDUCIBLE FACTOR (HIF) IN LUNG FIBROSIS.....	73
HYPOXIA MEDIATES A PRO-FIBROTIC PHENOTYPE IN ALVEOLAR EPITHELIAL CELLS	73
HIF SIGNALING REGULATES EXPRESSION OF PRO-FIBROTIC MEDIATORS IN ALVEOLAR EPITHELIAL CELLS	74
EPITHELIAL HIF SIGNALING IS NOT ESSENTIAL FOR MEDIATING THE EFFECTS OF HYPOXIA ON LUNG FIBROSIS IN THE ‘BLEOMYCIN + HYPOXIA’ MODEL.....	76
EPITHELIAL HIF MEDIATES LUNG FIBROSIS AFTER REPETITIVE BLEOMYCIN INJURY TO THE LUNG.....	80
DISCUSSION.....	81
VI. CONCLUDING REMARKS AND FUTURE DIRECTIONS.....	82
REFERENCES	88

LIST OF FIGURES

Figure 1:	Hematoxylin and eosin stained section from a lung biopsy showing findings of usual interstitial pneumonia.....	1
Figure 2:	Potential mechanism of IPF pathogenesis.....	3
Figure 3:	Schematic representation of endoplasmic reticulum (ER) stress.....	5
Figure 4:	Schematic illustration of the unfolded protein response (UPR).....	7
Figure 5:	Potential causes of ER stress.....	8
Figure 6:	Pro-fibrotic effects of ER stress in different cell types in lung fibrosis.....	12
Figure 7:	Domain structure of human CHOP.....	17
Figure 8:	Regulation of HIF-1 α stability and activity is oxygen dependent.....	19
Figure 9:	Repetitive bleomycin treatment results in ER stress and lung fibrosis.....	34
Figure 10:	CHOP mediates the effects of ER stress on epithelial cell apoptosis and lung fibrosis.....	37
Figure 11:	CHOP levels in inducible transgenic mice expressing L188Q surfactant protein C (L188Q SFTPC) treated with bleomycin compared to wild type mice.....	38
Figure 12:	Gene expression profiling of EpCAM positive epithelial cells isolated from wild type and CHOP deficient mice in the repetitive bleomycin model.....	40
Figure 13:	Immune/inflammatory cells identified in lungs of wild type and CHOP deficient mice following repetitive bleomycin treatment.....	42

Figure 14: Repetitive bleomycin treatment results in cellular hypoxia localized to type II AECs..... 44

Figure 15: Dual immunofluorescence between pimonidazole and markers of type I AECs, fibroblasts, endothelial cells, or macrophages in the repetitive dose bleomycin model..... 45

Figure 16: Exposure to hypoxia following bleomycin treatment increases ER stress and worsens lung fibrosis..... 47

Figure 17: Dual immunofluorescence between pimonidazole and markers of different cell types in lungs of mice treated with bleomycin followed by exposure to hypoxia (14% O₂)..... 49

Figure 18: CHOP deficient mice are protected from exaggerated lung fibrosis induced by exposure to hypoxia..... 51

Figure 19: Immune/inflammatory cells and M1/M2 markers in macrophages from lungs of wild type and CHOP deficient mice following single dose IT bleomycin treatment with or without subsequent exposure to hypoxia (14% O₂) and harvested at day 21 post-bleomycin..... 53

Figure 20: Immune/inflammatory cells and M1/M2 markers in macrophages from lungs of wild type and CHOP deficient mice following single dose IT bleomycin treatment with or without subsequent exposure to hypoxia (14% O₂) and harvested at day 10 post-bleomycin..... 55

Figure 21: CHOP expression in macrophages isolated from mice in the bleomycin followed by hypoxia model..... 56

Figure 22: CHOP and markers of hypoxia are prominently expressed in lungs of IPF patients..... 58

Figure 23: Hypoxia induces CHOP expression in AECs through the IRE1 α /XBP1 and PERK/ATF4 pathways..... 64

Figure 24: siRNA mediated-knockdown of IRE1 and ATF4 followed by evaluation of CHOP in MLE12 cells exposed to hypoxia. 65

Figure 25: Efficiency of HIF1 α knockdown by siRNA in MLE12 cells. MLE12 cells were transfected with HIF1 α siRNA or control NT siRNA and exposed to hypoxia for 6 hours..... 66

Figure 26: CHOP mediates hypoxia-induced apoptosis of AECs through expression of apoptosis regulating proteins..... 67

Figure 27: Expression of pro-apoptotic mediators in CHOP siRNA or control siRNA treated AECs exposed to hypoxia..... 68

Figure 28: Expression of CHOP-dependent apoptosis mediators in lungs of CHOP deficient mice treated with repetitive bleomycin..... 70

Figure 29: Hypoxia induces expression of pro-fibrotic mediators in AECs..... 74

Figure 30: Exposure to hypoxia induces HIF signaling in AECs peaking at 6 hours..... 75

Figure 31: HIF signaling regulates expression of pro-fibrotic mediators VEGF and PDGFB exposed to hypoxia..... 76

Figure 32: Evaluation of HIF1 α in the bleomycin + hypoxia model..... 77

Figure 33: Epithelial HIF deficient mice are not protected from exaggerated lung fibrosis induced by exposure to hypoxia..... 78

Figure 34: Epithelial HIF deficient mice and littermate controls have similar expression of pro-fibrotic mediators after bleomycin treatment followed by exposure to hypoxia..... 79

Figure 35: Epithelial HIF signaling plays an important role in mediating lung fibrosis after repetitive bleomycin injury..... 80

Figure 36: Model showing that tissue hypoxia leads to type II AEC dysfunction and augments lung fibrosis through ER stress and HIF signaling pathways..... 102

LIST OF TABLES

Table 1: Table showing genes in the Mouse Apoptosis RT2 Profiler PCR Array that were differentially regulated by CHOP siRNA treatment and confirmed by individual qPCR.....	69
--	----

LIST OF ABBREVIATIONS

AARE	amino acid regulatory element
AEC	alveolar epithelial cell
ANOVA	analysis of variance
AP-1	activator protein-1
ATF	activating transcription factor
Bak	Bcl2 homologous antagonist killer
Bax	Bcl2-associated X protein
BC12	B-cell lymphoma 2
BiP	binding immunoglobulin protein
BNIP3L	BCL2 interacting protein 3 like
CAMKII	calmodulin-dependent kinase II
COPD	chronic obstructive pulmonary disease
CHOP	C/EBP homologous protein
DOC	Downstream of CHOP
ECM	Extracellular matrix protein
EDEM	ER degradation enhancing α -mannosidase like protein
eIF2 α	eukaryotic translation initiation factor 2 α
EMT	endothelial mesenchymal transition
ER	endoplasmic reticulum
ERAD	ER-associated degradation
ERSE	ER stress-response element

FDA	Food and Drug Administration
GADD34	growth arrest and DNA damage-inducible protein 34
GADD45A	growth arrest and DNA damage-inducible protein 45A
HRE	hypoxia response element
IL-1 β	interleukin-1 β
ILD	interstitial lung disease
IPF	idiopathic pulmonary fibrosis
IRE1 α	inositol requiring enzyme 1 α
JNK	c-Jun NH2 terminal kinase
LC3-II	microtubule-associated protein 1A/1B-light chain 3-II
LPS	lipopolysaccharide
MLE	mouse lung epithelial
MOI	multiplicity of infection
NF- κ B	NF-kappa B
4-PBA	4-phenylbutyric acid
PCR	polymerase chain reaction
PDI	protein disulphide isomerase
PERK	PKR-like endoplasmic reticulum kinase
PI3K	Phosphoinositide 3-kinase
PINK1	PTEN-induced putative kinase 1
RIDD	IRE1 α -dependent decay of mRNA
ROS	reactive oxygen species
SFTPC	surfactant protein C

TGF β	transforming growth factor β
TNF α	tumor necrosis factor α
TRB3	tribbles-related protein 3
UIP	usual interstitial pneumonia
UPR	unfolded protein response
XBP-1	X-box binding protein-1
ZO-1	zona occludens-1

I. INTRODUCTION

What is IPF?

Idiopathic pulmonary fibrosis (IPF) is a severe form of interstitial lung disease (ILD) characterized by progressive dyspnea, exercise intolerance, hypoxemia, and respiratory failure (1). The pathological equivalent of IPF, known as usual interstitial pneumonia (UIP), is identified by the presence of patchy areas of fibrotic remodeling in the distal lung parenchyma with fibroblastic foci (1-3) (**Figure 1**). Collagen deposition occurs in association with accumulation of activated (myo)fibroblasts in areas subjacent to the epithelial surface, which can be composed of hyperplastic type II alveolar epithelial cells (AECs) or epithelium with bronchiolar appearance

(4). Collapse of remodeled alveoli creates focal areas of fibrosis and stretches adjacent lung parenchyma, resulting in micro-honeycombing and traction bronchiectasis, which are characteristic of this disorder. In addition to AECs and fibroblasts, inflammatory cells are thought to contribute to the development of fibrosis (5). Specifically, macrophages with the M2 phenotype are found within parenchymal areas in IPF and secrete mediators that can impact fibrosis (5, 6). The current paradigm to explain IPF is that repetitive epithelial injury, along with genetic factors, results in persistent fibroblast activation and ongoing collagen and matrix deposition.

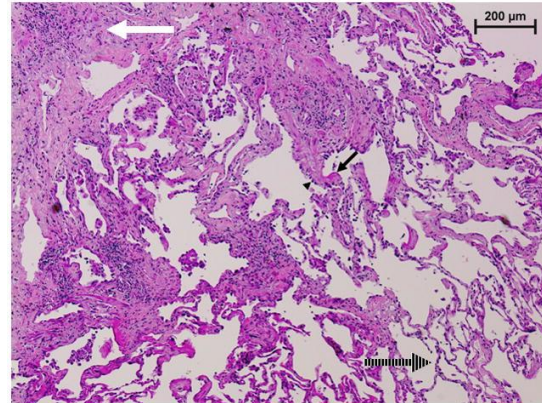


Figure 1. Hematoxylin and eosin (H&E) stained section from a lung biopsy showing findings of usual interstitial pneumonia (UIP). Hallmark findings of UIP are noted, including areas of dense fibrosis (white arrow) adjacent to areas of normal lung (striped arrow), fibroblastic foci (black arrow), and hyperplastic epithelial cells lining areas of fibrotic remodeling (black arrowhead). Adapted from Idiopathic Pulmonary Fibrosis: A Disorder of Epithelial Cell Dysfunction, Zoz et al., *Am J Med Sci.*;341(6):435-8, Copyright (2011), with permission from Elsevier.

The burden of IPF: an unmet medical need

IPF is a chronic, progressive, and irreversible lung disease. The prognosis of IPF is poor with median survival for patients being 3 - 5 years from the time of diagnosis (7). The prevalence of IPF ranges from 14 – 63 cases/100,000 people (8) and it leads to 30,000-50,000 deaths in the US every year (9). The mean age of onset for the disease is 65 years (10) and it is more common in men compared to women (11). Despite increasing efforts to understand disease pathogenesis and the performance of numerous clinical trials especially over the last two decades, treatment options for patients are limited. In 2014, Food and Drug Administration (FDA) approved the use of two antifibrotic agents, nintedanib and pirfenidone, for management of IPF (12); however, while these drugs may slow down disease progression, IPF remains an incurable disease. Due to absence of effective drugs, lung transplantation often becomes the only viable treatment option for IPF patients. Unfortunately, the 1- and 5-year survival rates for lung transplantation are the poorest compared to transplantation of any other solid organ (13). Additionally, from an economic standpoint, a 2012 study reviewing US claims database reported that the total direct cost for patients with IPF was \$26,000/person-year and the incremental cost over control subjects was \$12,124 (14). Taken together, it is clear that IPF poses a huge clinical and economic burden making it incumbent to advance our understanding of the pathophysiology of the disease to be able to develop effective therapeutic strategies.

Pathogenesis of IPF: dysfunction of the alveolar epithelium

Multiple lines of evidence implicate AEC dysfunction as pivotal in IPF (3). In IPF lung biopsies, epithelial abnormalities are common and include hyperplastic AECs lining areas of honeycombing (15). Although the critical mechanisms by which AECs contribute to IPF are incompletely understood, AEC apoptosis has been implicated in lung fibrosis based on human

disease and animal models (16). Furthermore, AECs produce key pro-fibrotic mediators that are implicated in lung fibrosis (17).

The current body of literature suggests that a combination of genetic and environmental factors produce a vulnerable type II AEC population (18). On encountering recurrent or persistent injurious stimuli, the vulnerable type II AECs exhibit aberrant behavior including enhanced apoptosis and increased expression of pro-fibrotic mediators; ongoing dysfunction of type II AECs impairs normal injury-repair responses and leads to failed re-epithelialization, fibroblast activation, excessive extracellular matrix (ECM) deposition, and progressive fibrosis. One of the ways in which genetic and environmental factors can affect AEC phenotype is by inducing ER stress, and increasing evidence now implicates endoplasmic reticulum (ER) stress in AECs as important in IPF pathogenesis (19-22) (**Figure 2**).

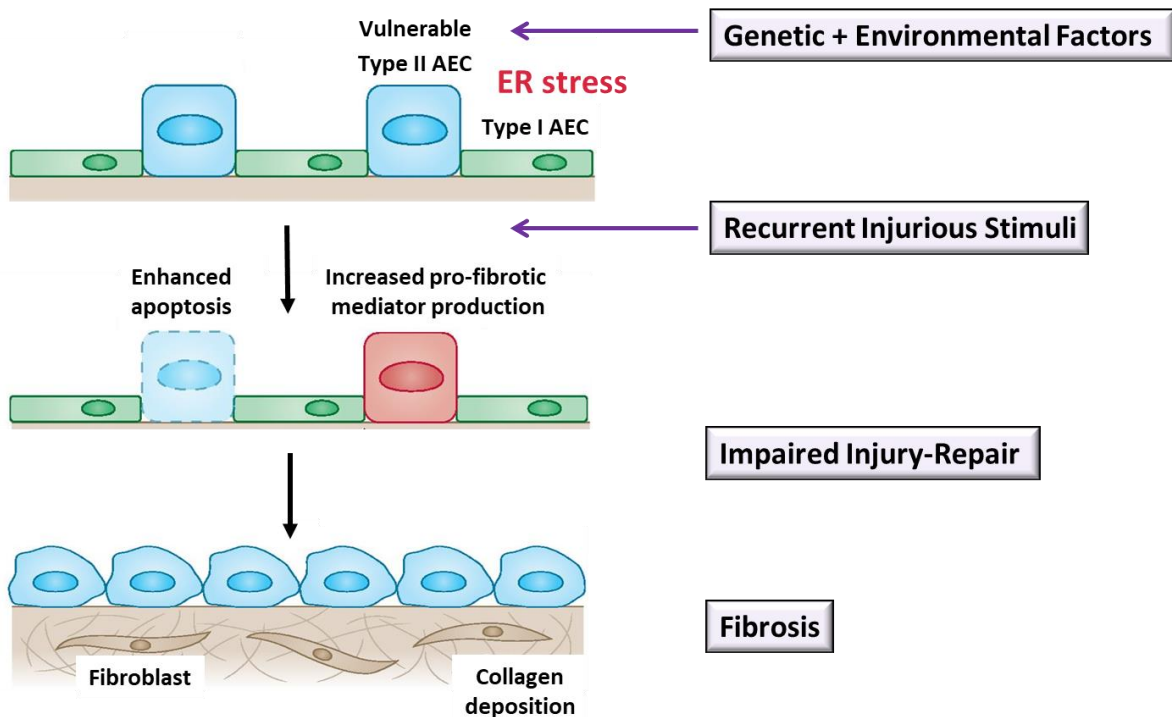


Figure 2. Potential mechanism of IPF pathogenesis. Adapted/modified from Genetic studies provide clues on the pathogenesis of idiopathic pulmonary fibrosis, Kropski JA, Dis Model Mech. 2013;6(1):9-17.

Endoplasmic reticulum stress as a pathogenic mechanism in lung fibrosis

The ER is a specialized organelle responsible for maintaining protein homeostasis or 'proteostasis'. The ER is primarily required for protein folding and performing quality control of proteins before they reach their intracellular or extracellular destinations. Any condition that perturbs protein processing can lead to accumulation of misfolded proteins in the ER – a condition termed ER stress (**Figure 3**). In response to ER stress, the cell launches a signaling cascade termed the unfolded protein response (UPR). The UPR initially aims to restore proteostasis but may result in cell death under prolonged or severe ER stress (20). Chronic ER stress is a key contributor to numerous diseases including neurodegeneration, diabetes, cancer, and metabolic diseases (23). Current evidence points to a critical pathogenic role of ER stress/UPR in fibrosis in a number of organs, including kidney, heart, liver, gastrointestinal tract, and lung (21). Potential mechanistic links between ER stress and lung fibrosis were first identified >15 years ago with the discovery that familial IPF can be caused by mutations in surfactant protein C (SFTPC), which is produced by type II AECs (24-26). When mutant SFTPC constructs were expressed in lung epithelial cell lines, the result was accumulation of mutant protein in ER and induction of ER stress (27-32). Subsequently, immunohistochemistry studies from our group (27) and others (33) showed that ER stress markers are common in the lungs of patients with both familial and sporadic IPF and are primarily localized to hyperplastic type II AECs in areas of fibrotic remodeling.

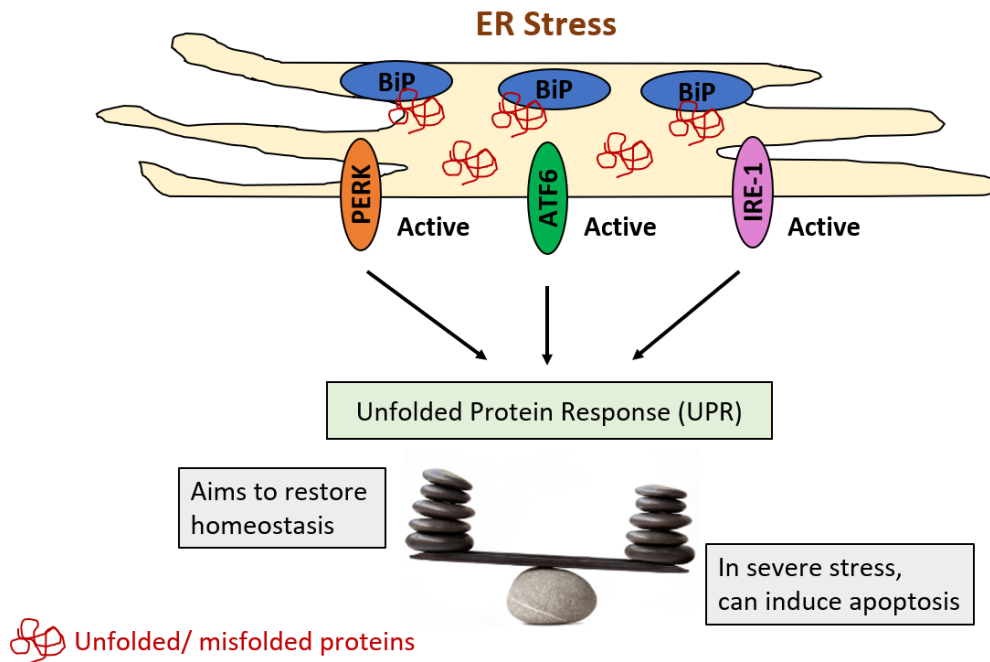


Figure 3. Schematic illustration of endoplasmic reticulum (ER) stress. On accumulation of unfolded or misfolded proteins in the ER, BiP is released from the three ER stress sensors and becomes bound to the proteins instead; release of BiP activates the three sensors, and together they launch a cell signaling network called the unfolded protein response or UPR.

The unfolded protein response (UPR) pathway: an overview

A cell produces up to 4×10^6 proteins every minute with the ER bearing the responsibility of folding and processing at least a third of those (34, 35). Functions of the ER include orchestrating biogenesis, folding, assembly, and trafficking of proteins, as well as degradation of defective proteins (36-39). ER function is tightly regulated by a combination of factors including protein load, metabolic demands of the cell, chaperone efficiency, redox balance, and calcium homeostasis (40-43). Perturbations in any of these factors can lead to ER stress and activation of the UPR.

The UPR pathway consists of three ER transmembrane proteins: 1) PKR-like endoplasmic reticulum kinase (PERK), 2) activating transcription factor 6 (ATF6), and 3) inositol requiring enzyme 1 α (IRE1 α) (36). In an unstressed cell, binding immunoglobulin protein (BiP), which is a chaperone that facilitates protein folding remains bound to PERK, ATF6 and IRE1 α , and maintains these sensors in an inactive state. In a stressed cell with accumulation of proteins in the ER, BiP is sequestered away from the sensors, resulting in their activation and initiation of the UPR, which is designed to restore cellular homeostasis through reduction in overall protein translation along with selective increases in expression of critical chaperone and redox proteins (44, 45) (**Figure 4**).

PERK: On sensing ER stress, PERK is activated and undergoes auto-phosphorylation and dimerization (46). PERK then phosphorylates the α subunit of eukaryotic translation initiation factor 2 α (eIF2 α) at Ser51, which is the only known direct target of PERK (47). Phosphorylation of eIF2 α leads to overall inhibition of protein synthesis. Phospho-eIF2 α , however, can selectively up-regulate activating transcription factor 4 (ATF4), which is a transcription factor that induces expression of a set of genes required for cellular homeostasis (47-51). ATF4 can also activate

expression of pro-apoptotic factors, including growth arrest and DNA damage-inducible protein 34 (GADD34) (48, 52) and C/EBP homologous protein (CHOP) (53, 54).

ATF6: After its release from BiP, ATF6 translocates to the Golgi where it is cleaved into amino terminal and carboxy terminal (cytoplasmic) domains by site1 and site2 proteases (55, 56). Cleaved cytoplasmic ATF6 then translocates to the nucleus where it activates transcription of several chaperones proteins, such as BiP, calreticulin, and protein disulphide isomerase (PDI) (57). Activated ATF6 also induces the expression of X-box binding protein 1 (XBP1), a downstream transcription factor activated through the IRE1 α pathway (58, 59).

IRE1 α : When released from chaperone binding, IRE1 α undergoes oligomerization and auto-phosphorylation, resulting in activation of an RNase domain that cleaves XBP1 into an active form. Spliced XBP1 (XBP1s) then activates expression of target genes, including ER degradation enhancing α -mannosidase like protein (EDEM), which promotes protein degradation through the ER-associated degradation (ERAD) pathway (60). In some settings, IRE1 α can be activated to degrade a wider range of ER-localized mRNAs through a process known as IRE1 α -dependent decay of mRNA (RIDD), thus affecting cell survival and other cellular phenotypes (61, 62).

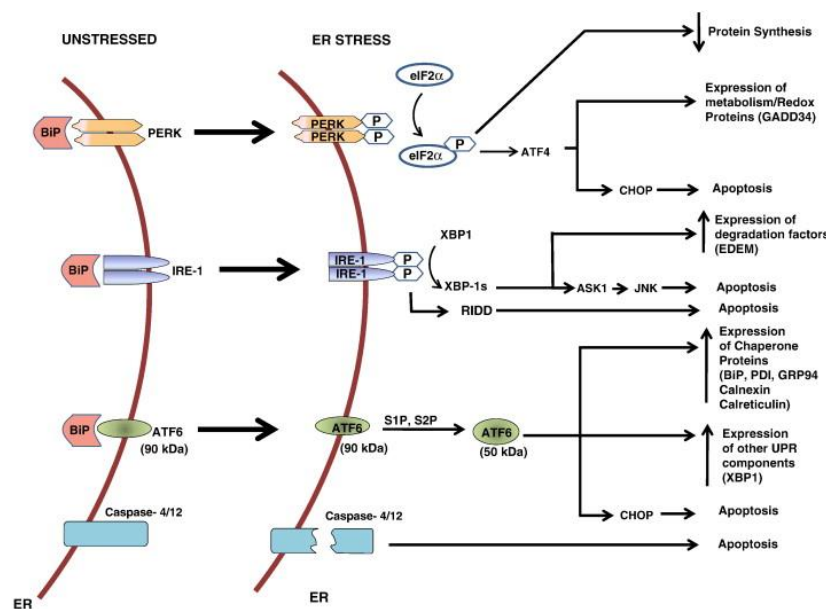


Figure 4. Schematic illustration of the UPR.

ATF = activating transcription factor; BiP = immunoglobulin heavy-chain-binding protein; EDEM = ER degradation enhancing α -mannosidase-like protein; eIF2 α = eukaryotic initiation factor 2 α ; ER = endoplasmic reticulum; GADD34 = growth arrest and DNA damage protein 34; IRE =

inositol-requiring enzyme 1 (IRE-1); PERK = PKR-like ER kinase; XBP1 = X-box binding protein 1; GADD34 = growth arrest and DNA damage-inducible protein; PDI = protein disulphide isomerase; GRP94 = glucose-regulated protein 98; CHOP = C/enhancer binding protein (EBP) homologous protein; ASK1 = apoptosis signal-regulating kinase 1; JNK = c-Jun N-terminal kinases; S1P = site-1 protease; S2P = site-2 protease; RIDD = regulated IRE1-dependent decay. Adapted/modified from Endoplasmic reticulum stress as a pro-fibrotic stimulus, Tanjore et al., *Biochimica et Biophysica Acta (BBA) - Molecular Basis of Disease*, 1832(7):940-947., Copyright (2013), with permission from Elsevier.

Factors influencing ER stress

In addition to genetically determined expression of mutant proteins, ER stress can be induced by: 1) exogenous factors that increase protein expression (e.g. viral infections) or produce reactive oxygen species (ROS) and/or impair redox balance in cells (e.g. cigarette smoke, inhaled particulates), and 2) intracellular processes that impair bioenergetics (e.g. hypoxia, aging), cause calcium shifts (e.g. mechanical stretch), or reduce clearance of misfolded proteins (e.g. proteasomal dysfunction, impaired autophagy) (**Figure 5**).

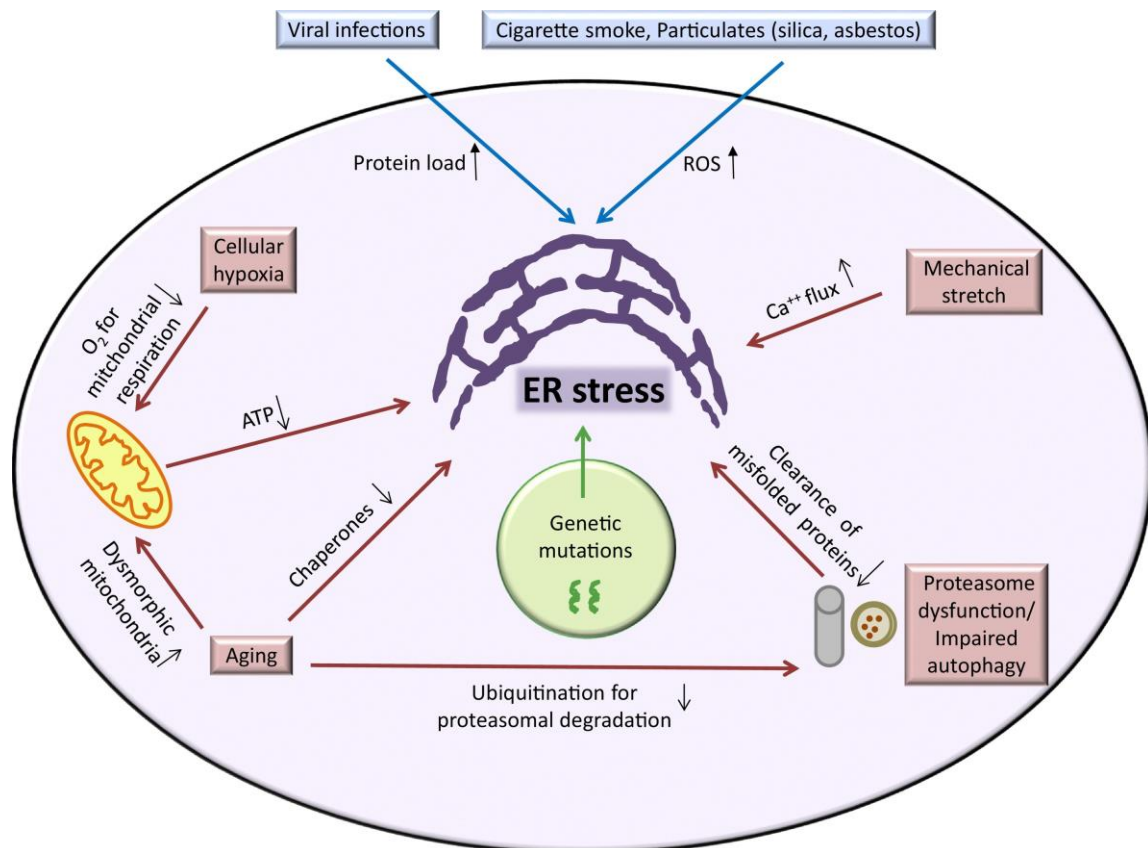


Figure 5. Potential causes of ER stress. Adapted from Burman A, *Matrix Biology*. 2018; 68-69:355-365

In IPF, several groups have detected herpesvirus antigens in lungs of patients by polymerase chain reaction (PCR) and immunohistochemistry (63). Our group has reported concomitant expression of herpesvirus antigens and ER stress markers in AECs in IPF patients (27) as well as in asymptomatic relatives of patients with familial IPF (64), thereby suggesting a role of herpesvirus-induced ER stress in lung fibrosis. Also, increased expression of a repertoire of hypoxia-inducible genes has been reported in IPF lungs (65, 66) and in single cell analysis of AECs in IPF (67) supporting the existence of cellular hypoxia, which can induce ER stress (68). Aging represents another ER stress-influencing factor in patients with IPF, whose median age of diagnosis is 65 years (8, 69). Aging can significantly impair ER function through reduction in chaperone production, increase in dysmorphic mitochondria (impacting bioenergetics), and inefficient proteasomal degradation of proteins (70-73). Torres-Gonzalez *et al.* reported increased ER stress markers in type II AECs in old mice compared to young mice in an experimental model of lung fibrosis, thus supporting a connection between ER stress and aging (74). In addition to direct effects of aging, impairment in ER quality control mechanism (e.g. ERAD, autophagy) can contribute to ER stress (75, 76). In this regard, staining for microtubule-associated protein 1A/1B-light chain 3-II (LC3-II), which is reflective of autophagy, was shown to be absent in type II AECs in fibrotic lesions while expression was prominent in non-fibrotic areas (76).

Regulation of effector pathways by ER stress

ER stress and UPR signaling have been linked to fibrosis through apoptotic cell death, activation/differentiation of fibroblasts, epithelial-mesenchymal transition (EMT), and activation or polarization of inflammatory responses (20, 21, 77).

Epithelial cell apoptosis is a key component of fibrotic diseases in a number of organs, including the lungs (4, 20). Prolonged or excessive ER stress can induce apoptosis in epithelial

cells through several UPR-dependent downstream mechanisms, including induction of CHOP, activation of the ER bound caspase (caspase-4 in humans, caspase-12 in mice), or activation of c-Jun NH2 terminal kinase (JNK) (36-38, 43). Of these three pathways, apoptosis through induction of CHOP is best studied. CHOP is a member of the C/EBP family of transcription factors. It functions both as an inhibitor of C/EBP transcriptional activity and an inducer of gene targets through interactions with alternative enhancer sites (78, 79). CHOP regulates the apoptotic pathway through activation of pro-apoptotic genes and downregulation of anti-apoptotic genes, such as B-cell lymphoma 2 (Bcl2) (80). In most reports, CHOP is primarily induced downstream of PERK/ATF4, but all 3 arms of the UPR can participate in CHOP induction (81). ER stress can also cause apoptosis through UPR-independent cell death mechanisms. For example, excessive ER stress releases calcium into the cytosol, which can trigger apoptosis through Bcl2-associated X protein (Bax) and Bcl2 homologous antagonist killer (Bak) (82).

In addition to effects on cell survival, ER stress can affect cell differentiation. In this regard, XBP1 contributes to plasma cell differentiation (83). In the context of fibrosis, ER stress has been shown to affect differentiation of fibroblasts to myofibroblasts, which are an activated subset of fibroblasts common in fibrotic diseases that produce large amounts of collagen and other extracellular matrix components. For example, fibroblasts treated with ER stress-inducing agents are more susceptible to myofibroblast differentiation induced by transforming growth factor β (TGF β) (84, 85). In epithelial cells, ER stress has been shown to induce EMT, resulting in a cellular phenotype that may directly participate in fibrotic remodeling (31, 32). In addition to *in vitro* studies showing ER stress-induced EMT, treatment of mice with cyclosporine, which can induce ER stress in renal tubular epithelial cells, has been shown to cause EMT through both TGF β dependent and independent mechanisms (86, 87).

Inflammation is linked to fibrosis in a number of organs, including lungs, and ER stress and the UPR pathway have been shown to regulate inflammatory signaling pathways, including nuclear factor kappa B (NF- κ B) and activator protein-1 (AP-1) (88). In inflammatory bowel disease, ER stress has been observed in colonic mucosa and the IRE1 α pathway has been shown to regulate disease progression (89). Accumulation of mutant muc2 (mucin in intestinal goblet cells) results in ER stress and inflammation in the large intestine with increased expression of interleukin-1 β (IL-1 β), tumor necrosis factor α (TNF α), and interferon- γ (90). In bone marrow derived macrophages subjected to LPS stimulation, ER stress is able to drive production and processing of pro-IL-1 β (91).

Macrophages can be polarized into M1 (pro-inflammatory) or M2 (pro-fibrotic) subsets based on microenvironmental stimuli (92). Based on available data, ER stress may be able to skew macrophage populations towards either a M1 or a M2 phenotype depending on the pathophysiological context. In obesity, IRE1 α deficiency has been reported to favor the M2 macrophage phenotype (93) and CHOP deficiency can increase both M1 and M2 macrophages (94). However, in diabetes, pulmonary fibrosis, and allergic airway inflammation, ER stress has been reported to drive M2 polarization through JNK or CHOP dependent mechanisms (95-97).

Pro-fibrotic effects of ER stress in individual lung cell types in lung fibrosis

Pro-fibrotic effects of ER stress may be transduced through several different cell types in the lungs, including alveolar epithelial cells, fibroblasts, and macrophages (**Figure 6**). The impact of ER stress on pro-fibrotic characteristics of each of these cell types is discussed below.

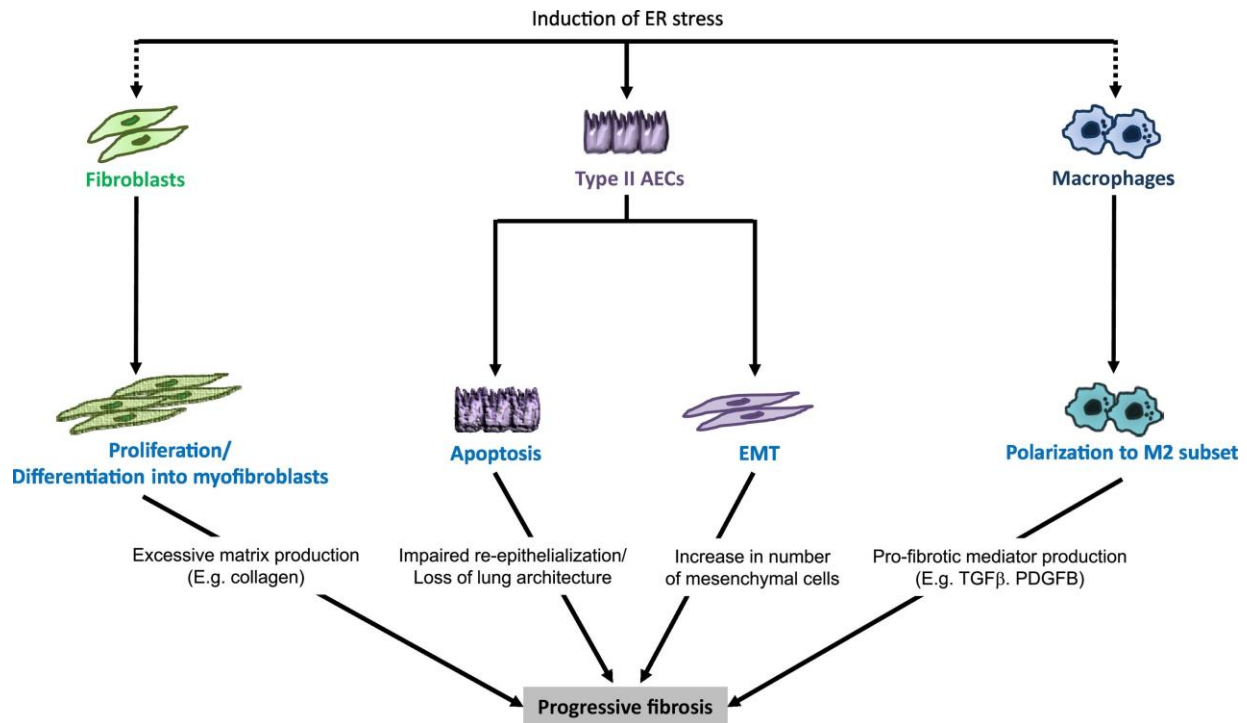


Figure 6. Pro-fibrotic effects of ER stress in different cell types in lung fibrosis. Adapted from Burman A, Matrix Biology. 2018; 68-69:355-365

Alveolar epithelial cells:

In lungs of IPF patients, ER stress markers have been identified primarily in type II AECs (27, 33). By immunohistochemistry, we identified increased expression of BiP, EDEM, and XBP1 in AECs from patients with both familial and sporadic IPF (27). In addition, Korfei *et al.* reported increased expression of ATF4, ATF6, and CHOP in AECs from lung sections obtained from IPF patients, along with evidence of apoptosis by immunostaining for cleaved caspase 3 (33).

In type II AEC lines, over-expression of mutant SFTPC genes (either exon 4 deleted or L188Q SFTPC) results in ER stress and increased apoptosis (27, 29, 30). Constitutive expression of exon 4 deleted SFTPC in mice resulted in fetal lethality with disrupted lung morphogenesis and defective surfactant protein processing (98). We generated doxycycline inducible transgenic mice in which mutant L188Q SFTPC is expressed in type II AECs (99). When this transgene was induced in type II AECs or when the ER-stress inducing agent tunicamycin was administered through direct intratracheal instillation into the lung, ER stress was observed in type II AECs; however, fibrosis did not develop, and AEC apoptosis was not identified. In contrast, treatment with low dose bleomycin resulted in a substantial increase in fibrosis with greater AEC apoptosis than treatment with bleomycin alone (99). Together, these data indicate that ER stress in AECs is not sufficient to induce lung fibrosis. Rather, ER stress appears to sensitize to development of fibrosis following epithelial injury.

The mechanisms by which ER stress regulates survival/apoptosis of AECs are incompletely understood and may be context dependent. In cultured type II AECs over-expressing mutant forms of SFTPC, Mulegeta *et al.* identified caspase 4/12 as an important mediator of apoptosis (30). Similarly, activation of caspase-12 and cleaved caspase-3 were detected in lungs of mice expressing L188Q SFTPC in type II AECs following bleomycin treatment (99). CHOP has also been implicated in ER stress-dependent AEC apoptosis (33) although prior studies show inconsistent effects of CHOP deletion on lung fibrosis. Tanaka *et al.* (100) reported that CHOP deficient mice have reduced AEC apoptosis and lung fibrosis after bleomycin treatment. In contrast, Ayaub *et al.* (101) found that CHOP deficient mice had higher mortality and increased fibrosis compared to wild-type controls following bleomycin treatment.

Several other mechanisms have been implicated in ER stress-induced AEC apoptosis, including regulation of ER Ca^{2+} . Calmodulin-dependent kinase II (CAMKII) is an important regulator of ER Ca^{2+} and can modulate apoptosis (102). Inhibition of CAMKII using transgenic mice with AEC specific expression of the CaMKII inhibitor peptide AC3-I resulted in decreased intracellular Ca^{2+} , reduced CHOP, decreased AEC apoptosis, and protection from fibrosis following bleomycin treatment (102). In addition, Bueno M. *et al.* (72) showed that the mitochondrial protective factor PTEN-induced putative kinase 1 (PINK1) is decreased in IPF lungs. In experimental models, ER stress induction resulted in decreased PINK1 in AECs, along with altered bioenergetics and increased AEC apoptosis (72). PINK1 loss can also induce ER stress, indicating the possibility of a feedback mechanism linking ER stress, mitochondrial dysfunction, and fibrotic remodeling (103).

In addition to AEC apoptosis, another possible mechanistic link between ER stress and fibrosis comes from studies in which ER stress-inducing agents or expression of mutant SFTPC were shown to induce EMT in AECs with increased expression of mesenchymal markers such as α smooth muscle actin (α SMA), vimentin, N-Cadherin and reduction of epithelial markers like E-Cadherin, and zona occludens-1 (ZO-1) (31, 32). Further studies suggested the IRE1 α /XBP1 pathway is critical for regulating EMT in type II AECs (31). Along these lines, induction of ER stress due to expression of mutant SFTPC (exon4 deletion) in A549 cells increased collagen production and secretion (104).

Fibroblasts:

Myofibroblast differentiation is involved in wound healing and is characteristic of fibrotic diseases since these activated myofibroblasts produce increased amounts of collagen and matrix components (105). In fibroblasts from IPF patients, pharmacological inhibition of ER stress

through 4-phenylbutyric acid (4-PBA) treatment reduced TGF β 1-induced myofibroblast differentiation, α SMA expression, and collagen production (84). Knockdown of the ER chaperone calreticulin using siRNA in mouse and human IPF fibroblasts reduced TGF β 1-induced collagen and fibronectin production (106). Similarly, treatment of fibroblasts with an IRE1 α inhibitor reduced collagen 1 α 2 and fibronectin expression and reduced autophagy in IPF lung fibroblasts following TGF β treatment (85). In addition, ER stress regulation of PI3K/AKT signaling has been implicated in fibroblast proliferation and differentiation (107). Together, current data implicate ER stress in regulating myofibroblast differentiation in the lungs; however, whether this is a critical pathogenic mechanism in IPF remains to be determined.

Macrophages:

Macrophages can contribute to lung fibrosis through secretion of pro-fibrotic mediators (e.g. TGF β), chemokines, and matrix metalloproteases (5, 108, 109). In the lungs, ER stress has been reported in macrophages obtained by bronchoalveolar lavage from asbestosis patients and alveolar macrophages from mice with asbestos-induced lung fibrosis (110). In IPF, Yao *et al.* reported expression of CHOP in M2 macrophages in IPF patients (96).

Several groups have shown that ER stress can affect macrophage phenotypes; however, current studies are inconsistent regarding the impact of ER stress on M2 macrophage polarization. In mouse obesity models, genetic deficiency of IRE1 α or CHOP resulted in increased M2 macrophages (93, 94). On the other hand, several studies have shown that induction of ER stress skews towards M2 polarization. Specifically, ER stress-induced JNK activation has been shown to induce M2 polarization in mouse peritoneal macrophages (95). In lung macrophages, CHOP has been reported to induce M2 polarization in the bleomycin model of pulmonary fibrosis and a model of allergic airway inflammation (96, 97). Similarly, treatment of murine bone marrow-

derived macrophages with PBA was reported to prevent palmitate-induced M2 polarization (111). Although available studies suggest that the effects of ER stress on macrophage polarization depend on the disease context, ER stress in lung macrophages appears to favor the M2 phenotype.

In addition to effects on macrophage polarization, ER stress may impact fibrosis by inducing macrophage apoptosis, thereby abrogating the effects of M2 polarization. Ayaub *et al.* showed that CHOP expression induced macrophage apoptosis and protected from bleomycin-induced lung fibrosis (101). Similarly, silica has been shown to induce alveolar macrophages apoptosis via ER stress *in vitro* (112). Taken together, these data reveal a complex interplay between ER stress and macrophage phenotype. Further studies are needed to clarify whether the net effect of ER stress in macrophages is pathogenic or protective in different models of lung fibrosis.

C/EBP homologous protein (CHOP)

Over the past few years, several studies have reported a role of CHOP in lung fibrosis. CHOP, also known as growth arrest and DNA damage inducible gene 153 (GADD153), is a member of the C/EBP family of transcriptions factors and is a primary mediator of ER stress-induced apoptosis. It is a 29 kDa protein comprising of 169 amino acids in humans and 168 amino acids in rodents. CHOP is ubiquitously expressed at low levels in homeostatic conditions while cellular stress (e.g. ER stress, amino acid starvation) leads to increased expression of CHOP and its accumulation in the nucleus (113).

CHOP can act both as a dominant negative inhibitor of other members of the C/EBP family and as a transcription factor. Specifically, CHOP heterodimerizes with other members of the C/EBP family, which have a strong preference for homodimerization; while CHOP-C/EBP heterodimers cannot bind to the consensus C/EBP site on the promoters of target genes, these

heterodimers can bind to a unique site on a unique set of target genes and activate them. CHOP consists of an N-terminal transcriptional activation domain and a C-terminal basic leucine zipper (bZIP) domain responsible for DNA binding and dimerization (113) (**Figure 7**).

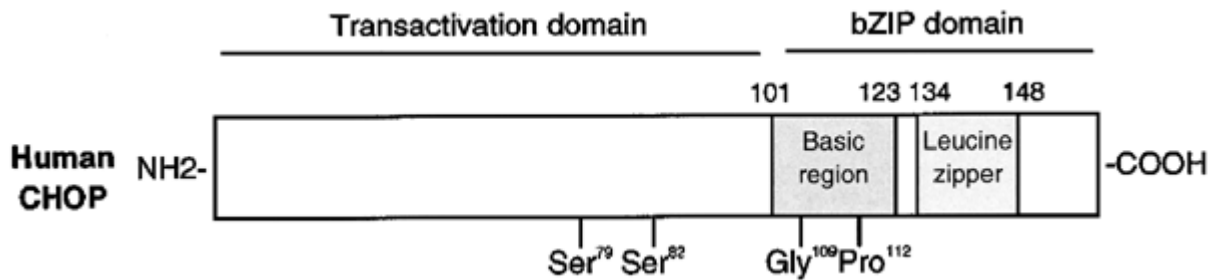


Figure 7. Domain structure of human CHOP. CHOP is composed of its N-terminal putative transactivation domain and a C-terminal bZIP domain that contains a DNA-binding basic region and a leucine zipper dimerization region. The basic region contains conserved glycine (109) and proline (112) residues, which are essential for binding to the unique CHOP binding site on target genes. Two serine residues (79 and 82) in the transactivation domain are phosphorylated by p38 MAP kinase, and this phosphorylation is required for the enhanced transcriptional activation. Adapted with permission from Springer Nature: Nature, Cell Death and Differentiation, Roles of CHOP/GADD153 in endoplasmic reticulum stress, Oyadomari S, Cell Death Differ. 2003;11(4):381-9, Copyright (2003).

CHOP is primarily regulated at the transcriptional level. The human CHOP promoter contains two amino acid regulatory element (AARE) and at least two ER stress-response element (ERSE) cis-acting motifs. On induction of ER stress, the upstream ER stress mediators ATF4, ATF6, and XBP1 bind to these motifs on the CHOP promoter and induce expression of CHOP; specifically, ATF4 binds to the AARE1 and AARE2 motifs whereas ATF6 and XBP1 bind to the ERSE1 and ERSE2 motifs. While all the three UPR pathways namely PERK/ATF4, ATF6 and IRE1/XBP1 are required for maximal induction of CHOP, it has been shown that the PERK/ATF4 pathway is essential for CHOP induction in ER stress and dominates over the ATF6 and IRE1/XBP1 pathways (113).

CHOP has been implicated in diseases such as diabetes and neurodegenerative disorders where enhanced apoptosis may contribute to the disease process. Overexpression of CHOP leads to apoptosis in cells and CHOP deficient cells have reduced ER stress-induced apoptosis. As a transcription factor, CHOP can regulate the expression of numerous apoptosis-related genes including DOCs (down-stream of CHOP), B-cell lymphoma-2 (BCL-2), tribbles-related protein3 (TRB3), and growth and DNA damage 34 (GADD34) (114).

Hypoxia and fibrosis

Hypoxia is a common factor in the microenvironment of injured/damaged tissue in fibrosis in several organs (115). Following tissue damage, an imbalance created by decreased oxygen supply (due to compromised perfusion) and increased oxygen demand (due to infiltration of inflammatory and mesenchymal cells) may lead to tissue hypoxia. While transient hypoxia often helps in tissue repair, chronic hypoxia may be maladaptive and promote excessive scarring (115). Chronic hypoxia has been implicated as a pathogenic factor in kidney, liver, and heart fibrosis (116-118). In the lungs, hypoxia is known to contribute to vascular remodeling in pulmonary hypertension (119); however, the role of tissue hypoxia in lung fibrosis is unclear. Mechanistically, in addition to induction of ER stress, studies have suggested a potential role of hypoxia in several cellular processes including inflammatory pathways, expression of pro-fibrotic mediators, secretion of collagen, oxidative stress, EMT, and apoptosis (120-126). Taken together, tissue hypoxia is a potentially pathogenic microenvironmental factor that needs to be considered while investigating the pathophysiology of fibrosis.

Hypoxia-inducible factor (HIF) signaling

The cellular responses to hypoxia occur primarily through signaling via the hypoxia inducible factors, HIF1 α and HIF2 α . The stability of HIF1 α and HIF2 α is determined by the availability of oxygen. In normoxia, HIF1 α and HIF2 α are hydroxylated at specific proline residues by prolyl hydroxylases, which leads to their subsequent ubiquitination and degradation. In hypoxia, lack of oxygen inhibits the activity of prolyl hydroxylases leading to stabilization of HIF1 α and HIF2 α . These isoforms of HIF are then transported to the nucleus where they dimerize with the ubiquitously expressed subunit HIF1 β and form transcriptionally active HIF1 or HIF2. HIFs bind to hypoxia response element (HRE) on promoters of specific target genes and activate them (127) (**Figure 8**).

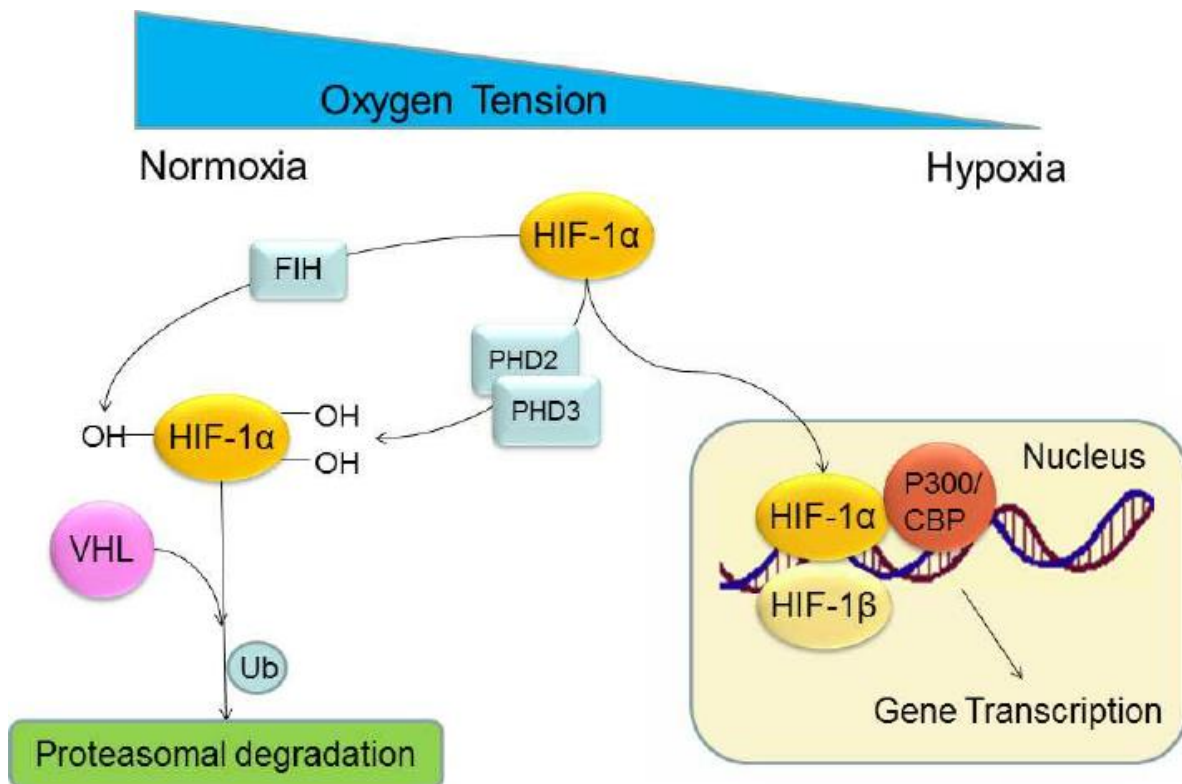


Figure 8. Regulation of HIF-1 α stability and activity is oxygen-dependent. In normal oxygen tension, HIF-1 α undergoes two prolyl hydroxylations within its degradation domain by PHD-2 and PHD-3, enabling its interaction with VHL protein. VHL functions as the recognition component of an E3 ubiquitin ligase that targets HIF-1 α for ubiquitination (Ub) and proteosomal degradation. In addition, FIH acts as an asparaginyl hydroxylase, leading to asparaginyl hydroxylation within the C-transactivation domain of HIF-1 α and preventing interaction of HIF-1 α with various coactivators, such as p300/CBP, thus resulting in its inactivation. During hypoxia, activity of the prolyl and asparaginyl hydroxylases, which is oxygen-dependent, is markedly reduced. The accumulating HIF-1 α combines with HIF-1 β to form a heterodimer that binds to DNA and interacts with its coactivators p300/CBP, driving transcription of various HIF-1 α inducible genes. Adapted from Tal et al., The Role of Hypoxia and Hypoxia-Inducible Factor-1 Alpha in Preeclampsia Pathogenesis, *Biology of Reproduction*, 2012;134:1-8 by permission of Oxford University Press.

HIF signaling has been implicated in tissue repair and fibrosis in several organs (116, 117). For example, targeted deletion of HIF1 α in the renal tubular epithelium was shown to attenuate kidney fibrosis following unilateral ureteral obstruction (128). Similarly, reduced liver fibrosis was

observed in HIF1 α deficient mice in a bile-duct ligation model (129), and HIF2 α has been shown to regulate hepatic fibrogenesis in the setting of steatohepatitis (130). Also, HIF1 α has been reported to induce fibrogenesis in white adipose tissue (131). HIFs may impact tissue fibrosis in various ways including effects on pro-fibrotic mediators, cell survival, cell migration, inflammation, and angiogenesis (119, 132).

In conclusion, research over the last two decades has established that injury and dysfunction of type II AECs are critical in the pathogenesis of IPF. While available studies provide compelling evidence for ER stress in type II AECs in IPF, the etiology of ER stress in the vast majority of IPF lungs is unknown. In addition, the mechanisms by which ER stress contributes to fibrosis in the lungs have been challenging to unravel. Our studies described in Chapter III suggest hypoxia to be an etiological factor underlying ER stress observed in lung fibrosis and show CHOP to be a critical molecular mechanistic link between ER stress and lung fibrosis. Our work described in Chapter IV provides insight into the signaling pathways important in induction of CHOP and those in CHOP-mediated cell death in AECs in hypoxia. While HIF, a primary mediator of cellular responses to hypoxia, has been implicated in fibrosis in several organs, its role in lung fibrosis is not clear. Our investigations described in Chapter V focus on the role of HIF in two distinct mouse models of lung fibrosis and the effect of HIF signaling on phenotype of AECs. While Chapters III and IV of this dissertation have been published in *JCI Insight* (133), Chapter V consists of both published (133) and unpublished work.

II. MATERIALS AND METHODS

Human samples

Lung samples were obtained from surgical lung biopsies or explanted lung tissue obtained at the time of organ transplantation. Explanted donor lungs that were rejected for transplantation were used as controls.

Mice

We used 8- to 10-week-old male and female mice for these experiments (C57BL/6J background). WT and CHOP^{-/-} mice were purchased from The Jackson Laboratory. Doxycycline-inducible transgenic mice that express a mutant form of human SFTPC (L188Q SFTPC) (99) driven by a murine SFTPC promoter construct were crossed with CHOP^{-/-} mice to generate L188Q SFTPC/CHOP^{-/-} mice. L188Q SFTPC mice were used as controls. HIF1 α -floxed (128) and HIF2 α -floxed (134) mice were crossed to generate HIF1 α /HIF2 α -floxed mice. Transgenic mice in which both HIF1 α and HIF2 α are deleted in the lung epithelium were generated by crossing the HIF1 α /HIF2 α -floxed mice with SPC.Cre.Rosa.STOP.LacZ mice, in which Cre recombinase expression is under the control of a 3.7-kb human SPC promoter as described previously (128, 135-137). Mice with HIF1 α /HIF2 α deleted in lung epithelium were designated as HIF Δ/Δ . Littermate controls used were negative for Cre expression and designated as HIF^{fl/fl}. Mice were housed in the animal care facility at the Vanderbilt University Medical Center and given food and water ad libitum.

Lung fibrosis models

Bleomycin (Hospira Inc.) was purchased from Vanderbilt University Medical Center pharmacy. Bleomycin (0.04 units or 0.08 units) in 100 μ l saline was delivered by direct i.t. instillation under anesthesia as described previously (135, 137, 138). Mice were administered a single-dose or repetitive doses (6 doses at intervals of 2 weeks) of bleomycin, depending on the experimental strategy. Doxycycline-inducible transgenic mice were treated with doxycycline in drinking water (2 g/l) for 1 week prior to bleomycin instillation, and doxycycline was continued through the course of experiments. Lungs were harvested following euthanasia by exposure to carbon dioxide at designated time points. Right lungs were tied off and snap frozen for estimation of collagen and extraction of RNA and protein, and left lungs were inflated with 10% formalin for histology under constant pressure using a 25-cm pressure column as previously described (135).

Exposure of mice to hypoxia

Mice were exposed to hypoxia in a normobaric hypoxia chamber (Biospherix), in which oxygen concentration is controlled through flow of nitrogen to achieve the desired FiO₂. Ventilation ensures that carbon dioxide concentration remains below 1,000 parts per million.

Detection of cellular hypoxia

Mice were treated with pimonidazole (60 μ g/g body weight; HypoxyProbe Inc.) in 75 μ l sterile normal saline by intraperitoneal (i.p.) injection at 3 hours prior to lung harvest. Subsequently, IHC for pimonidazole adducts was performed on lung sections.

Morphometry

Left lungs were formalin-fixed, paraffin-embedded, sectioned, and stained with Masson's trichrome as previously described (135, 137). Lung morphometry was performed as previously

described (135). For each lung sample, images were captured at $\times 4$ using an Olympus BX81 research microscope. Areas of fibrosis or hyperplastic cells were measured using Cell Sens Dimension (Olympus).

IHC and immunofluorescence

IHC was performed on paraffin-embedded lung tissue sections as previously published (135, 137) using the following primary antibodies: pro-SPC (1:1,000 dilution, AB3786, MilliporeSigma), CHOP (1:300 dilution, SC-575, Santa Cruz Biotechnology), HIF1 α (1:300 dilution, SC-10790, Santa Cruz), pyruvate kinase (1:300 dilution, GTX107977, Genetex), CA-IX (1:300 dilution, NB100-417, Novus Biologicals), pimonidazole (biotin-conjugated antibody, Mouse-Biotin-Mab, HypoxyProbe Inc.). Primary antibodies were developed using Vectastain Elite anti-rabbit ABC peroxidase kits and Vectastain Elite antimouse ABC peroxidase kits (both from Vector Laboratories). Peroxidase substrate was developed with VECTOR NovaRED Peroxidase (HRP) Substrate Kit (Vector Laboratories). For quantification of CHOP, CHOP+ AECs (based on morphology and location) were counted in 10 high-power fields (HPFs) on each lung section. To detect cellular hypoxia in different cell types, dual immunofluorescence staining for pimonidazole adducts was performed with pro-SPC (1:1,000 dilution, AB3786, MilliporeSigma), S100A4 (1:400 dilution) (139), T1 α (1:500 dilution, 8.1.1, Developmental Studies Hybridoma Bank, Iowa City, Iowa, USA), CD34 (1:300 dilution, 119302, BioLegend), and F4/80 (1:300 dilution, MCA497G, AbD Serotec). For immunofluorescent detection of HIFs, HIF1 α (1:300 dilution, SC-10790, Santa Cruz) and HIF2 α (1:200 dilution, NB100-122, Novus Biologicals) primary antibodies were used. Following primary antibody incubation, appropriate fluorescent secondary antibodies (Jackson Immunoresearch) were used and nuclear counterstaining was performed using Vectashield mounting media with DAPI (Vector Laboratories). Dual fluorescent images were

captured using an Olympus IX81 Inverted Research Microscope configured with an Olympus IX2 Biological Disk Scanning Unit (Olympus). Quantification of pro-SPC, pimonidazole, and dual-positive cells was performed in 10 HPFs on each lung section

Evaluation of cell death

For evaluation of apoptosis in lung tissue, TUNEL staining was performed using the Fluorescent In Situ Cell Death Detection Kit (MilliporeSigma). The total number of TUNEL+ type II AECs (based on morphology and location) was quantified in 10 HPFs on each lung section as previously published (140). In addition, dual immunofluorescence was performed for TUNEL and pro-SPC, and double-positive cells were quantified in 10 HPFs on each lung section. To detect cytotoxicity in vitro, the lactate dehydrogenase (LDH) assay (Promega) was performed as per the manufacturer's instructions.

Measurement of collagen and fibronectin

Total soluble collagen in right lower lobes of the lung was measured using the Sircol assay (Biocolor; Accurate Chemical and Scientific Corporation) as per the manufacturer's instructions and as previously published (141). Fibronectin in lung tissue was measured using the Mouse Fibronectin ELISA Kit (Abcam) as per the manufacturer's instructions.

Quantification of immune/inflammatory cell types by flow cytometry

Lungs were enzymatically digested using collagenase XI (MilliporeSigma) and DNase IV (Macs Miltenyi Biotec) for 45 minutes at 37°C to obtain single-cell suspensions, followed by incubation with viability dye (Thermo Fisher Scientific) for 20 minutes according to the manufacturer's instructions. Cells were then incubated with anti-CD16/32 antibodies and further labeled with the following fluorescent dye-conjugated mAbs: CD45-eFluor 650 (95-0451- 42,

eBioscience/Thermo Fisher Scientific), Ly6C-APC-Cy7 (128025, BioLegend), Ly6G-Alexa Fluor 700 (127621, BioLegend), CD11b-APC (101212, BioLegend), CD11c-PE-Cy7 (25-01140-81, eBioscience/Thermo Fisher Scientific), F4/80-PE-Cy5 (123111, BioLegend), CD103-PE (12-1031-81, eBioscience/Thermo Fisher Scientific), CD19-PE (12-0193-81, eBioscience/Thermo Fisher Scientific), and CD3-Alexa Fluor 488 (100321, BioLegend). Samples were acquired on an LSRII machine (BD Biosciences), and data were analyzed using FlowJo software.

M1/M2 macrophage polarization

The M1 and M2 macrophage phenotype was determined as previously published (142). In brief, freshly isolated lungs were digested with collagenase XI (0.7 mg/ml; MilliporeSigma) and type IV bovine pancreatic DNase (30 mg/ml; MilliporeSigma) in RPMI-1640 media to obtain single-cell suspensions. Red blood cells (RBCs) were lysed in RBC Lysis Buffer (BioLegend), followed by adherence on 6-well culture plates for 2 hours. Cells were supplemented with RPMI-1640 media with 10% FBS. Supernatant was discarded, mRNA was isolated from adherent macrophages, and qPCR was performed. The following primer sets were used: TNF- α — forward, 5'-AAGCCTGTAGCCCACGTCGTA-3', reverse, 5'-GGCACCACTAGTTGGTTGTCTTTG-3'; IL-6 — forward, 5'-TCCTCTGGTCTTCTGGAGTA-3', reverse, 5'-CTTAGCCACTCCTTCTGTGA-3'; IL-12p35 — forward, 5'-TGGACCTGCCAGGTGTCTTAG-3', reverse, 5'-CAATGTGCTGGTTTGGTCCC-3'; iNOS — forward, 5'-CACCTTGGAGTTCACCCAGT-3', reverse, 5'-ACCACTCGTACTTGGGATGC-3'; IL-10 — forward, 5'-ATAACTGCACCCACTTCCCA-3', reverse, 5'-GGGCATCACTTCTACCAGGT-3'; arginase-1 — 5'-ATGGAAGAGACCTTCAGCTAC-3', reverse, 5'-GCTGTCTTCCCAAGAGTTGGG-3'; Ym1 — forward, 5'-GGGCATACCTTTATCCTGAG-3', reverse, 5'-CCACTGAAGTCATCCATGTC-3'; mannose

receptor — forward, 5'-CAAGGAAGGTTGGCATTGT-3', reverse, 5'-CCTTTCAGTCCTTTGCAAGC-3'; and GAPDH — forward, 5'-TGAGGACCAGGTTGTCTCCT-3', reverse: 5'-CCCTGTTGCTGTAGCCGTAT-3'. mRNA expression in each sample was normalized to GAPDH.

Cell culture and hypoxia exposure

Mouse lung epithelial cells (MLE12) were purchased from ATCC. The cells were maintained in DMEM (Invitrogen, Life Technologies) with 2 mM L-glutamine, supplemented with FBS (10%) and antibiotics (100 units/ml penicillin and 100 µg/ml streptomycin). MLE12 cells were plated at 70%–80% confluence in 6-well plates. Twenty-four hours later, media were changed to fresh DMEM with FBS and antibiotics, and cells were exposed to hypoxia (1.5% O₂) using an in vitro hypoxia chamber (Coy Laboratory) or normoxia (21% O₂) for an additional 24–48 hours.

HIF reporter cells

MLE12 cells were seeded at 70% confluency in 96 well plates. Signal lenti HIF reporter was obtained from Qiagen. Cells were transfected with 10 multiplicity of infection (MOI) Lenti HIF reporter in antibiotic free conditions using SureENTRY™ Transduction Reagent (Qiagen) (5ug/ml) as per the manufacturer's instructions. 24 hours after transfection, the cells were switched into medium containing 10% fetal bovine serum. Stable cells were generated using puromycin-based (10µg/ml) selection. For measurement of HIF activity after hypoxia exposure, activity of firefly luciferase (that is indicative of HIF activity) was measured as relative light units (RLU) using the Dual-Luciferase Reporter Assay System (Promega).

siRNA studies

On-Target Smartpool siGenome siRNAs were used to target ER stress pathways and HIF1 α in MLE12 cells as previously described (31). The following mouse constructs were used for siRNA targeting: IRE1 α (L-041030-00), ATF4 (L-042737-01), HIF1 α (L-040368-00), CHOP (L-062068-00), and nontarget control (D-001210-04-05) (all from Dharmacon). In brief, MLE12 cells were plated at 40%–50% confluence in 6-well plates in DMEM with FBS but no antibiotics and cultured overnight in a standard cell culture incubator. Cells were transfected with 25 nM Smartpool siRNA using Lipofectamine RNAi Max (Life Technologies) as per the manufacturer's instructions. Twenty-four hours later, the media were replaced with fresh DMEM (with FBS and antibiotics), and cells were exposed to hypoxia (1.5% O₂) or normoxia (21% O₂) for an additional 48 hours.

Small molecule-mediated inhibition of UPR pathways

For chemical inhibition of IRE1 α and PERK, MLE12 cells were plated at 70% confluence in 6-well plates in DMEM. Twenty-four hours later, media were replaced with 2 ml fresh DMEM in each well. 10 μ M PCP-101 (Mannkind Corporation) or 0.3 μ M GSK2606414 (MilliporeSigma) in DMSO was added to the treatment groups, and 2 μ l DMSO (MilliporeSigma) was added to the vehicle control groups.

Western blotting

Total protein extracts were prepared from lungs using RIPA lysis buffer with protease and phosphatase inhibitors (Life Technologies Corporation) as previously described (27, 31). The following primary antibodies were used: CHOP (1:300 dilution, SC-7351, Santa Cruz Biotechnology), PDI (1:1,000 dilution, C81H6, Cell Signaling), ATF4 (1:1,000 dilution, 10835-1-AD, Proteintech Group Inc.), XBP1s (1:1,000 dilution, 658802, BioLegend), β -actin (1:25,000

dilution, A5316, MilliporeSigma), IRE1 α (1:1,000 dilution, 14C10, Cell Signaling), ATF6 (1:500 dilution, NB1-40256SS, Novus Biologicals), and HIF1 α (1:500 dilution, NB-100-479, Novus Biologicals). Western blots were developed using corresponding fluorescent-conjugated IRDye secondary antibodies and the Odyssey Infrared Imaging System (LI-COR Biosciences). Densitometry was performed using ImageJ software (NIH), and band intensities were normalized to β -actin.

RNA isolation and quantitative PCR

Total mRNA was isolated from lung tissue or MLE12 cells using a RNeasy Mini kit (Qiagen) as per the manufacturer's instructions. Following RNA isolation, DNA digestion was performed using the DNA-free DNA Removal kit (Ambion Thermo Scientific), and cDNA was synthesized using Superscript III Reverse Transcriptase (Invitrogen) or Superscript VILO Master Mix (Invitrogen) as per the manufacturer's instructions. qPCR was performed using SYBR green PCR master mix (Applied Biosystems) as per the manufacturer's instructions. The following primer sets were used: XBP1 spliced forward 5'-GAGTCCGCAGCAGGTG-3' and XBP1 spliced reverse 5'-GTGTCAGAGTCCATGGGA-3', XBP1 unspliced forward 5'-GACTATGTGCACCTCTGCAG-3' and XBP1 unspliced reverse 5'-CTGGGAGTTCCTCCAGACTA-3', ATF4 forward 5'-GGGTTCTGTCTTCCACTCCA-3' and ATF4 reverse 5'-AAGCAGCAGAGTCAGGCTTTC-3', CHOP forward 5'-CCACCACACCTGAAAGCAGAA-3' and CHOP reverse 5'-AGGTGAAAGGCAGGGACTCA-3', HIF1 α forward 5'-TGGAGATGCTGGCTCCCTAT-3' and HIF1 α reverse 5'-TGGAGGGCTTGGAGAATTGC-3', GADD45A forward 5'-TGCGAGAACGACATCAACAT-3' and GADD45A reverse 5'-TCCCGGCAAAAACAAATAAG-3', ATF5 forward 5'-GGCTGGCTCGTAGACTATGG-3' and ATF5 reverse 5'-CCAGAGGAAGGAGAGCTGTG-3',

BNIP3L forward 5'-CCTCGTCTTCCATCCACAAT-3' and BNIP3L reverse 5'-GTCCTGCTGGTATGCATCT-3', CCN1 forward 5'-GGGTTGGAATGCAATTTTCG-3' and CCN1 reverse 5'-CAGCCCAACTGTAAACACCA-3', CTGF forward 5'-CTGCCAGTGAGTTCAAATGC-3' and CTGF reverse 5'-TCATTGTCCCCAGGACAGTTG-3', collagen-1 forward 5'-TGTGTTCCCTACTCAGCCGTCT-3' and collagen-1 reverse 5'-CATCGGTCATGCTCTCTCCAA-3', PDGF-B forward 5'-CCCACAGTGGCTTTTCATTT-3' and PDGF-B reverse 5'-GTGGAGGAGCAGACTGAAGG-3', VEGF forward 5'-CGCGAGTCTGTGTTTTTGCA-3' and VEGF reverse 5'-CAGAGCGGAGAAAGCATTGT-3', TGF β forward 5'-CAATACGTCAGACATTCGGGAAGC-3' and TGF β reverse 5'-CTGGTAGAGTTCTACGTGTTGCTC-3', and RPL19 forward 5'-ATGCCAACTCCCGTCAGCAG-3' and RPL19 reverse 5'-TCATCCTTCTCATCCAGGTCACC-3'. Expression values of XBP1s were normalized to that of XBP1us using the $2\Delta Ct$ method. Expression values of all other genes were normalized to RPL19 also using the $2\Delta Ct$ method. Evaluation of XBP1 splicing by separation of spliced and unspliced cDNA products on an agarose gel was performed as previously described. For cDNA synthesis for this evaluation, the following primers were used: XBP1 forward 5'-CTGGAAAGCAAGTGGTAGA-3' and XBP1 reverse 5'-CTGGGTCCTTCTGGGTAGAC-3'.

Mouse apoptosis PCR array

The Mouse Apoptosis RT2 Profiler PCR Array (Qiagen) was used. MLE12 cells were plated at 40%–50% confluence in 6-well plates in antibiotic-free DMEM media. Twenty-four hours later, MLE12 cells were transfected with Smartpool siRNA for CHOP or control nontargeted siRNA. Following transfection, cells were exposed to hypoxia (1.5% O₂) or normoxia (21% O₂)

for an additional 48 hours. After mRNA isolation, cDNA was synthesized using the RT2 First Strand Kit (Qiagen) and qPCR was performed using RT2 qPCR master mixes (Qiagen).

Isolation of EpCAM⁺ cells

Lungs were enzymatically digested using Dispase II (MilliporeSigma) for 45 minutes at 37°C and passed through 100- μ M and 40- μ M SwiftStrain Cell Strainers (Denville), followed by the 20- μ M Steriflip vacuum filter (EMD Millipore) to obtain single-cell suspensions. The single-cell suspension was then coated with mouse CD45 microbeads as per the manufacturer's instructions (Macs Miltenyi Biotech). CD45⁺ cells were depleted by passing the CD45-coated single-cell suspension through LD columns on a QuadroMACS Separator (Macs Miltenyi Biotech) as per the manufacturer's instructions. The flow through containing CD45⁻ cells was then coated with mouse EpCAM microbeads as per the manufacturer's instructions (Macs Miltenyi Biotech). EpCAM⁺ cells were collected by passing EpCAM-coated single-cell suspension through LS columns on a QuadroMACS Separator as per the manufacturer's instructions.

RNA-sequencing

Total RNA was isolated from EpCAM⁺ cells using Direct-Zol RNA MiniPrep (Zymo Research), followed by DNA Digestion (Ambion, Invitrogen). The quality check of the RNA, mRNA enrichment, and cDNA library preparation utilizing stranded mRNA (polyA selected) were conducted at Vanderbilt Technologies for Advanced Genomics. RNA sequencing was performed on an Illumina NovaSeq6000 system with a paired-end mRNA library prep, PE-150, with 30 million reads. Initial alignment and quantification were performed using the Partek Flow package. STAR 2.5.3a was used to align RNA-sequencing reads, with quantification performed by Ensembl Transcripts Release 83 using Partek E/M. Reads were normalized to total count. Differentially expressed genes were determined based on >2-fold change (\log_2 ratio > 1) between groups, with

$P < 0.05$ and $FDR < 0.05$. Annotation of overrepresented pathways was done using WebGestalt (WEB-based Gene SeT AnaLysis Toolkit).

Statistics

Statistical analyses were performed using GraphPad Prism Software. Data are presented as mean \pm SEM. Survival data were assessed using a Kaplan-Meier survival analysis. Pairwise comparisons were made using 2-tailed, unpaired Student's t test. Comparisons between groups were made by 1-way ANOVA, followed by Tukey's post hoc test. P values of less than 0.05 were considered significant.

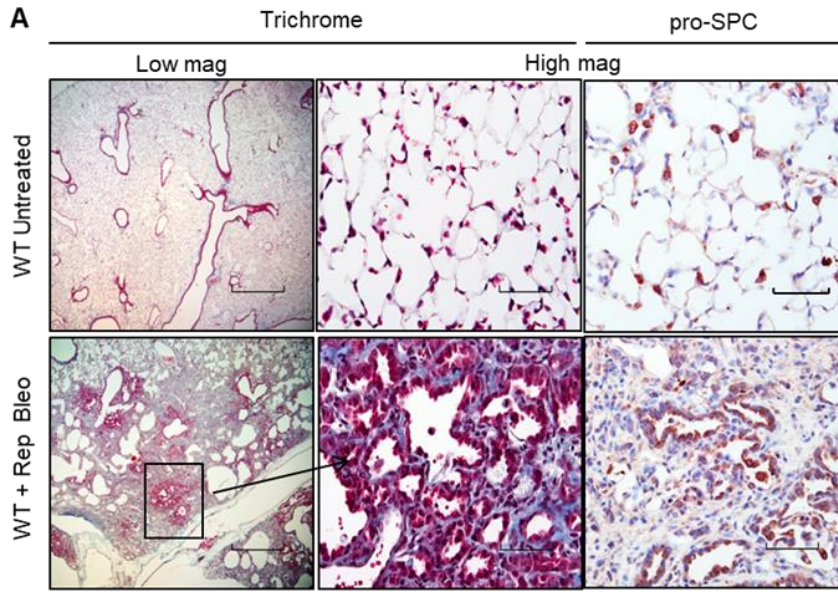
Study approval

Tissue collection and studies were approved by the Vanderbilt University Institutional Review Board (060165). All experimental protocols were approved by the Animal Care and Utilization Institutional Committee at Vanderbilt University Medical Center.

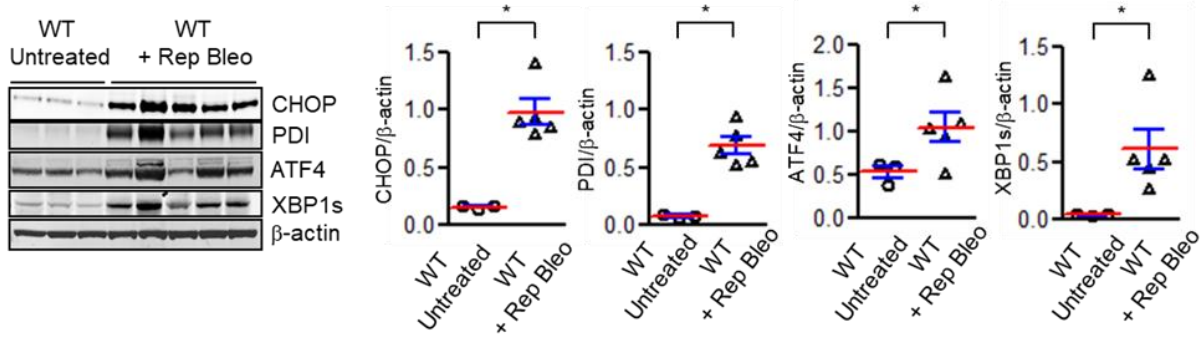
III. HYPOXIA WORSENS LUNG FIBROSIS THROUGH EXPRESSION OF ER STRESS EFFECTOR C/EBP HOMOLOGOUS PROTEIN (CHOP)

CHOP regulates epithelial cell survival and mediates lung fibrosis in the presence of ER stress

We investigated the mechanisms by which ER stress contributes to pulmonary fibrosis using a repetitive intratracheal (i.t.) bleomycin injury model; we have previously demonstrated that this model recapitulates important features of human IPF, including hyperplastic AECs and persistent fibrosis (135). In this model, we treated 8 to 10 week old male and female WT mice (C57BL/6J background) with 6 doses of bleomycin (0.04 units) delivered by direct i.t. instillation at 2-week intervals. Mice were euthanized and lungs were harvested 2 weeks after the final bleomycin instillation. Consistent with previous findings (135), we observed distinct areas of parenchymal fibrosis with type II AEC hyperplasia (**Figure 9A**). Markers of ER stress were markedly upregulated, as shown by western blotting of lung lysates, including CHOP, protein disulphide isomerase (PDI), activating transcription factor 4 (ATF4), and spliced X-box binding protein 1 (XBP1s) (**Figure 9B**). By IHC, we found that CHOP expression was localized primarily to type II AECs in areas of fibrosis (**Figure 9C**).



B



C

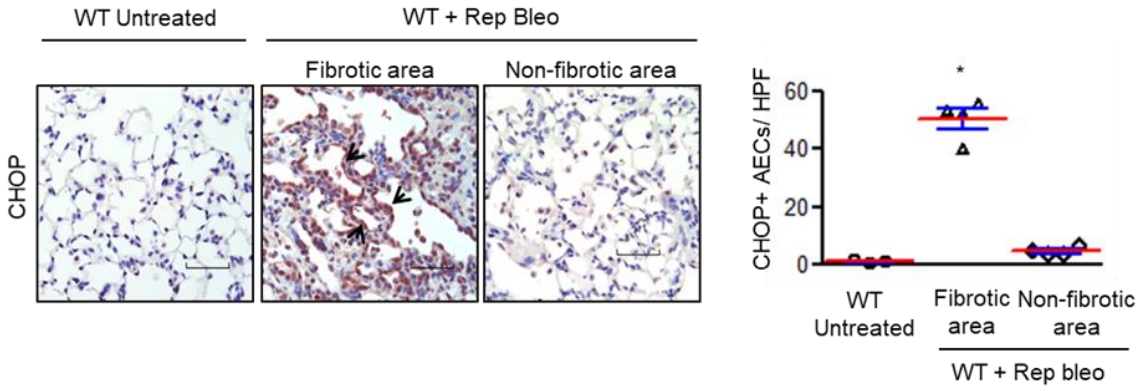


Figure 9. Repetitive bleomycin treatment results in ER stress and lung fibrosis. (A) Representative Masson's trichrome stained lung sections and immunostaining for pro-surfactant protein C (pro-SPC) showing areas of fibrosis and hyperplastic type II alveolar epithelial cells (AECs) following intratracheal (IT) injection of bleomycin (0.04 units) every 2 weeks for 6 doses (Rep Bleo) compared to untreated controls. Scale bars - low mag: 800 μ m, high mag: 60 μ m. (B) Western blots and densitometry for CHOP, PDI, ATF4, and XBP1s from lung tissue lysates (left panel) and densitometry (right panel). β -actin was used as a loading control. Comparisons between groups were made using unpaired, two-tailed Student's t-test. $*=p<0.05$ compared to untreated WT. (C) Representative immunostaining for CHOP (arrows indicate CHOP staining) and quantification of CHOP positive AECs per high power field (HPF) on lung sections. $*=p<0.05$ compared to other groups by one way ANOVA with Tukey's post-hoc test.

Next, we performed experiments using repetitive i.t. bleomycin in CHOP-deficient (CHOP^{-/-}) mice to determine whether CHOP is an important profibrotic mediator in this model (Figure 10, A-E). In these studies, we observed significant protection of CHOP^{-/-} mice from development of lung fibrosis, with a marked reduction in fibrotic area, reduced soluble collagen content, and decreased fibronectin level by ELISA (Figure 10, A-D). Since AEC apoptosis is an important antecedent of bleomycin-induced fibrosis, we quantified apoptotic AECs by colocalization of pro-SPC and TUNEL staining. We found that the number of TUNEL⁺ AECs was significantly lower in repetitive bleomycin-treated CHOP^{-/-} mice compared with WT controls (Figure 10E). Together, these studies suggest that CHOP deficiency protects from lung fibrosis following repetitive bleomycin by reducing AEC apoptosis. To more directly test the role of CHOP in AECs, we investigated whether selective induction of ER stress in type II AECs affects lung fibrosis via CHOP induction. For these studies, we utilized a doxycycline-inducible transgenic model in which expression of a mutant form of human SFTPC (L188Q SFTPC) is limited to type II AECs (99), resulting in ER stress and enhanced fibrotic susceptibility (99). After crossing CHOP^{-/-} mice into this model to generate L188Q SFTPC/CHOP^{-/-} mice, we treated these mice with doxycycline in drinking water (2 g/l) for 1 week and then administered a single i.t. injection

of bleomycin (0.08 units). At 3 weeks after bleomycin instillation, L188Q SFTPC mice had increased lung fibrosis compared with WT controls, but CHOP deficiency (L188Q SFTPC/CHOP^{-/-} mice) reduced fibrosis to WT levels (**Figure 10, F and G**). Notably, no difference in fibrosis was observed between WT and CHOP^{-/-} mice used as controls in these experiments. Single-dose i.t. bleomycin did not induce robust CHOP upregulation in WT mice, potentially explaining why CHOP deletion was not protective in this model (**Figure 10 and 11**). Collectively, these studies in two different fibrosis models indicate that CHOP is a key mediator of lung fibrosis when expressed in AECs.

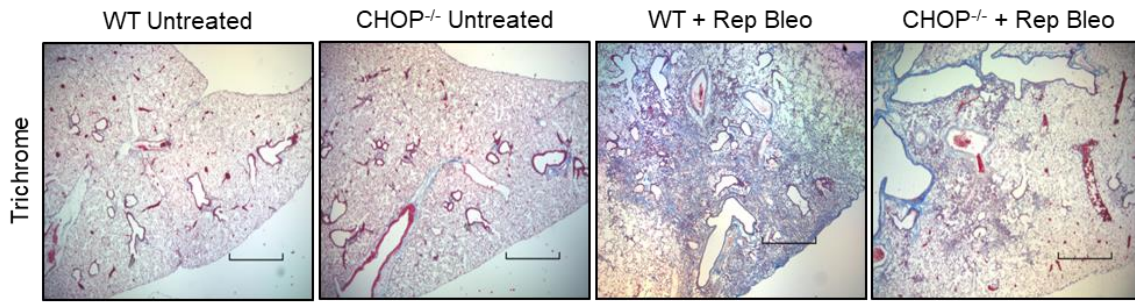
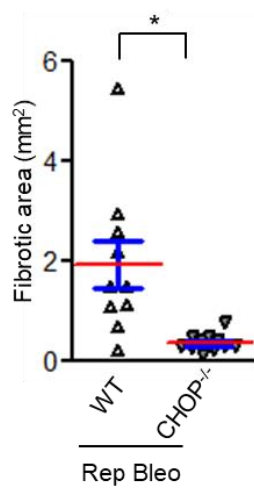
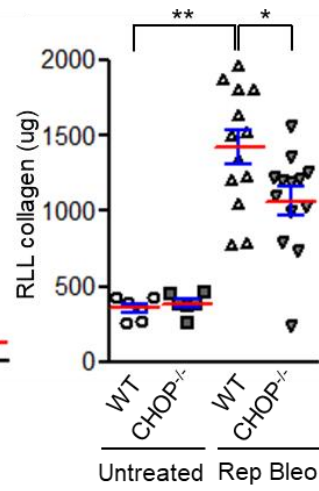
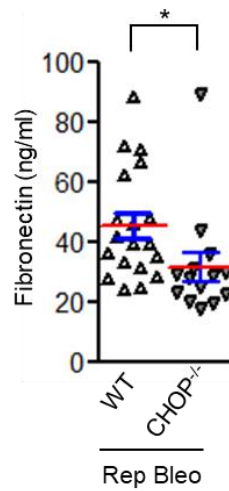
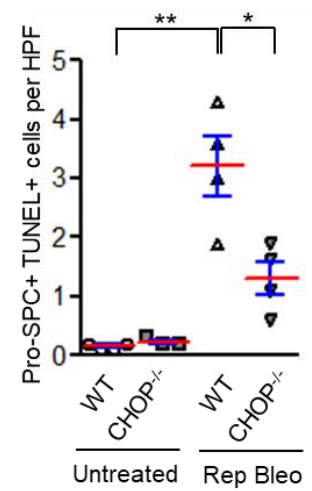
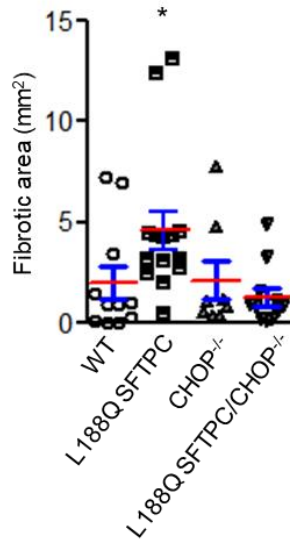
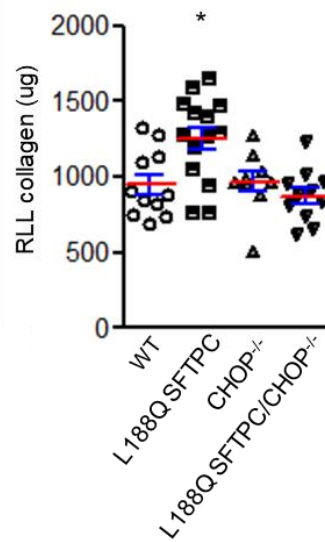
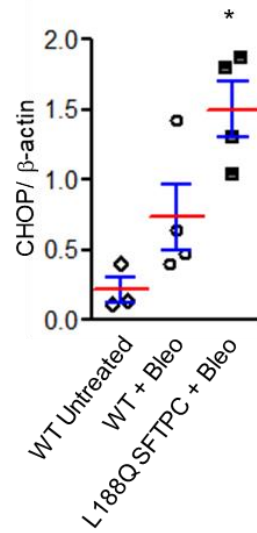
A**B****C****D****E****F****G****H**

Figure 10. CHOP mediates the effects of ER stress on epithelial cell apoptosis and lung fibrosis. (A-E) WT and CHOP^{-/-} mice were studied using the repetitive bleomycin model (Rep Bleo) and lungs were harvested 2 weeks after the last dose. (A) Representative Masson's trichrome stained lung sections. Scale bars: 800 μm. (B) Evaluation of fibrosis by morphometry. (C) Quantification of total soluble collagen in right lower lobe (RLL) by sircol assay. (D) Fibronectin measurement by ELISA. (E) Quantification of dual immunofluorescence for pro-SPC positive and TUNEL positive cells per high power field (HPF) on lung sections. Comparisons between groups were made using unpaired, two-tailed Student's t-test (B and D) or one way ANOVA with Tukey's post-hoc test (C and E). *= $p < 0.05$ compared to WT + rep bleo, **= $p < 0.05$ compared to untreated WT. (F-H) Inducible transgenic mice expressing L188Q mutant surfactant protein C (L188Q SFTPC), CHOP^{-/-} mice, L188Q SFTPC/CHOP^{-/-} mice, and WT mice were treated with doxycycline (2 g/l) for 1 week followed by intratracheal injection of bleomycin (0.08 units) and lungs were harvested 3 weeks post-bleomycin. (F) Morphometric evaluation of fibrosis. (G) Total soluble collagen in right lower lobe (RLL) by sircol assay. (H) Densitometry on western blot for CHOP from lung tissue lysates. β-actin was used for normalization. *= $p < 0.05$ compared to other groups by one way ANOVA with Tukey's post-hoc test (F-H).

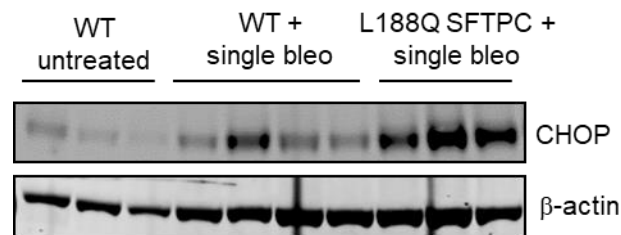


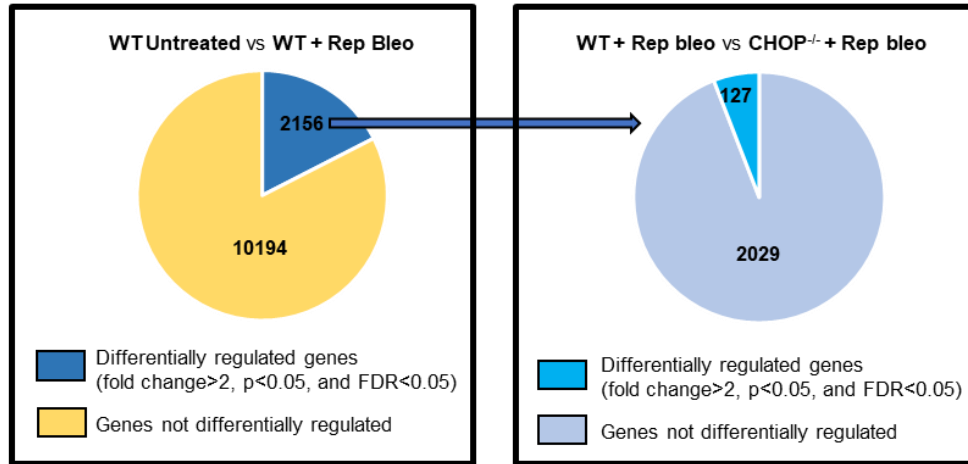
Figure 11. CHOP levels in inducible transgenic mice expressing L188Q surfactant protein C (L188Q SFTPC) treated with bleomycin compared to wild type mice. L188Q SFTPC and WT controls were treated with doxycycline (2 g/l) for 1 week followed by intratracheal injection of bleomycin (0.08 units) and lungs were harvested 3 weeks later. Untreated WT mice were used as an additional control. Western blot for CHOP from lung tissue lysates is shown along with β-actin as loading control.

CHOP regulates epithelial cell responses and inflammation following repetitive bleomycin treatment

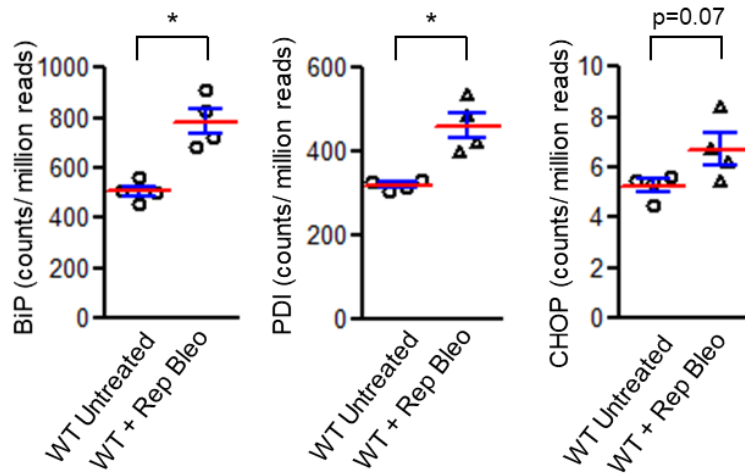
To evaluate the effect of CHOP on potential profibrotic pathways, we analyzed gene expression by RNA sequencing of EpCAM⁺ (EpCAM is also known as CD326) cells isolated from lungs of WT and CHOP^{-/-} mice following repetitive bleomycin treatment (**Figure 12**). Compared with that in lung epithelial cells from untreated WT mice, 2,156 genes were

differentially expressed (fold change > 2, P < 0.05, FDR < 0.05), including some ER stress genes, in repetitive bleomycin-treated WT mice (**Figure 12, A and B**). From among this set of differentially expressed genes, 127 genes were differentially expressed in epithelial cells from WT and CHOP^{-/-} mice following repetitive bleomycin (**Figure 12A**). By gene ontology analysis, 46 of these gene products were grouped into the following 4 categories: (a) cellular response to growth factor stimulus, (b) epithelial cell differentiation, (c) epithelium development, and (d) cell migration (**Figure 12C**), thereby suggesting several profibrotic pathways in the epithelial compartment that could be regulated by CHOP. We also investigated whether CHOP regulates inflammatory cell recruitment or function. We compared the inflammatory response in CHOP^{-/-} mice with that of WT controls following repetitive bleomycin treatment. As shown in **Figure 13**, significant differences were not detected in numbers of immune/inflammatory cells in the lungs of WT and CHOP^{-/-} mice (alveolar macrophages, interstitial macrophages, B or T lymphocytes), with the exception of neutrophils and dendritic cells, which were reduced in the lungs of CHOP^{-/-} mice.

A



B



C

Differentially regulated GO pathways in 'CHOP ^{-/-} + Rep Bleo' compared to 'WT + Rep Bleo' that are relevant to fibrosis	
Pathways	Genes
Cellular response to growth factor stimulus	Mmrn2, Ltbp4, Acvr1, Bmp6, Cdh5, Cldn5, Dll1, Edn1, Eng, Flt1, Fzd4, Ltbp1, Postn, Pde3a, Fgfbp3, Adgra2
Epithelial Cell Differentiation	Acvr1, Bmp6, Cd34, Cdh5, Cldn5, Dll1, S1pr1, Eng, Notch4, Rbpj, Sox17, Sox18, Ppp1r16b, Podxl
Epithelium Development	Acvr1, Aqp1, Cd34, Cdh5, Cldn5, S1pr1, Edn1, Eng, Flt1, Gja4, Notch4, Podxl, Sem3c, Sox17, Sox18, Ppp1r16b, Dact2, Podxl, Shank3, Bmp6
Cell Migration	Mmrn2, Arap3, Acvr1, Aqp1, S1pr1, Edn1, Eng, Flt1, Gata2, Kit, Plat, Sem3c, Sox18, Nav1, Tie1, Sem3g, Gpm6a, Pkn3, Podxl, Cxcl3, Egfl7, Postn, Adgra2, Plvap, Sem7a, Sox17

Figure 12. Gene expression profiling of EpCAM positive epithelial cells isolated from wild type and CHOP deficient mice in the repetitive bleomycin model. WT and CHOP^{-/-} mice were intratracheally injected with 6 doses of bleomycin (0.04 units) at intervals of 2 weeks and lungs were harvested 2 weeks after the last dose. EpCAM positive epithelial cells were isolated from the lungs of bleomycin-treated (Rep Bleo) mice and control (untreated) WT mice. Total RNA was extracted from the isolated EpCAM positive cells and used for RNA-sequencing. n=3-4 mice in each group. **(A)** Pie-charts showing differentially regulated genes (fold change>2, p value<0.05, and FDR<0.05) between groups. The subset of genes differentially regulated between the WT + Rep Bleo group and WT Untreated group was examined in epithelial cells from the CHOP^{-/-} + Rep Bleo group. **(B)** Plots showing expression of representative ER stress genes. Comparisons between groups were made using unpaired, two-tailed Student's t-test. *p<0.05 compared to WT Untreated. **(C)** Differentially regulated GO pathways in CHOP^{-/-} + Rep Bleo compared to WT + Rep Bleo.

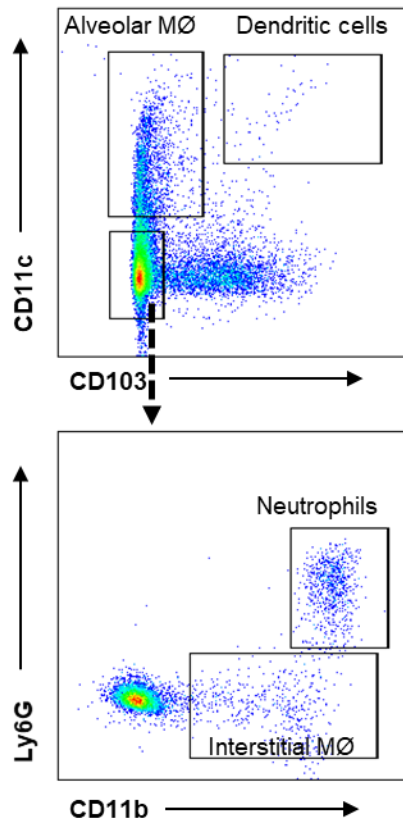
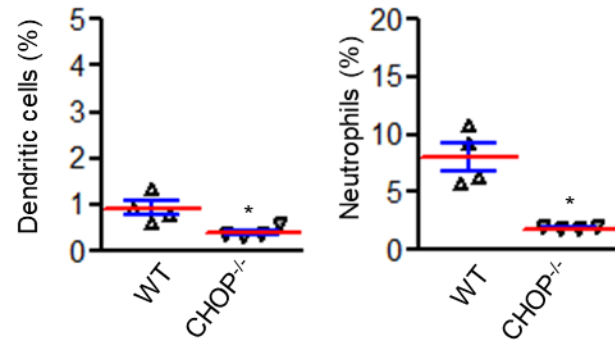
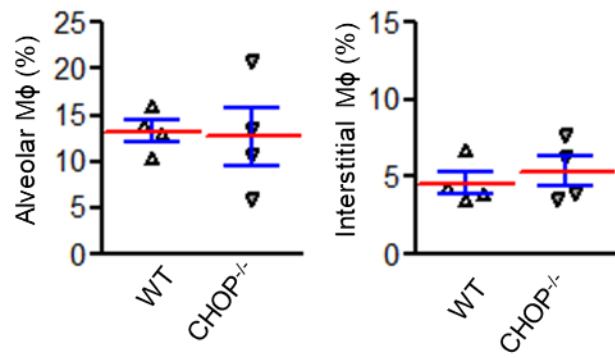
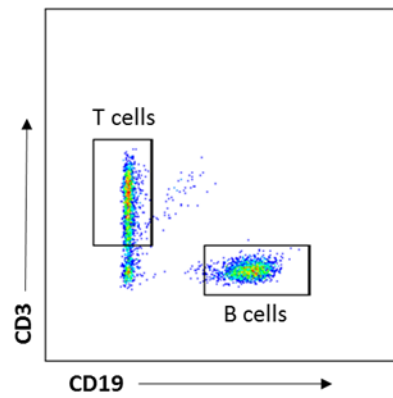
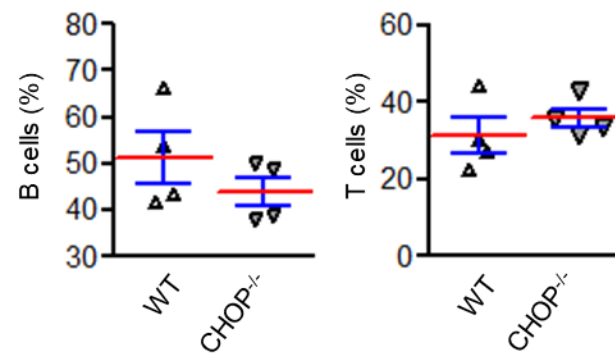
A**B****C****D**

Figure 13. Immune/inflammatory cells identified in lungs of wild type and CHOP deficient mice following repetitive bleomycin treatment. Mice were intratracheally injected with 6 doses of bleomycin (0.04 units) at intervals of 2 weeks and lungs were harvested 2 weeks after the last dose for flow cytometry analysis. **(A-B)** Gating strategy and quantification of myeloid cell subsets obtained from single cell suspensions of lung tissue. Viable (DAPI-) CD45+ cells were gated and percentages of alveolar macrophages (CD103-CD11c+), interstitial macrophages (CD103-CD11c-CD11b+Ly6G-), dendritic cells (CD103+CD11c+), and neutrophils (CD103-CD11c-Ly6G+CD11b+) were determined. **(C-D)** Gating strategy and quantitation of lymphocytes. Viable (DAPI-) CD45+ cells were gated and percentages of B cells (CD19+) and T cells (CD3+) were determined. Comparison between groups was made using unpaired, two-tailed Student's t-test. *= $p < 0.05$ compared to WT.

Repetitive bleomycin injury results in localized tissue hypoxia

Although a variety of factors can affect protein processing in the ER, the mechanism by which repetitive lung injury causes ER stress is unknown. Since hypoxia has been shown to cause ER stress in vitro (143), we postulated that localized areas of hypoxia in lung parenchyma could induce ER stress during repetitive cycles of lung injury and repair. To evaluate this possibility, we utilized pimonidazole as a chemical marker of cellular hypoxia (144) delivered by i.p. injection (60 $\mu\text{g/g}$) 3 hours prior to euthanasia in the repetitive bleomycin model. We then harvested lungs and performed IHC for pimonidazole adducts. Strong immunostaining was observed in areas of fibrosis, while minimal pimonidazole staining was identified in lungs of control (non bleomycin-treated) mice and in nonfibrotic areas of lungs of mice treated with repetitive bleomycin (**Figure 14A**). Using dual immunofluorescence for pimonidazole adducts and the type II AEC marker pro-SPC, we found that pimonidazole staining colocalized in this cell population. Quantification of dual immunofluorescence revealed that $65.3\% \pm 1.2\%$ of pro-SPC+ cells were also positive for pimonidazole staining in areas of fibrosis, whereas almost none of the pro-SPC+ cells in control (non bleomycin-treated) mice stained for pimonidazole (**Figure 14, B and C**).

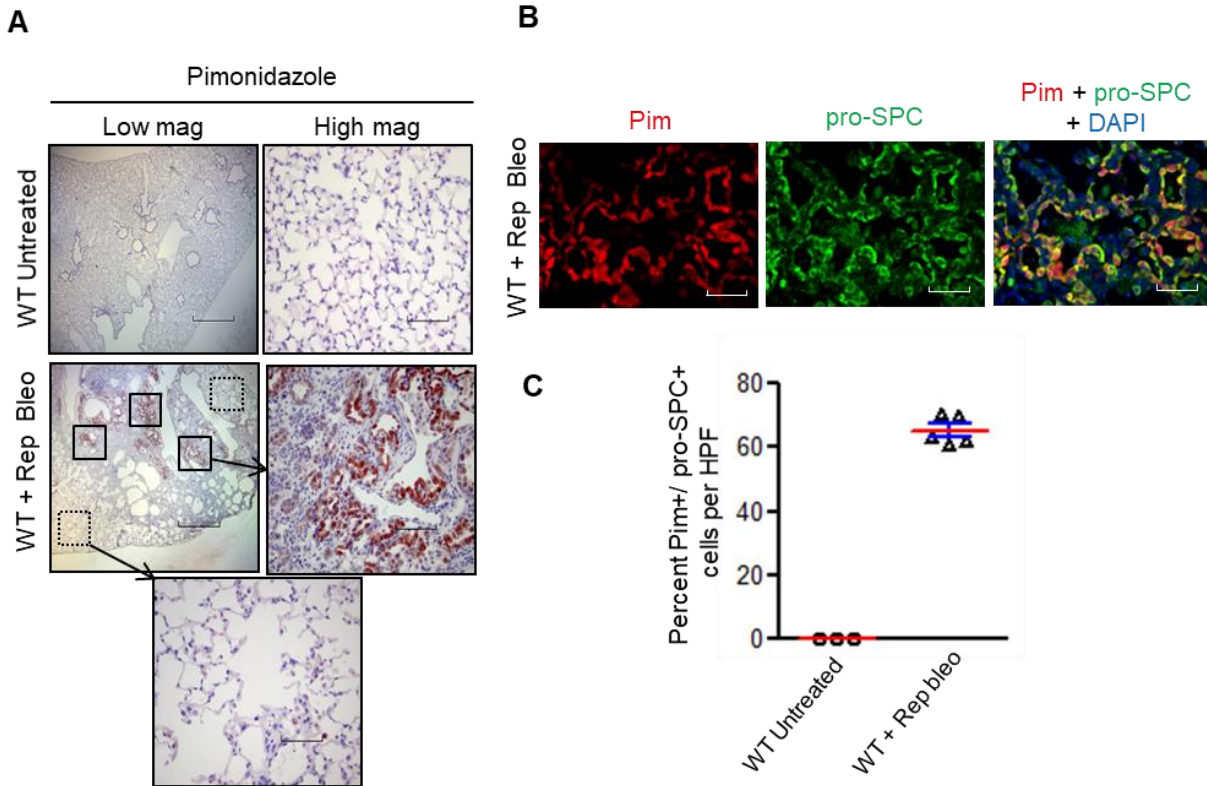


Figure 14. Repetitive bleomycin treatment results in cellular hypoxia localized to type II AECs. (A) Intraperitoneal injection of pimonidazole (60 $\mu\text{g/g}$) was performed 3 hours before euthanasia in mice treated with repetitive intratracheal bleomycin, followed by immunostaining for pimonidazole adducts on lung sections. Scale bars - low mag: 800 μm , high mag: 80 μm . (B) Dual immunofluorescence for pimonidazole adducts (red) and pro-SPC for type II AECs (green). Nuclei were counterstained with DAPI (blue). White arrows point to cells with co-localization (yellow). Scale bar: 80 μm . (C) Quantification of the percentage of pro-SPC positive cells which were also positive for pimonidazole per high power field (HPF).

We also performed dual immunofluorescence for pimonidazole adducts and markers of type I AECs, fibroblasts, endothelial cells, and macrophages and found minimal colocalization in all of these cell types (**Figure 15**). Based on these data, we concluded that repetitive bleomycin injury results in localized hypoxia in lung parenchyma that is primarily detectable in type II AECs.

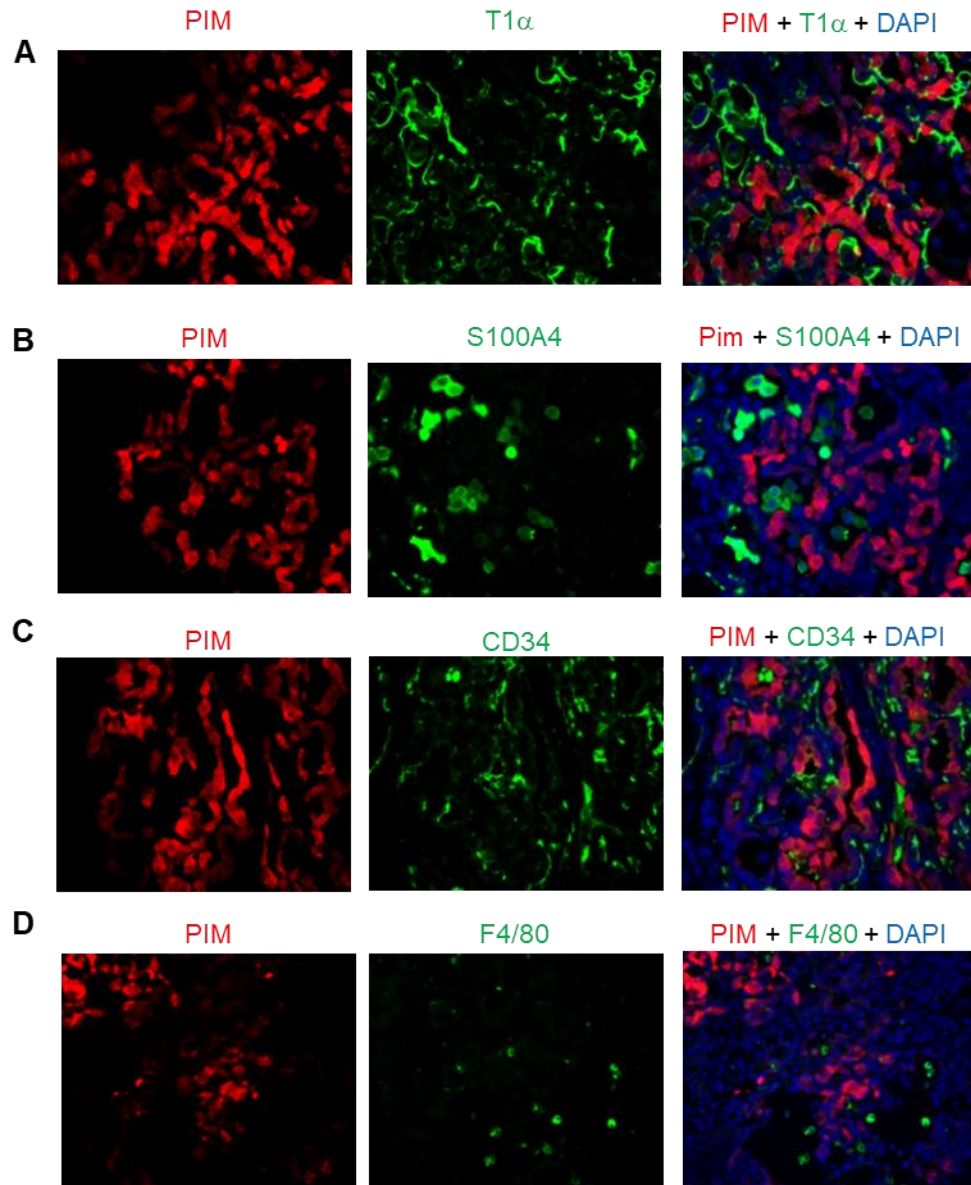


Figure 15. Dual immunofluorescence between pimonidazole and markers of type I AECs, fibroblasts, endothelial cells, or macrophages in the repetitive dose bleomycin model. (A-D) Dual immunofluorescence for pimonidazole (red) and markers for type I AECs (T1 α), fibroblasts (S100A4), endothelial cells (CD34), or macrophages (F4/80) (all green) was performed on lung sections of mice treated in the repetitive bleomycin model. Nuclei were counterstained with DAPI (blue).

Exposure to hypoxia following bleomycin injury increases ER stress and worsens lung fibrosis

Since our studies suggested that cellular hypoxia could cause ER stress and promote CHOP expression in type II AECs, we sought to develop a model to test this idea. We reasoned that exposure of bleomycin-treated mice to normobaric hypoxia could exacerbate local hypoxia in the lungs and worsen fibrosis. Therefore, we treated mice with a single dose of i.t. bleomycin (0.04 units) and then exposed mice to hypoxia from day 7 to day 21 after bleomycin (**Figure 16**). As shown in **Figure 16B**, 10% O₂ was uniformly lethal and 12% O₂ resulted in 50% mortality by day 21; however, 14% O₂ was relatively well tolerated (10% mortality). To determine whether exposure to 14% O₂ was sufficient to exacerbate cellular hypoxia in the lungs, we injected pimonidazole and performed IHC on lung sections obtained at day 21 after bleomycin treatment (14 days of hypoxia). While no pimonidazole staining was observed in unchallenged mice exposed to 14% O₂ and minimal staining was detected in bleomycin-challenged mice maintained in normoxia, there was robust pimonidazole staining in areas of bleomycin-induced fibrosis in mice exposed to 14% O₂ (**Figure 16C**). As in the repetitive bleomycin model, pimonidazole staining strongly colocalized with pro-SPC⁺ type II AECs (**Figure 17, A and B**), while S100A4⁺ fibroblasts, T1α⁺ type I AECs, CD34⁺ endothelial cells, and F4/80⁺ macrophages did not have detectable colocalization with pimonidazole adducts (**Figure 17, C–F**). With evidence that exposure to 14% O₂ following bleomycin injury was associated with cellular hypoxia in AECs, we evaluated ER stress markers and found that CHOP, PDI, ATF4, and XBP1s were upregulated in lung tissue from mice treated with bleomycin followed by 14% O₂ (**Figure 16D**). By quantification of IHC, we found a marked induction of CHOP in AECs in lungs of mice treated with bleomycin followed by 14% O₂ (**Figure 16, C and E**).

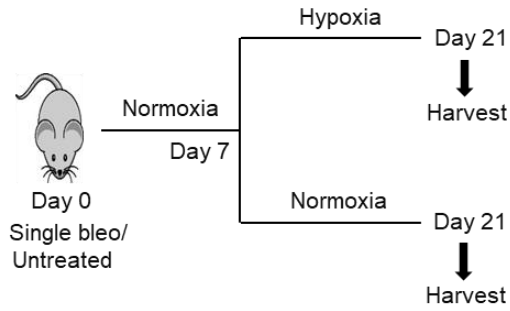
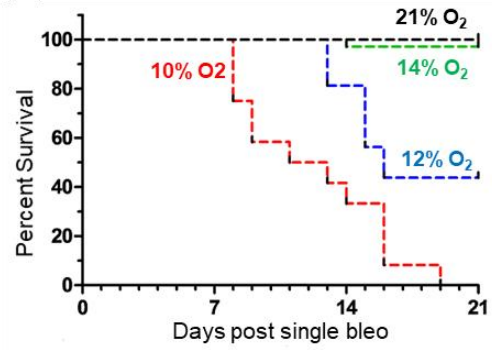
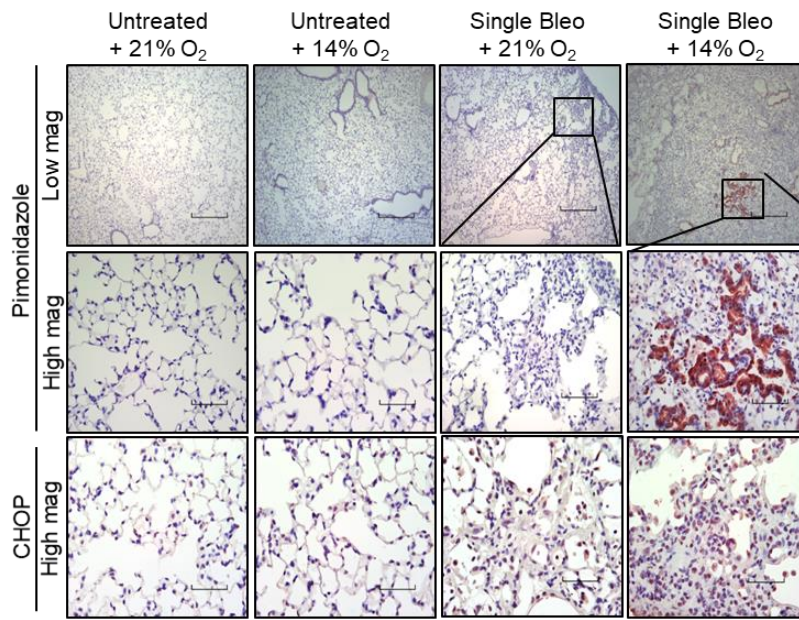
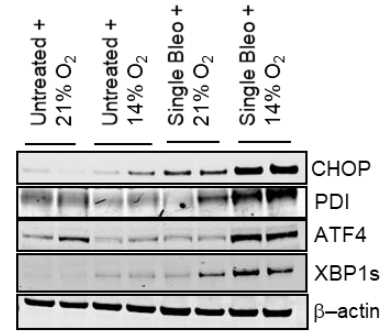
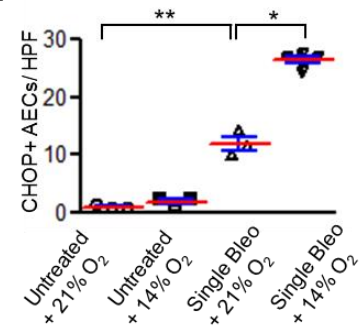
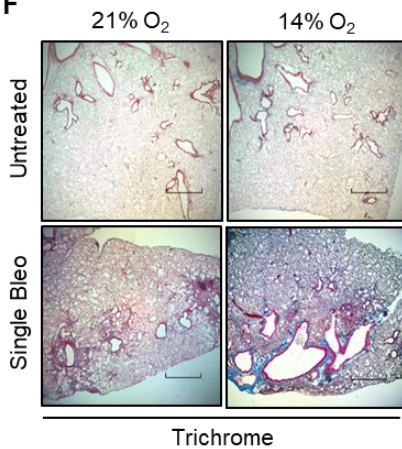
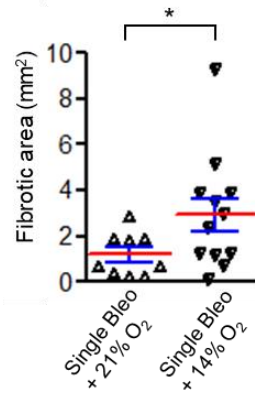
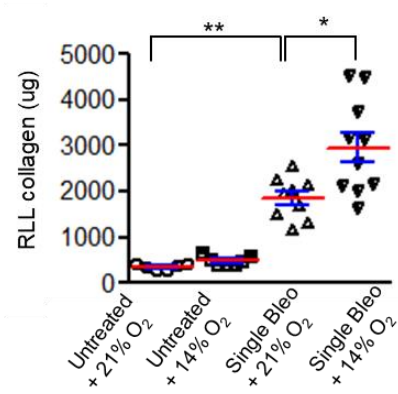
A**B****C****D****E****F****G****H**

Figure 16. Exposure to hypoxia following bleomycin treatment increases ER stress and worsens lung fibrosis. (A) Schematic representation of experimental design in which a single dose of bleomycin (0.04 units) was injected intratracheally followed 7 days later by exposure to normobaric hypoxia or normoxia (21% O₂) for an additional 14 days. (B) Kaplan-Meier survival plot for mice treated with bleomycin and exposed to 21%, 14%, 12%, or 10% O₂. n = 48 (in 21% O₂), 35 (in 14% O₂), 16 (in 12% O₂), and 12 (in 10% O₂). (C) Representative immunostaining for CHOP expression and pimonidazole adducts in mice injected with pimonidazole (60 µg/g) at 3 hours before lung harvest. Mice were treated with bleomycin followed 7 days later by exposure to 14% O₂ for an additional 14 days or maintained in 21% O₂. Additional controls were only exposed to 14% O₂ for 2 weeks or were maintained in 21% O₂. Scale bars - low mag: 800 µm, high mag: 60 µm. (D) Western blots for ER stress markers CHOP, PDI, ATF4, and XBP1s in lung tissue lysates. β-actin was used as a loading control. (E) Quantification of CHOP positive AECs per high power field (HPF) on lung sections. (F) Masson's trichrome staining and (G) Morphometric evaluation of lung fibrosis. (H) Total soluble collagen in right lower lobe (RLL) by sircol assay. Comparisons between groups were made using unpaired, two-tailed Student's t-test (G) or one way ANOVA with Tukey's post-hoc test (E and H). *= $p < 0.05$ compared to single bleo + 21% O₂, **= $p < 0.05$ compared to untreated + 21% O₂.

Consistent with our findings in other fibrosis models characterized by robust induction of ER stress, mice treated with bleomycin followed by 14% O₂ had a marked exacerbation of fibrosis compared with bleomycin-treated mice maintained in normoxia (**Figure 16, F–H**).

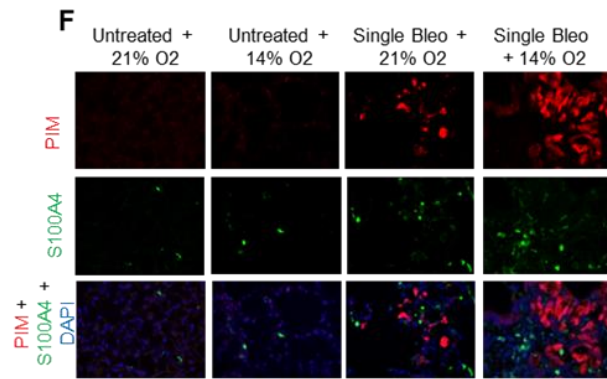
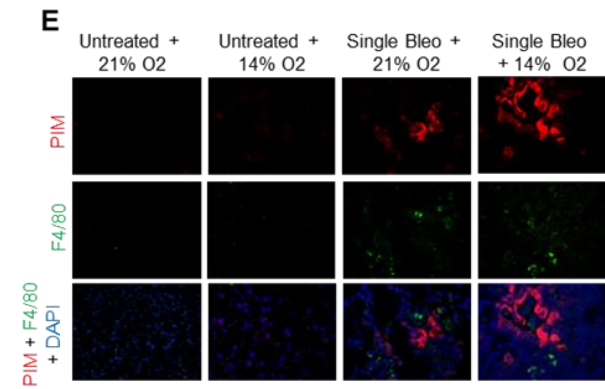
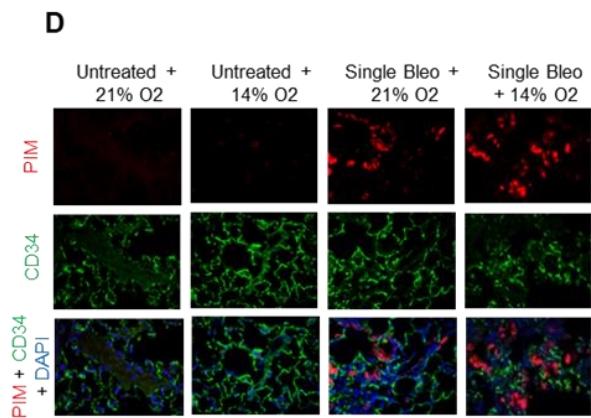
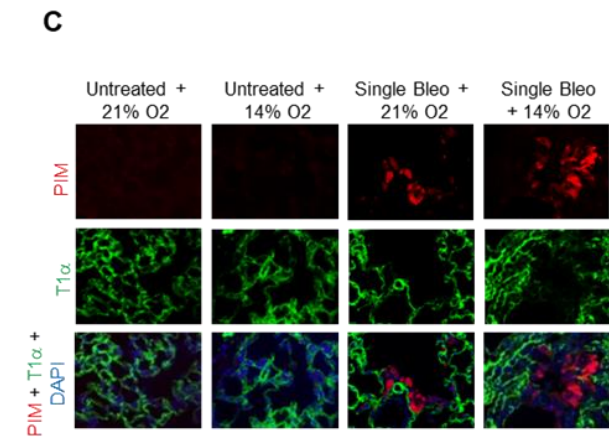
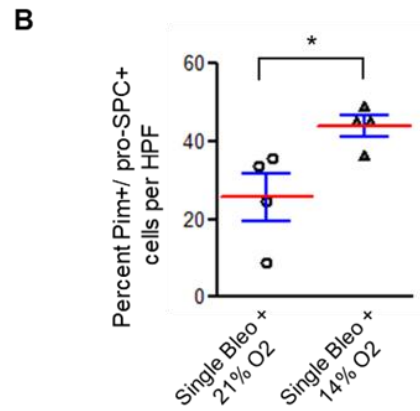
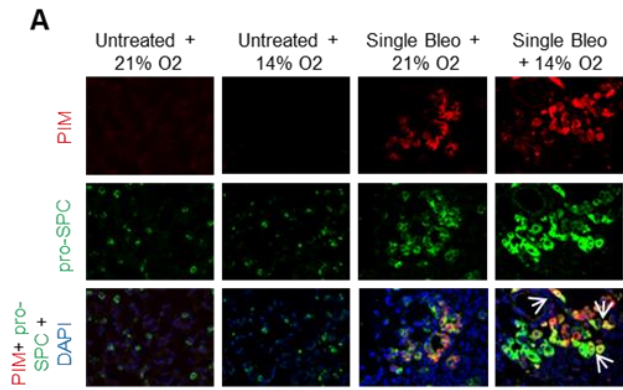


Figure 17. Dual immunofluorescence between pimonidazole and markers of different cell types in lungs of mice treated with bleomycin followed by exposure to hypoxia (14% O₂). Dual immunofluorescence (IF) for pimonidazole (red) and cell specific markers (green) was performed in lungs of mice treated with intratracheal bleomycin (0.04 units) followed 7 days later by exposure to 14% O₂ for an additional 14 days or maintained in 21% O₂. Additional controls were only exposed to 14% O₂ for 2 weeks or were maintained in 21% O₂. **(A)** Dual IF is shown for type II AECs (pro-SPC). Nuclei were counterstained with DAPI (blue). White arrows point to cells with co-localization (yellow) of pimonidazole (red) and pro-SPC (green). **(B)** Quantification of the percentage of pro-SPC positive cells which were also positive for pimonidazole per high power field (HPF). Comparison between groups was made using unpaired, two-tailed Student's t-test. *= $p < 0.05$ compared to single bleo + 21% O₂. Dual IF is also shown for **(C)** type I AECs (T1 α), **(D)** endothelial cells (CD34), **(E)** macrophages (F4/80), and **(F)** fibroblasts (S100A4). Nuclei were counterstained with DAPI (blue).

CHOP^{-/-} mice are protected from exaggerated lung fibrosis induced by exposure to hypoxia

To test whether CHOP mediates the excess lung fibrosis resulting from exposure to hypoxia following bleomycin treatment, we treated WT and CHOP^{-/-} mice with a single i.t. injection of bleomycin (0.04 units) followed by randomization to normoxia (21% O₂) or hypoxia (14% O₂) between day 7 and day 21 after bleomycin. As shown in **Figure 18, A–C**, the hypoxia-induced exacerbation of lung fibrosis was completely abrogated in CHOP^{-/-} mice. CHOP deficiency had no detectable effects in mice treated with single-dose bleomycin and maintained in normoxia. Since AEC apoptosis following single-dose bleomycin is most prominent within the first 2 weeks after treatment (145), we tested whether exposure of bleomycin-treated mice to 14% O₂ for 3 days (between day 7–10 after bleomycin) exacerbates AEC apoptosis and if this effect is mediated by CHOP. In lungs harvested at 10 days after bleomycin, quantification of pro-SPC and TUNEL dual-positive cells showed that AEC apoptosis was increased in WT mice exposed to hypoxia compared with WT mice maintained in normoxia and that this increase was mitigated in lungs of CHOP^{-/-} mice (**Figure 18D**).

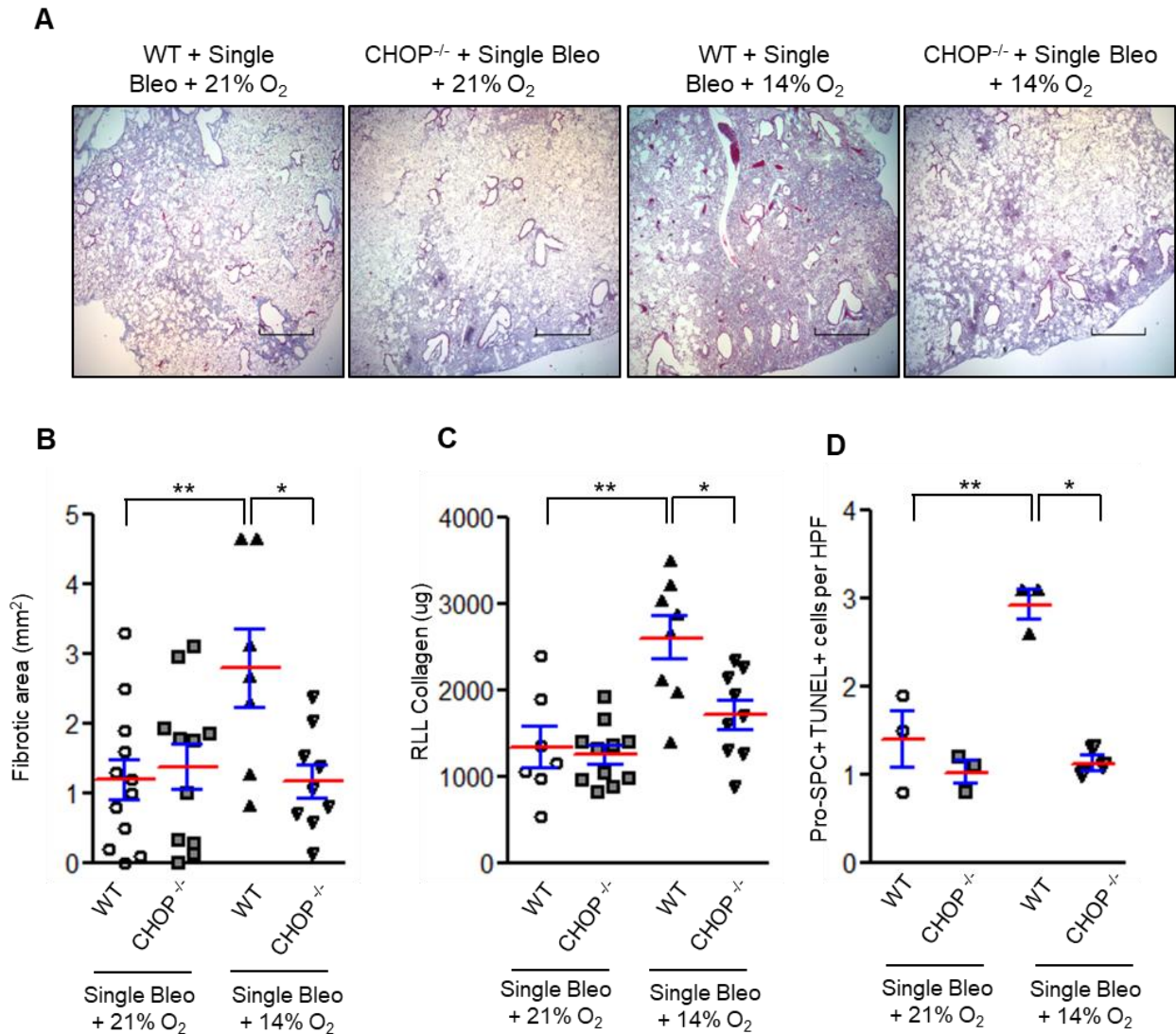


Figure 18. CHOP deficient mice are protected from exaggerated lung fibrosis induced by exposure to hypoxia. (A-D) WT and CHOP^{-/-} mice received an intratracheal injection of bleomycin (0.04 units) followed 7 days later by exposure to 14% O₂ or 21% O₂. (A) Representative Masson's trichrome staining (Scale bars: 800 μ m) and (B) Morphometric evaluation of lung fibrosis at 21 days after bleomycin injection. (C) Total soluble collagen in right lower lobe (RLL) by sircol assay. (D) Quantification of dual immunofluorescence for pro-SPC positive and TUNEL positive cells per high power field (HPF) on sections from lungs harvested 3 days after randomization to 21% O₂ or 14% O₂ (10 days after bleomycin injection).

We also examined whether CHOP^{-/-} mice had differences in lung immune/inflammatory cell populations in the bleomycin followed by hypoxia model. At 21 days after bleomycin treatment, we found no differences in myeloid cell subsets (**Figure 19A**) or lymphocytes (**Figure 19B**) between CHOP^{-/-} and WT mice exposed to 14% O₂ or maintained in normoxia. Since M2 macrophage polarization has been associated with lung fibrosis (146-148), we also isolated lung macrophages and examined whether CHOP deficiency alters macrophage polarization; however, no M1/M2 phenotype shift was observed in CHOP^{-/-} mice following bleomycin treatment in either the normoxia or hypoxia groups (**Figure 19C**).

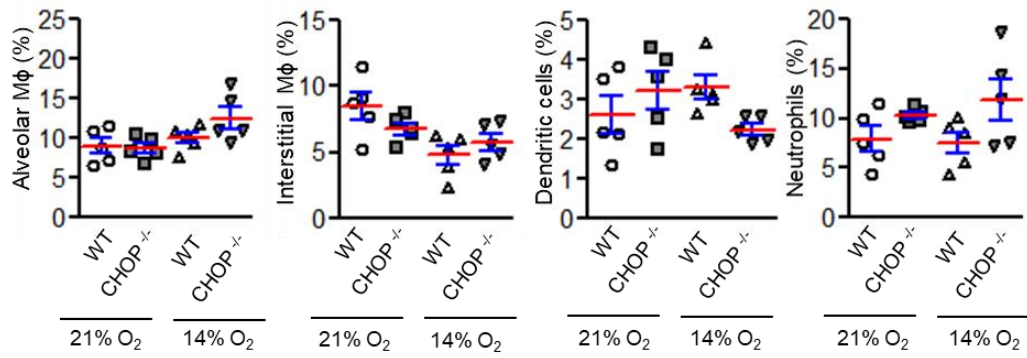
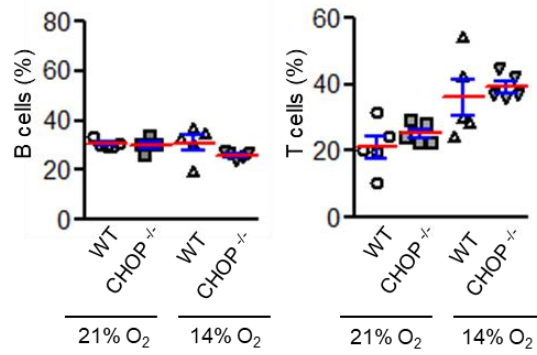
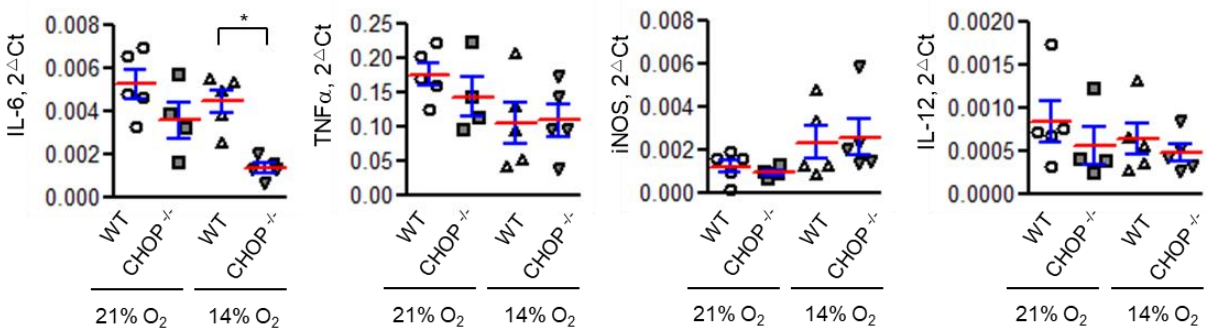
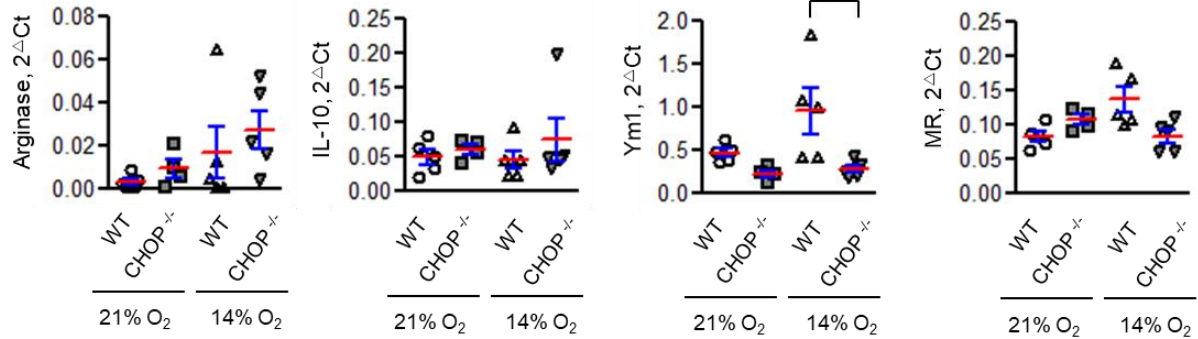
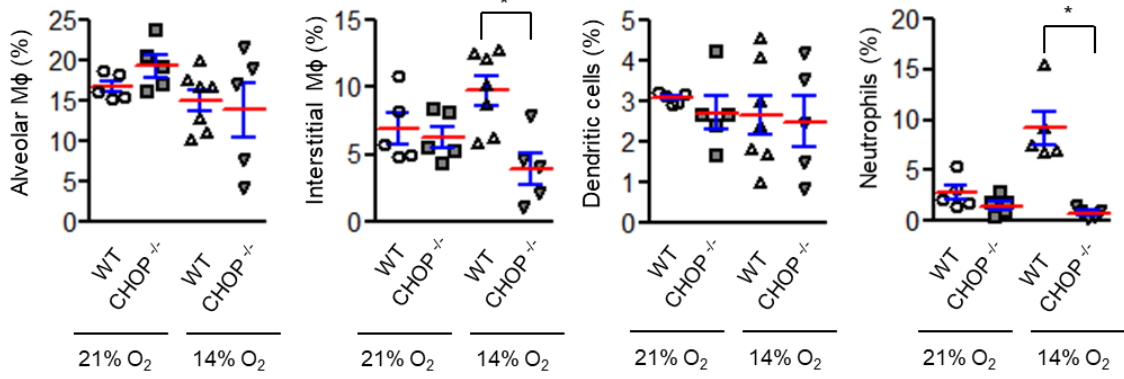
A**B****C****M1 markers****M2 markers**

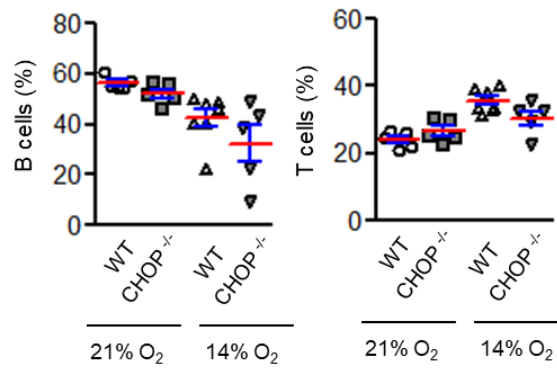
Figure 19. WT and CHOP^{-/-} mice were treated with intratracheal bleomycin (0.04 units) followed 7 days later by exposure to 14% O₂ for an additional 14 days or maintained in 21% O₂. Lungs were harvested at 21 days post-bleomycin and immune/inflammatory cells were analyzed by flow cytometry. (A) Percentage of viable CD45⁺ cells in the lungs identified as alveolar macrophages (CD103-CD11c⁺), interstitial macrophages (CD103-CD11c-CD11b+Ly6G⁻), dendritic cells (CD103+CD11c⁺), or neutrophils (CD103-CD11c-Ly6G+CD11b⁺). (B) Percentage of viable CD45⁺ cells in the lungs identified as B cells (CD19⁺) and T cells (CD3⁺). (C) WT and CHOP^{-/-} mice were treated with intratracheal bleomycin (0.04 units) followed 7 days later by exposure to 14% O₂ for an additional 14 days or maintained in 21% O₂. Lungs were harvested at 21 days post-bleomycin and macrophages were isolated from single cell suspensions by adherence to plastic and mRNA was isolated for qPCR quantification of M1 macrophage markers (IL-6, TNF α , iNOS, and IL-12) and M2 macrophage markers (Arginase, IL-10, Ym1, Mannose Receptor). GAPDH was used for normalization. Comparisons between groups were made using one way ANOVA with Tukey's post-hoc test. *= $p < 0.05$ compared to WT +14% O₂.

Since bleomycin results in inflammation that peaks between 1 and 2 weeks after exposure, we also evaluated inflammation during this time period at 10 days after bleomycin injection (exposure to 21% O₂ or 14% O₂ for 3 days between 7 and 10 days after bleomycin). Similar to our findings at day 21 after bleomycin, numbers of lymphocytes were similar in the lungs of WT and CHOP^{-/-} mice in normoxia and hypoxia. In contrast, neutrophils and interstitial macrophages were reduced in bleomycin-treated CHOP^{-/-} mice compared with WT mice in hypoxia, while numbers of alveolar macrophages and dendritic cells were similar (**Figure 20, A and B**). Regarding macrophage polarization, no difference in the pattern of M1/ M2 markers was observed between WT and CHOP^{-/-} mice following bleomycin treatment in normoxia or hypoxia (**Figure 20C**).

A



B



C

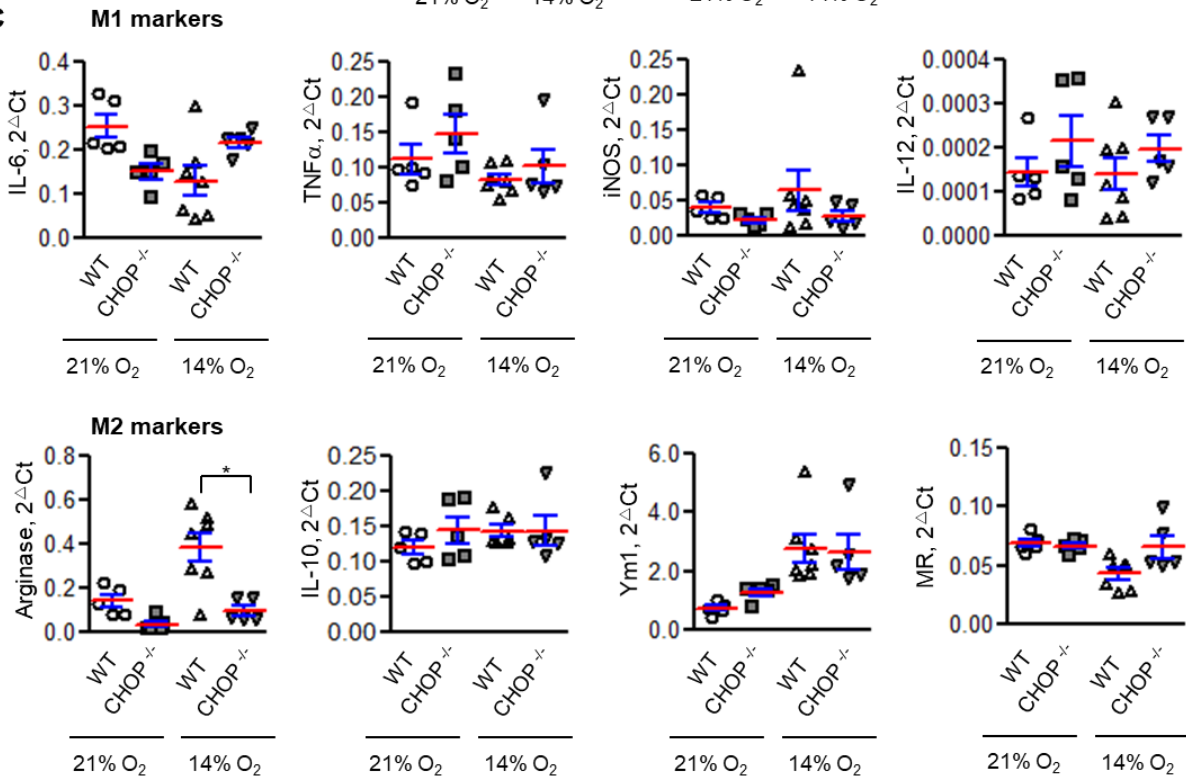


Figure 20. Immune/inflammatory cells and M1/M2 markers in macrophages from lungs of wild type and CHOP deficient mice following single dose IT bleomycin treatment with or without subsequent exposure to hypoxia (14% O₂) and harvested at day 10 post-bleomycin. WT and CHOP^{-/-} mice were treated with intratracheal bleomycin (0.04 units) followed 7 days later by exposure to 14% O₂ for an additional 3 days or maintained in 21% O₂. Lungs were harvested at 10 days post-bleomycin and immune/inflammatory cells were analyzed by flow cytometry. (A) Percentage of viable CD45⁺ cells in the lungs identified as alveolar macrophages (CD103-CD11c⁺), interstitial macrophages (CD103-CD11c-CD11b+Ly6G⁻), dendritic cells (CD103+CD11c⁺), or neutrophils (CD103-CD11c-Ly6G+CD11b⁺). (B) Percentage of viable CD45⁺ cells in the lungs identified as B cells (CD19⁺) and T cells (CD3⁺). (C) WT and CHOP^{-/-} mice were treated with intratracheal bleomycin (0.04 units) followed 7 days later by exposure to 14% O₂ for an additional 3 days or maintained in 21% O₂. Lungs were harvested at 10 days post-bleomycin and macrophages were isolated from single cell suspensions by adherence to plastic. mRNA was isolated for qPCR quantification of M1 macrophage markers (IL-6, TNF α , iNOS, and IL-12) and M2 macrophage markers (Arginase, IL-10, Ym1, Mannose Receptor). GAPDH was used for normalization. Comparisons between groups were made using one way ANOVA with Tukey's post-hoc test. *= $p < 0.05$ compared to WT + 14% O₂.

Consistent with similar macrophage polarization among treatment groups, no evidence of CHOP induction was observed in macrophages isolated from bleomycin-treated WT mice in either hypoxia or normoxia (**Figure 21**)

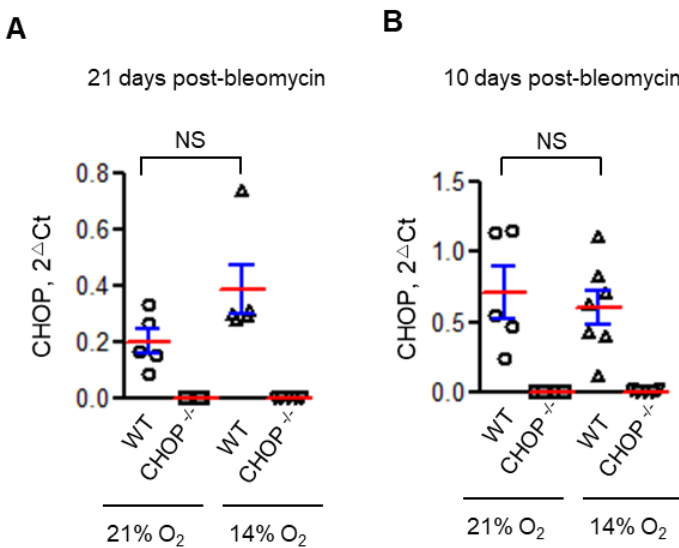


Figure 21. CHOP expression in macrophages isolated from mice in the bleomycin followed by hypoxia model. WT and CHOP^{-/-} mice were treated with intratracheal bleomycin (0.04 units) followed 7 days later by exposure to 14% O₂ for an additional 14 days (A) or 3 days (B). Control mice were maintained in 21% O₂. Lungs were harvested and macrophages were isolated from single cell suspensions by adherence in tissue culture plates. mRNA was isolated for qPCR quantification of CHOP and GAPDH was used for normalization. Comparisons between groups were made using one way ANOVA with Tukey's post-hoc test. NS= non-significant.

CHOP and markers of hypoxia are prominently expressed in lungs of IPF patients

We evaluated the expression of CHOP and hypoxia markers in lungs of IPF patients and non-IPF controls. We observed induction of CHOP in IPF lungs by IHC on lung sections and by Western blotting of lung tissue homogenates. CHOP was predominantly expressed in hyperplastic type II AECs in areas of fibrosis. Additionally, we observed prominent expression of hypoxia markers HIF1 α , pyruvate kinase, and carbonic anhydrase IX in hyperplastic type II AECs in IPF lungs, with a pattern similar to CHOP staining (**Figure 22**). Together, these studies in lung specimens from IPF patients provide further evidence for a connection between localized hypoxia and ER stress in this disease.

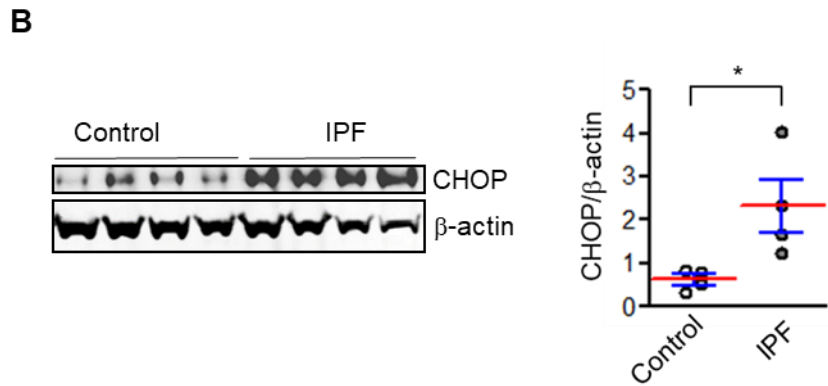
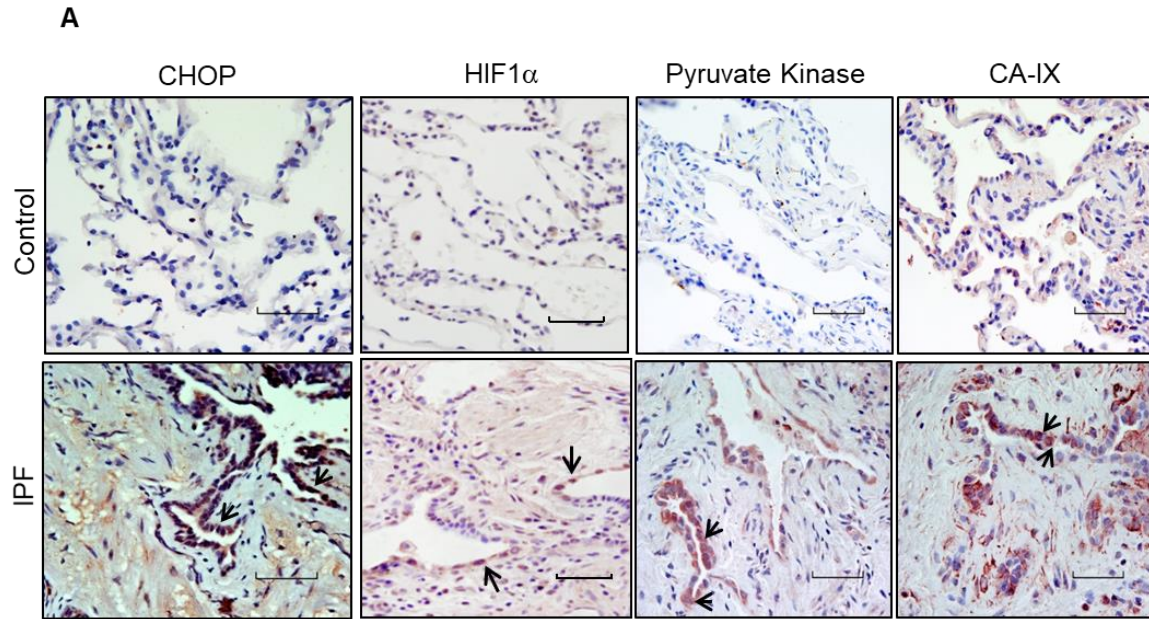


Figure 22. CHOP and markers of hypoxia are prominently expressed in lungs of IPF patients. (A) Representative immunostaining for CHOP, HIF1 α , pyruvate kinase, and carbonic anhydrase IX (CA-IX) on lung sections of IPF patients and non-IPF control lungs. Arrows indicate positive staining in type II AECs. Scale bars: 60 μ m. (B) Western blot (left panel) and densitometry (right panel) for CHOP on protein from lung tissue lysates of IPF patients and non-IPF controls. β -actin was used as a loading control. Comparisons between groups were made using unpaired two-tailed Student's t-test. $^* = p < 0.05$.

DISCUSSION

Our studies indicate that localized hypoxia augments ER stress and induces CHOP expression in AECs, thus favoring fibrotic remodeling over effective repair. These studies point to a distinction between the standard injury-repair model (single-dose i.t. bleomycin) and models involving sequential or repetitive injuries that worsen or prolong fibrotic remodeling. CHOP was not required for fibrosis in the single-dose bleomycin model, where CHOP induction was minimal. In contrast, CHOP was shown to be a critical mediator of fibrosis in models with substantial ER stress, including repetitive-dose bleomycin, bleomycin treatment in mice with L188Q SFTPC-induced ER stress in AECs, and bleomycin followed by hypoxia, thereby suggesting that CHOP (and ER stress) may be more important in progression, rather than initiation, of fibrosis.

CHOP expression has been linked to a number of ER stress-mediated pathologies in the kidneys, pancreas, heart, and liver, including diseases with progressive remodeling and organ dysfunction (20, 21, 149, 150). In lung fibrosis, prior studies regarding the role of CHOP have yielded conflicting results, with two reports showing that CHOP^{-/-} mice have reduced fibrosis after single-dose i.t. bleomycin treatment (96, 100) and another report showing markedly worse survival and increased fibrosis in CHOP^{-/-} mice after single-dose i.t. bleomycin treatment (101). The latter study also found that mice with heterozygous deletion of binding immunoglobulin protein (BiP), which should exacerbate ER stress through reduced chaperone function, were protected from lung fibrosis through increased CHOP-dependent macrophage apoptosis. In contrast to these studies, we found no effects of CHOP deficiency in the standard single-dose bleomycin model using two different doses of bleomycin (0.04 units and 0.08 units). Although the explanation for the discrepancy between these studies is not obvious, our findings suggest that CHOP regulation of fibrosis differs depending on the ER stress-dependent contribution to the fibrotic phenotype.

Specifically, CHOP deficiency in bleomycin-treated L188Q SFTPC/CHOP^{-/-} mice reduced fibrosis only to the level observed in bleomycin-treated WT mice, and similarly, CHOP^{-/-} mice exposed to hypoxia following single-dose bleomycin developed lung fibrosis equivalent to that of WT mice treated with single-dose bleomycin and maintained in normoxia.

CHOP is a transcription factor that plays an important role in regulating ER stress-induced apoptosis (151). Our studies implicate CHOP-induced AEC apoptosis as an important mechanism influencing fibrosis severity. Several studies have implicated CHOP in regulating inflammatory signaling (152). In this regard, CHOP was reported to regulate M2 macrophage polarization in lung fibrosis induced by single-dose bleomycin (96); however, in our studies, we did not observe induction of CHOP in macrophages and CHOP deficiency did not affect macrophage polarization in any of our models. CHOP deficiency did reduce the number of neutrophils in the lungs following repetitive-bleomycin treatment and at day 10 in the bleomycin followed by hypoxia model (interstitial macrophages were reduced at day 10 in this model as well). It is unclear whether these changes in inflammatory cells effect fibrosis in these models; we speculate that the observed decrease in these inflammatory cell subtypes may be secondary to reduced epithelial injury and death, rather than a direct effect of CHOP in inflammatory cells. In addition to epithelial cell survival and regulation of inflammation, our epithelial cell expression profiling studies suggested that CHOP may affect a number of other cellular phenotypes that could affect fibrotic remodeling, including epithelial differentiation, growth factor responses, and cell migration.

Our finding of localized hypoxia in the repetitive bleomycin model is an important advance in understanding how ER stress could be generated in IPF. In our studies, we identified pimonidazole adducts, which require a very low pO₂ (≤ 10 mmHg) for generation, as a marker of cellular hypoxia in type II AECs in the repetitive bleomycin treatment model and the single-dose

bleomycin followed by hypoxia model. Depletion of oxygen to the level required for pimonidazole adduct formation may occur preferentially in AECs because of the high metabolic activity of these cells (145). Our model of exposure to 14% O₂, which is equivalent to ascension to an altitude of approximately 10,500 feet above sea level, after bleomycin injury makes it possible for future studies to further investigate the specific contribution of hypoxia to development of lung fibrosis.

In summary, these data (a) provide evidence that the UPR-downstream effector CHOP plays a critical role in mediating the effects of ER stress in lung fibrosis, likely through increasing apoptosis of AECs and impairing re-epithelialization and restoration of lung architecture, and (b) suggest localized hypoxia in the injured/damaged lung parenchyma to be a potential explanation for ER stress, almost universally observed in lungs of IPF patients.

IV. REGULATION AND DOWNSTREAM FUNCTION OF C/EBP HOMOLOGOUS PROTEIN (CHOP) IN ALVEOLAR EPITHELIAL CELLS IN HYPOXIA

Hypoxia induces CHOP expression in AECs through the IRE1 α /XBP1 and PERK/ATF4 pathways

To investigate the regulation of CHOP expression by hypoxia, we exposed a type II AEC line (MLE12 cells) to hypoxia (1.5% O₂) for 24–48 hours. By Western blotting and qPCR, we found upregulation of CHOP in hypoxic cells compared with cells cultured in room air (21% O₂) (**Figure 23A**). In addition, we found increased expression of ATF4 (a measure of activation of PKR-like ER kinase [PERK]) and spliced XBP1 (a measure of activation of inositol-requiring enzyme 1 [IRE1]) following hypoxia exposure. In contrast, cleaved activating transcription factor 6 (ATF6) and IRE1 α levels remained unchanged after exposure to hypoxia (**Figure 23, B and C**). To determine the regulation of CHOP expression in hypoxia, we used small-molecule inhibitors to disrupt IRE1 α or PERK activity in MLE12 cells. We treated MLE12 cells with a small-molecule inhibitor of IRE1 α (PCP-101, Mannkind Corporation), which interacts directly with the RNase active site of IRE1 α and blocks XBP1 mRNA splicing (153-155), or DMSO as vehicle control. Following treatment, cells were exposed to 1.5% O₂ or room air for 48 hours. Treatment of MLE12 cells with PCP-101 efficiently blocked XBP1 splicing and markedly reduced CHOP induction in hypoxia, without affecting ATF4 induction (**Figure 23, D and E**). These data show an important role of the IRE1 α /XBP1 pathway in hypoxia-induced CHOP expression. In confirmation of this finding, treatment of MLE12 cells with an IRE1 siRNA also prevented CHOP induction in hypoxia (**Figure 24**). Next, to evaluate the role of the PERK/ATF4 pathway, we treated MLE12 cells with a small-molecule inhibitor of PERK (GSK2606414) or DMSO as vehicle control, followed by

exposure to hypoxia for 48 hours. PERK inhibition led to a reduction in ATF4 expression and a concomitant decrease in CHOP expression, without affecting XBP1 splicing (**Figure 23F**). siRNA-mediated inhibition of ATF4 signaling led to a slight reduction in CHOP levels in hypoxia (**Figure 24**). Taken together, these data suggest that both the IRE1/XBP1s and the PERK/ATF4 arms of the UPR pathways contribute to CHOP induction in hypoxia. To evaluate the role of HIF signaling in regulating CHOP expression in AECs, we treated MLE12 cells with siRNA directed toward HIF1 α , followed by exposure to hypoxia (1.5% O₂). While we observed efficient HIF1 α knockdown (**Figure 25**), hypoxia-induced CHOP expression was unchanged (**Figure 23G**), suggesting that HIF and CHOP are independently regulated.

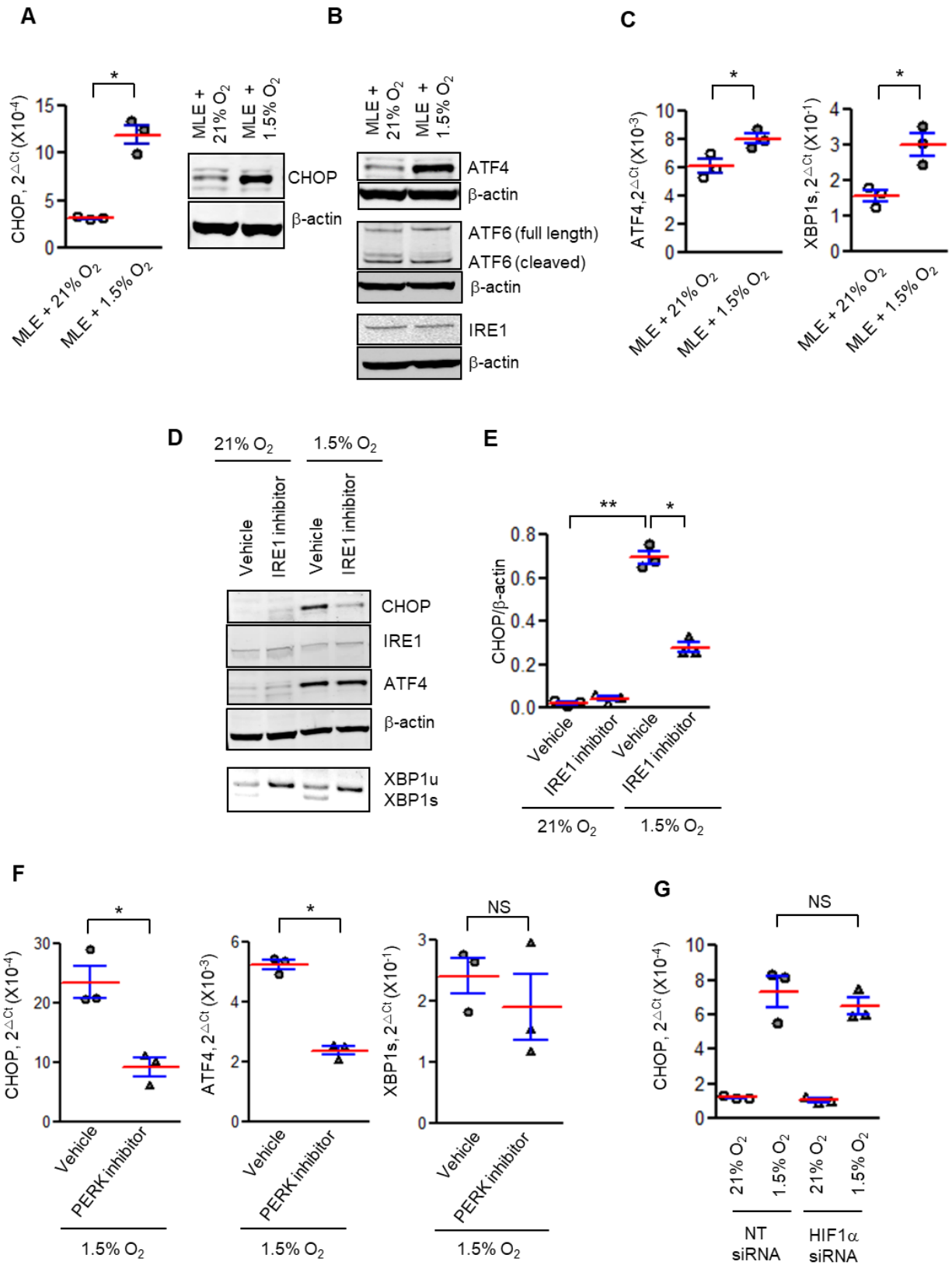


Figure 23. Hypoxia induces CHOP expression in AECs through the IRE1 α /XBP1 and PERK/ATF4 pathways. MLE12 cells were exposed to normoxia (21% O₂) or hypoxia (1.5% O₂) for 24 or 48 hours. **(A)** qPCR for CHOP normalized to RPL19 in left panel and western blot for CHOP in right panel at 48 hours. **(B)** Western blots for ATF4, ATF6, IRE1 and β -actin at 48 hours. **(C)** qPCR for ATF4 normalized to RPL19 and spliced XBP1 normalized to unspliced XBP1 at 24 hours. Comparisons between groups were made using unpaired, two-tailed Student's t-test for A and C. $\ast = p < 0.05$ compared to MLE12 + 21% O₂. **(D)** MLE12 cells were treated with small molecule inhibitor of IRE1 (PCP101) or DMSO (vehicle control) and exposed to hypoxia for 48 hours. Western blots for CHOP, IRE1, and ATF4, and RTPCR gel showing XBP1 splicing. XBP1u: XBP1 unspliced, XBP1s: XBP1 spliced. **(E)** Densitometry of CHOP normalized to β -actin. **(F)** MLE12 cells were treated with small molecule inhibitor of PERK (GSK2606414) or DMSO (vehicle control) and exposed to hypoxia for 48 hours. qPCRs for ATF4 and CHOP normalized to RPL19 and spliced XBP1 normalized to unspliced XBP1. **(G)** MLE12 cells were transfected with HIF1 α siRNA or control NT siRNA and exposed to hypoxia for 48 hours. Comparisons between groups were made using unpaired, two-tailed Student's t-test (F) or one way ANOVA with Tukey's post-hoc test (E,G). $\ast = p < 0.05$ compared to Vehicle + 1.5% O₂, $\ast\ast = p < 0.05$ compared to Vehicle + 21% O₂, NS = non-significant.

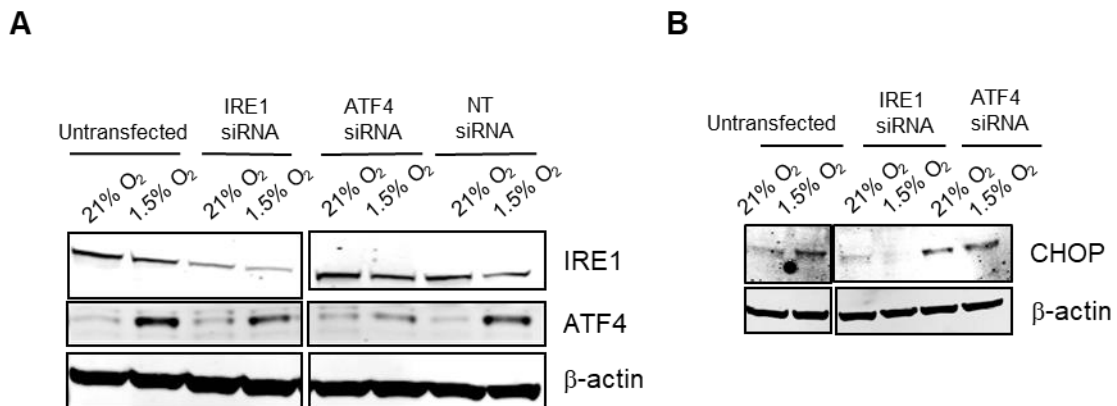


Figure 24. siRNA mediated-knockdown of IRE1 and ATF4 followed by evaluation of CHOP in MLE12 cells exposed to hypoxia. MLE12 cells were transfected with IRE1, ATF4 or control non-targeted (NT) siRNA and exposed to hypoxia for 48 hours. Western blots for **(A)** IRE1, ATF4 and **(B)** CHOP. β -actin is shown as loading control.

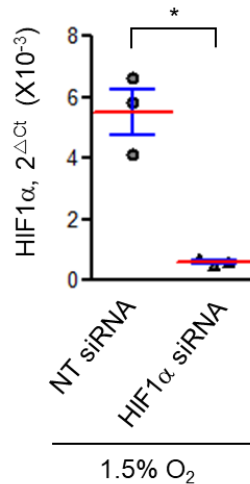


Figure 25. Efficiency of HIF1 α knockdown by siRNA in MLE12 cells. MLE12 cells were transfected with HIF1 α siRNA or control NT siRNA and exposed to hypoxia for 6 hours. qPCR for HIF1 α normalized to RPL19. Groups were compared using unpaired, two-tailed Student's t-test. *= $p < 0.05$ compared to NT siRNA + 1.5% O $_2$.

CHOP regulates hypoxia-induced apoptosis of AECs

To determine the mechanism through which CHOP regulates hypoxia-induced apoptosis of AECs, we transfected MLE12 cells with an siRNA targeting CHOP (or non-targeted control siRNA), followed by exposure to 1.5% O $_2$ for 48 hours. We confirmed efficient CHOP knockdown and found that CHOP $^{-/-}$ cells were protected from hypoxia-induced cell death (**Figure 26, A and B**). To identify the mediators regulated by CHOP in AECs, we utilized the Mouse Apoptosis RT2 Profiler PCR Array (Qiagen) to assess mRNA expression of proapoptotic and antiapoptotic genes in MLE12 cells treated with CHOP siRNA or nontargeted siRNA and exposed to 1.5% O $_2$. Of the 59 genes expressed in MLE12 cells (cycle threshold < 30), 13 were significantly downregulated and 1 was upregulated in CHOP $^{-/-}$ cells (**Figure 26C and Figure 27**). Following PCR validation of this set of apoptosis-related genes, 8 genes remained that were differentially expressed (all downregulated) in the setting of CHOP deficiency (**Table 1**).

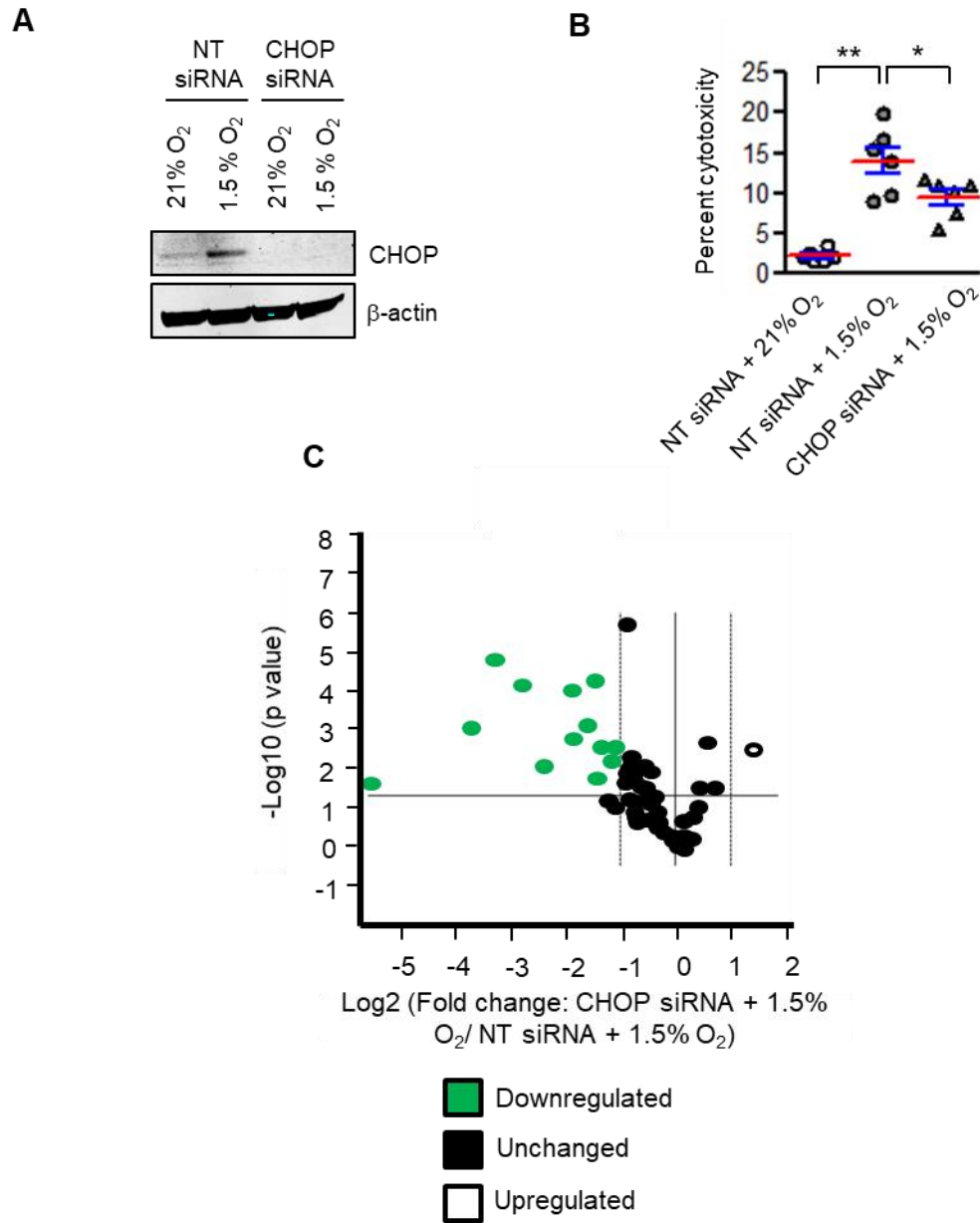
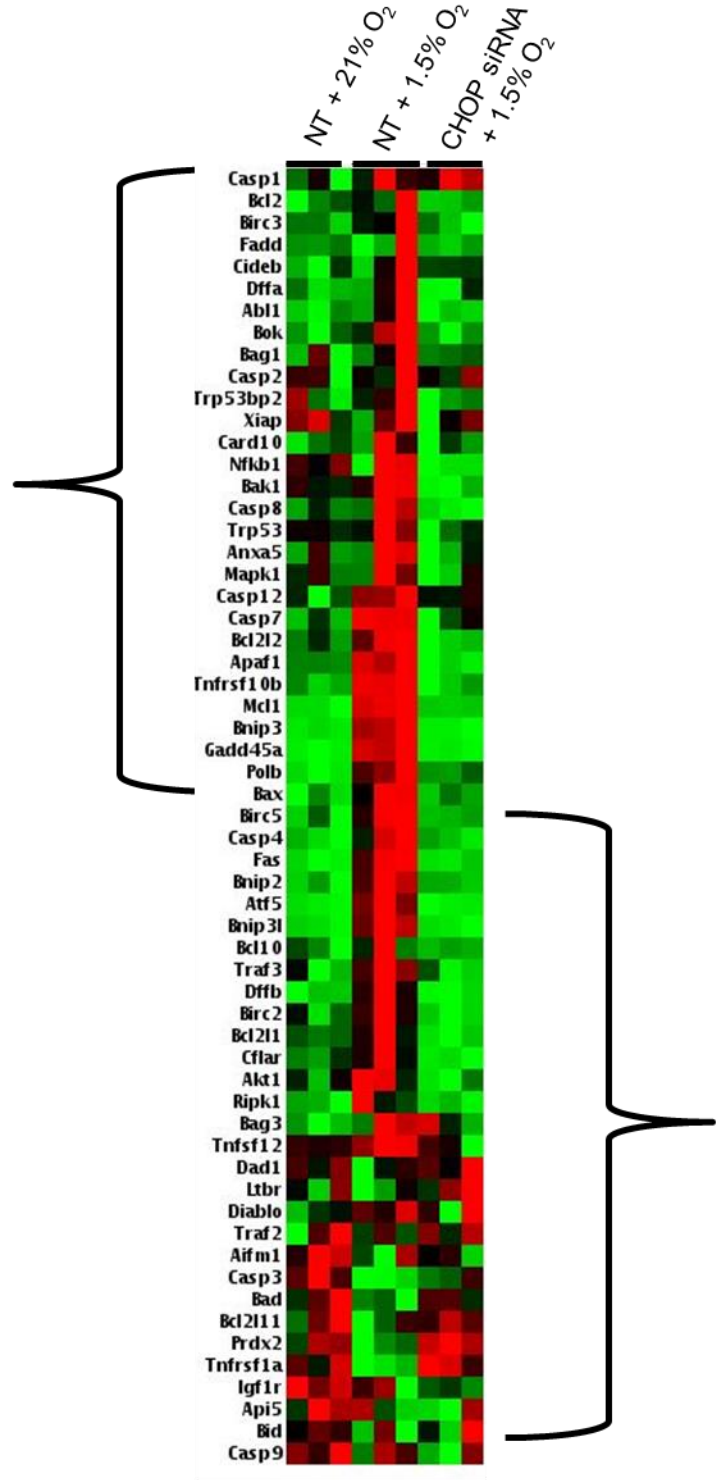


Figure 26. CHOP mediates hypoxia-induced apoptosis of AECs through expression of apoptosis regulating proteins. MLE12 cells were transfected with CHOP siRNA or non-target (NT) siRNA and exposed to hypoxia for 48 hours. (A) Western blot for CHOP. β -actin was used as a loading control. (B) Cell death measured by LDH assay. Comparisons between groups were made using one way ANOVA with Tukey's post-hoc test. $*=p<0.05$ compared to NT siRNA + 1.5% O₂, $**=p<0.05$ compared to NT siRNA + 21% O₂. (C) Volcano plot showing differentially regulated genes (cycle threshold < 30) using the Mouse Apoptosis RT² Profiler PCR Array comparing MLE12 cells treated with CHOP siRNA or NT siRNA followed by hypoxia exposure for 48 hours. $n = 3$ samples in each group.

Casp1
Bcl2
Birc3
Fadd
Cideb
Dffa
Abl1
Bok
Bag1
Casp2
Trp53bp2
Xiap
Card10
Nfkb1
Bak1
Casp8
Trp53
Anxa5
Mapk1
Casp12
Casp7
Bcl2l2
Apaf1
Tnfrsf10b
Mcl1
Bnip3
Gadd45a
Polb
Bax



Birc5
Casp4
Fas
Bnip2
Atf5
Bnip3l
Bcl10
Traf3
Dffb
Birc2
Bcl2l1
Cflar
Akt1
Ripk1
Bag3
Tnfrsf12
Dad1
Ltbr
Diablo
Traf2
Aifm1
Casp3
Bad
Bcl2l11
Prdx2
Tnfrsf1a
Igf1r
Api5
Bid
Casp9

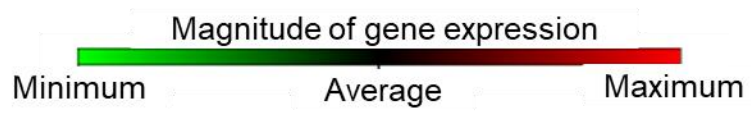


Figure 27. Expression of pro-apoptotic mediators in CHOP siRNA or control siRNA treated AECs exposed to hypoxia. MLE12 cells were transfected with CHOP siRNA or NT control siRNA and exposed to hypoxia for 48 hours. Clustergram analysis of results from Mouse Apoptosis RT² Profiler PCR Array is shown. n = 3 samples per group.

Validated Genes	Fold Regulation in array (CHOP siRNA/ NT siRNA in 1.5% O ₂)
Atf5	-12.62
Gadd45a	-9.48
Bnip3	-6.85
Dffb	-5.06
Bnip3l	-2.92
Apaf1	-2.77
Cflar	-2.60
Bnip2	-2.44

Table 1. MLE12 cells were transfected with CHOP siRNA or non-target (NT) siRNA and exposed to hypoxia for 48 hours. Table showing genes in the Mouse Apoptosis RT2 Profiler PCR Array that were differentially regulated by CHOP siRNA treatment and confirmed by individual qPCR. n = 3 samples in each group.

Following PCR validation of this set of apoptosis-related genes, 8 genes remained that were differentially expressed (all downregulated) in the setting of CHOP deficiency (Table 1). Subsequently, we evaluated these targets in vivo and found that expression of activating transcription factor 5 (ATF5), growth arrest and DNA damage inducible α (GADD45A), and BCL2-interacting protein 3 like (BNIP3L) were reduced in lungs of CHOP^{-/-} mice compared with WT mice after repetitive bleomycin injury (**Figure 28**), thus validating these targets as potential downstream CHOP mediators affecting AEC survival in this model.

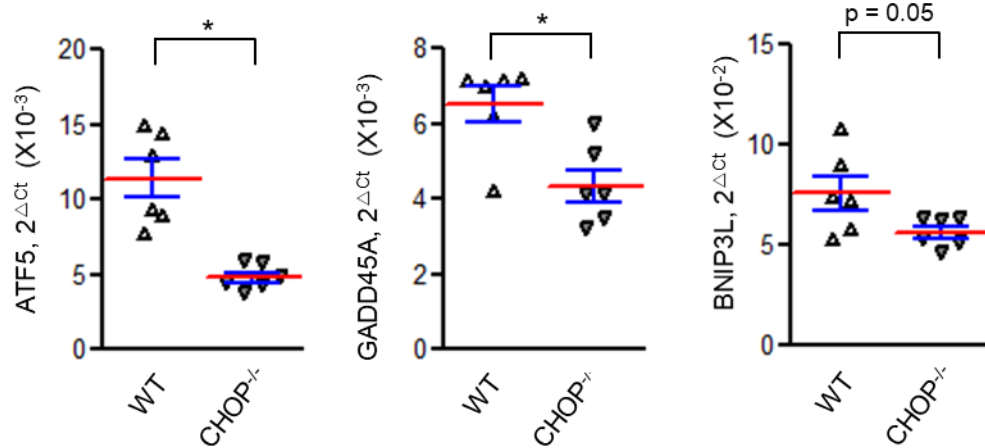


Figure 28. Expression of CHOP-dependent apoptosis mediators in lungs of CHOP deficient mice treated with repetitive bleomycin. Wild type and CHOP^{-/-} mice were studied using the repetitive bleomycin model and lungs were harvested 2 weeks after the last dose. qPCR for ATF5, GADD45A, and BNIP3L normalized to RPL19. Groups were compared using unpaired two-tailed Student's t-test. *=p<0.05.

DISCUSSION

We found that (a) in addition to the PERK/ATF4 arm, generally considered to be predominant in CHOP activation, the IRE1 α /XBP1 arm of the UPR is also necessary for hypoxia-induced upregulation of CHOP in AECs, and (b) CHOP upregulates expression of several apoptosis-related genes in AECs following exposure to hypoxia, including GADD45A, ATF5, and BNIP3L, which we verified in lungs of CHOP^{-/-} mice after recurrent bleomycin injury.

In our studies, CHOP expression in AECs was unrelated to HIF signaling but was induced by ER stress through the IRE1 α /XBP1 and PERK/ATF4 pathways in hypoxia. In disease models, the PERK pathway has been implicated in liver fibrosis (156), and the IRE1 α pathway has been reported to regulate both liver and skin fibrosis (157-159). Together with our studies, these data indicate that these UPR pathways may be most relevant for regulating fibrotic remodeling.

Our data showed that CHOP induces apoptosis of AECs in hypoxia, likely via expression of CHOP target genes. Although the molecular mechanisms underlying CHOP-induced apoptosis may be context dependent, our studies showed that CHOP upregulates expression of numerous apoptosis-related genes in AECs following exposure to hypoxia, including GADD45A, ATF5, and BNIP3L. GADD45A can regulate cell cycle checkpoints, apoptosis, and DNA repair by contributing to activation of p53 (160), a protein that is upregulated in AECs in IPF (161). ATF5 has been identified as a direct downstream target of CHOP in mouse embryonic fibroblasts and has been reported to cooperate with CHOP for full induction of a specific subset of downstream genes (162). BNIP3L functions in B cell lymphoma 2-mediated (Bcl-2-mediated) cell death, production of reactive oxygen species, and mitophagy (163). While the effect of CHOP may be multifactorial, further work is needed to precisely define the pathways through which CHOP regulates AEC apoptosis during lung fibrosis.

Taken together, these studies have furthered our understanding of regulation of CHOP and the molecular mediators involved in CHOP-induced apoptosis in AECs in hypoxia.

V. THE ROLE OF HYPOXIA-INDUCIBLE FACTOR (HIF) IN LUNG FIBROSIS

Hypoxia mediates a pro-fibrotic phenotype in alveolar epithelial cells

We wondered whether hypoxia could influence the expression of pro-fibrotic mediators in AECs. Therefore, we exposed MLE12 cells to hypoxia (1.5% O₂) or normoxia (21% O₂) for 48 hours and measured the expression of several pro-fibrotic mediators including cysteine-rich angiogenic inducer 61-CYR61 (CCN1), connective tissue growth factor (CTGF/CCN2), collagen1, platelet derived growth factor B (PDGFB), transforming growth factor β (TGF β), and vascular endothelial growth factor (VEGF) by qPCR. We found that exposure to hypoxia led to a significant increase in expression of each of these mediators (**Figure 29**).

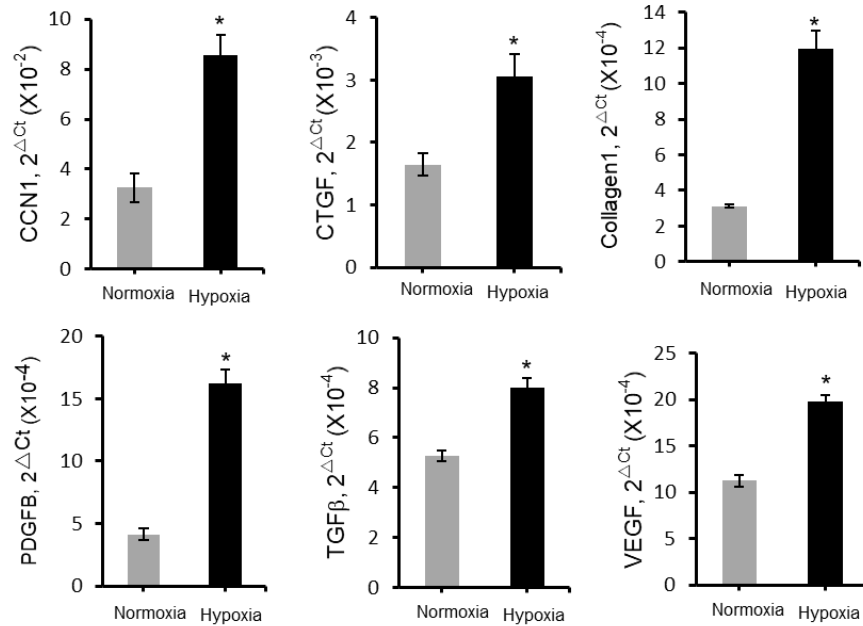


Figure 29. Hypoxia induces expression of pro-fibrotic mediators in AECs. MLE12 cells were exposed to normoxia or hypoxia for 48 hours. qPCRs for CCN1, CTGF, Collagen-1, PDGFB, TGFβ, and VEGF normalized to RPL19. Comparisons between groups were made using unpaired, two-tailed Student's t-test. *=p<0.05 compared to normoxia.

HIF signaling regulates expression of pro-fibrotic mediators in alveolar epithelial cells

We tested for induction of HIFs in MLE12 cells exposed to hypoxia (**Figure 30**). We exposed MLE12 cells to hypoxia (1.5% O₂) or normoxia (21% O₂) for 6, 24, or 48 hours. By western blotting for HIF1α on cell lysates, we found that exposure to hypoxia stabilized HIF1α with maximum stabilization at 6 hours (**Figure 30A**). Also, immunofluorescence staining showed prominent expression of both HIF1α and HIF2α in the nuclei of MLE12 cells exposed to hypoxia at this time point (**Figure 30B**). To evaluate for HIF transcriptional activity, we generated stable MLE12 cells containing a hypoxia response element (HRE) driven luciferase construct. These cells were then exposed to hypoxia (1.5% O₂) or maintained in normoxia (21% O₂) for 2, 4, 6, or 15 hours. Consistent with our findings of HIF stabilization, reporter cells exposed to hypoxia

showed HRE-dependent luciferase activity (reflective of transcriptional activity of HIF) that peaked at 6 hours (**Figure 30C**).

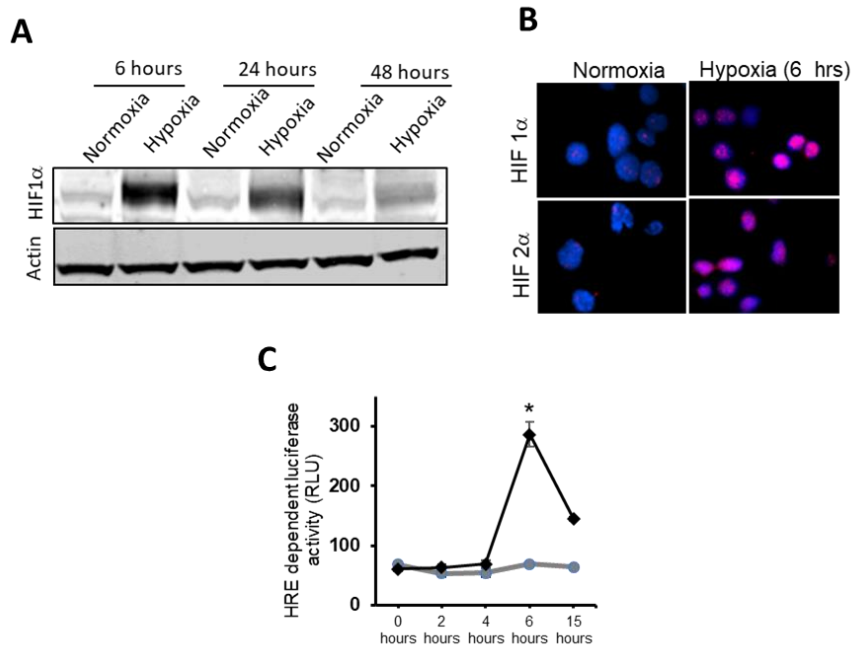


Figure 30. Exposure to hypoxia induces HIF signaling in AECs peaking at 6 hours. (A) MLE12 cells were exposed to hypoxia or normoxia for for 6, 24, or 48 hours. Western blotting for HIF1α. β-actin was used as loading control. (B) MLE12 were exposed to hypoxia or normoxia for 6 hours and immunofluorescence staining was performed with rabbit antibodies to HIF1α or HIF2α, Cy3 conjugated secondary antibodies, and DAPI. Red nuclei indicate positive staining (C) Stably transfected MLE12 cells were generated with a hypoxia responsive element (HRE)-luciferase construct using puromycin selection. Reporter cells were then exposed to hypoxia or normoxia for 2, 4, 6, or 15 hours. Luciferase activity was measured as relative light units (RLU).

Next, we evaluated the effect of HIF signaling on the expression of pro-fibrotic mediators in AECs. We transfected MLE12 cells with siRNA against HIF1α or control non-target siRNA and exposed them to hypoxia (1.5% O₂) or normoxia (21% O₂) for 48 hours. Following hypoxia, cells with HIF1α deficiency showed a significant decrease in expression of pro-fibrotic mediators VEGF and PDGFB (**Figure 31**). Together, these studies suggest that hypoxia increases expression of pro-fibrotic mediators in AECs, at least some of which are regulated through HIF signaling.

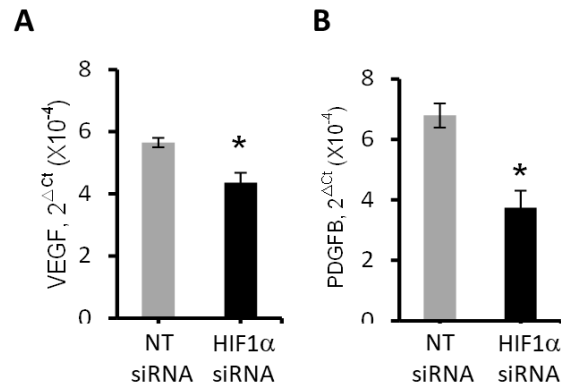


Figure 31. HIF signaling regulates expression of pro-fibrotic mediators VEGF and PDGFB exposed to hypoxia. MLE12 cells were transfected with HIF1 α siRNA or non-targeted (NT) siRNA and exposed to hypoxia or normoxia for 48 hours. qPCRs for VEGF and PDGFB normalized to RPL19. * $p < 0.05$ compared to NT siRNA.

Epithelial HIF signaling is not essential for mediating the effects of hypoxia on lung fibrosis in the ‘bleomycin + hypoxia’ model

To evaluate whether epithelial HIF signaling affects lung fibrosis in mice, we generated mice with lung epithelial cell-specific deletion of HIF1 α and HIF2 α . Epithelial HIF1/2-deficient (HIF1/2 Δ/Δ) mice and littermate controls (HIF1/2 $^{fl/fl}$) were treated with bleomycin (0.04 units), followed by exposure to 14% O₂ or 21% O₂ between day 7 and 21. We found that despite substantial HIF activation (**Figure 32**), epithelial HIF1/2 deletion did not alter lung fibrosis (**Figure 33**) in mice treated with bleomycin followed by exposure to hypoxia.

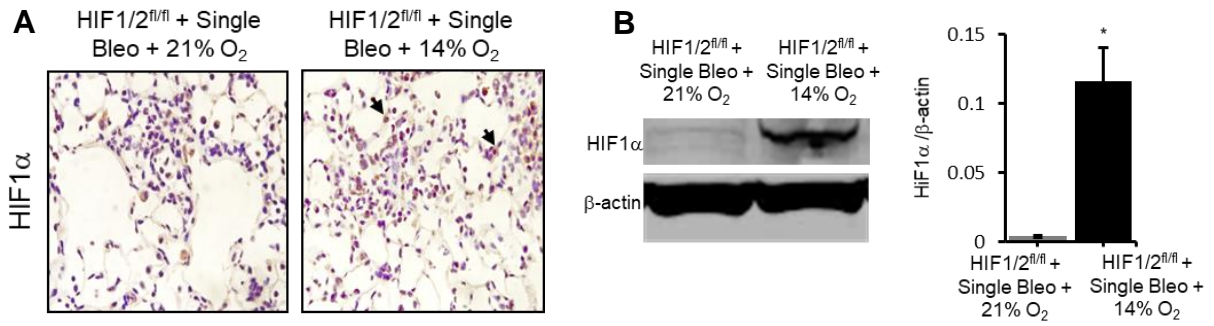


Figure 32. Evaluation of HIF1 α in the bleomycin + hypoxia model. Mice were treated with intratracheal bleomycin (0.04 units) followed 7 days later by exposure to 14% O₂ for an additional 14 days or maintained in 21% O₂. Lungs were harvested at 21 days post-bleomycin. **(A)** Representative immunohistochemistry for HIF1 α on lung sections. **(B)** Western blot for HIF1 α in lung tissue lysates. β -actin was used as a loading control. Comparisons between groups were made using unpaired two-tailed Student's t-test. *= $p < 0.05$.

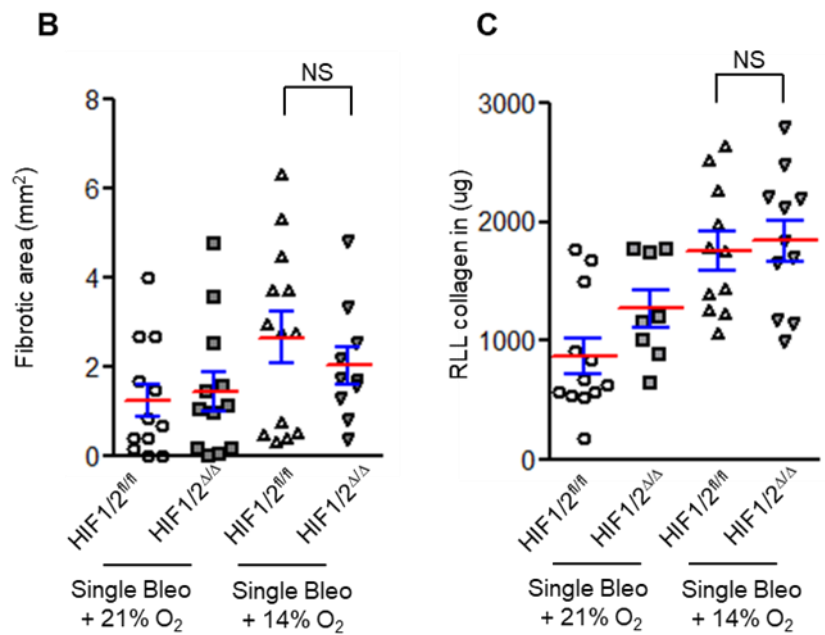
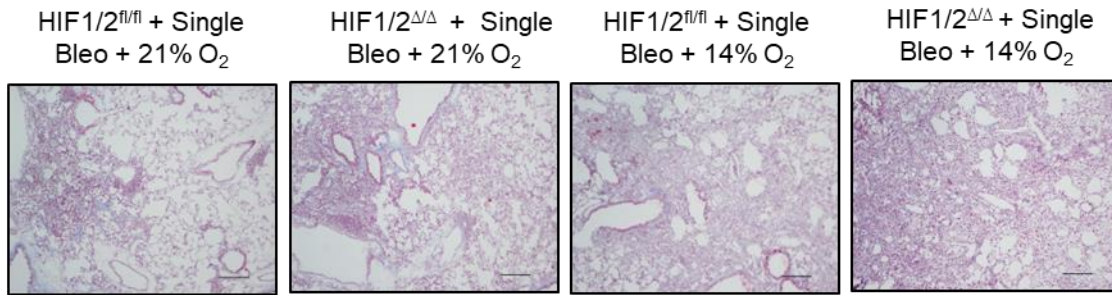
A

Figure 33. Epithelial HIF deficient mice are not protected from exaggerated lung fibrosis induced by exposure to hypoxia. Mice with targeted deletion of HIF1/2 in lung epithelium (HIF1/2^{Δ/Δ}) and controls (HIF1/2^{fl/fl}) were studied in the bleomycin + hypoxia model. (A) Representative Masson's trichrome staining on lung sections. Scale bars: 800 μm. (B) Morphometric evaluation of fibrosis at 21 days after bleomycin injection. (C) Total soluble collagen in right lower lobe (RLL) by sircol assay. Comparisons between groups were made using one way ANOVA with Tukey's post-hoc test. NS = non-significant.

Although epithelial HIF signaling did not protect from lung fibrosis in mice treated with bleomycin followed by exposure to hypoxia, we wondered whether HIF signaling could regulate the expression of pro-fibrotic mediators in this model. Therefore, we performed qPCRs for TGF β , CTGF, PDGFB and VEGF on mRNA isolated from lung lysates of HIF1/2 $^{\Delta/\Delta}$ and HIF1/2 $^{fl/fl}$ mice. However, similar to our finding of no difference in fibrosis between HIF1/2 $^{\Delta/\Delta}$ and HIF1/2 $^{fl/fl}$ mice, we found no significant difference in expression of any of the pro-fibrotic mediators in HIF1/2 $^{\Delta/\Delta}$ mice compared to HIF1/2 $^{fl/fl}$ mice (**Figure 34**).

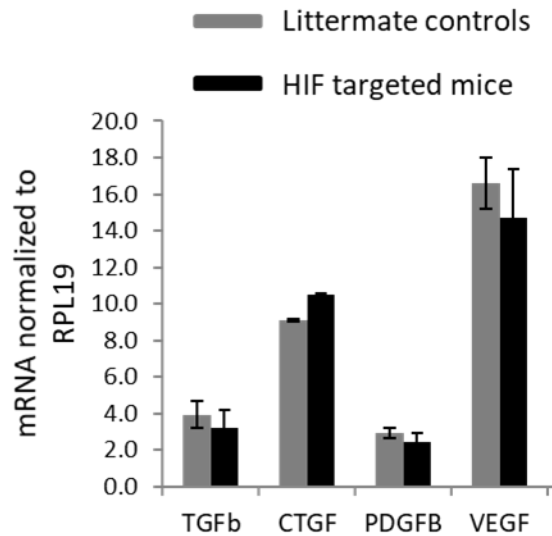


Figure 34. Epithelial HIF deficient mice and littermate controls have similar expression of pro-fibrotic mediators after bleomycin treatment followed by exposure to hypoxia. Mice with targeted deletion of HIF1/2 in lung epithelium (HIF1/2 $^{\Delta/\Delta}$) and controls (HIF1/2 $^{fl/fl}$) were studied in the bleomycin + hypoxia model. qPCR for TGF β , CTGF, PDGFB and VEGF on mRNA isolated from lung lysates was performed. RPL19 was used for normalization. Comparisons between groups were made using unpaired two-tailed Student's t-test.

In summary, these studies demonstrate that epithelial HIF is not essential in mediating the effects of hypoxia on lung fibrosis in the 'bleomycin + hypoxia' model.

Epithelial HIF mediates lung fibrosis after repetitive bleomycin injury to the lungs

Next, we performed experiments using repetitive i.t. bleomycin in HIF1/2^{ΔΔ} and HIF1/2^{fl/fl} mice to determine whether epithelial HIF is an important profibrotic mediator in this model (Figure 35). In these studies, we observed significant protection of HIF1/2^{ΔΔ} mice from development of lung fibrosis, with a marked reduction in fibrotic area (Figure 35A), reduced hyperplastic AECs (Figure 35B), reduced collagen content (Figure 35C), and decreased collagen-1 mRNA expression (Figure 35D).

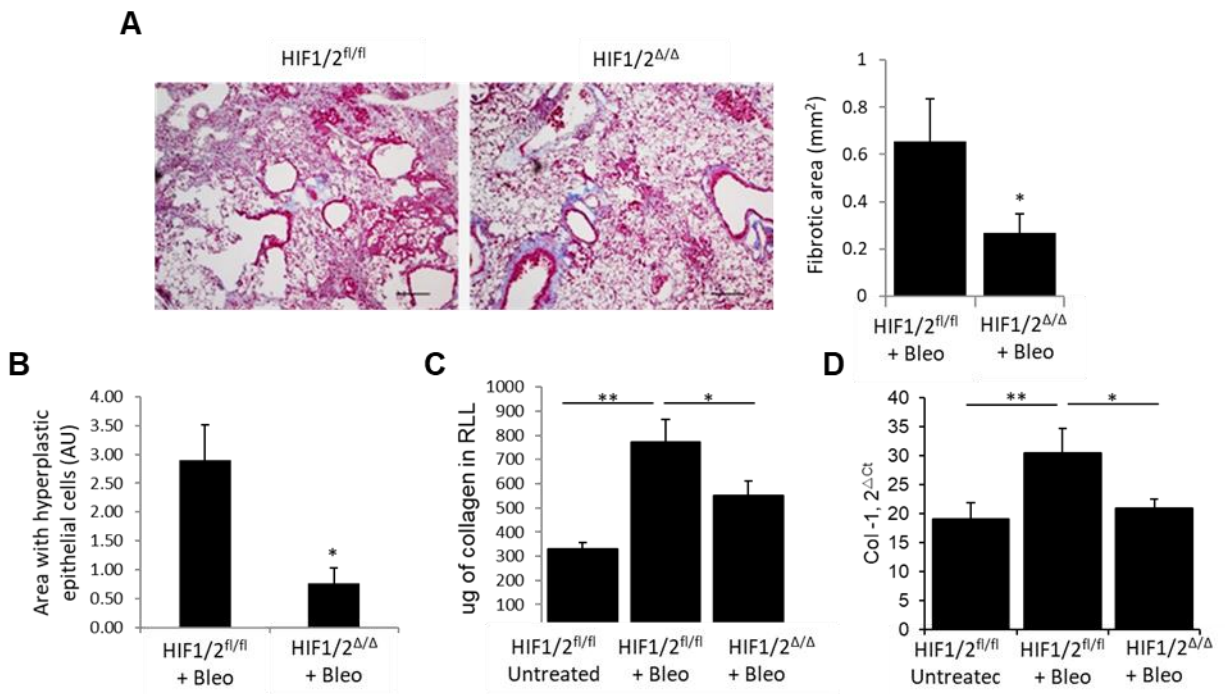


Figure 35. Epithelial HIF signaling plays an important role in mediating lung fibrosis after repetitive bleomycin injury. HIF1/2^{ΔΔ} and HIF1/2^{fl/fl} mice were studied using the repetitive bleomycin model and lungs were harvested 2 weeks after the last dose. (A) Representative Masson's trichrome stained lung sections. Scale bars: 800 μm. (B) Evaluation of fibrosis by morphometry. (C) Quantification of hyperplastic AECs. (D) Quantification of total soluble collagen in right lower lobe (RLL) by sircol assay. (E) qPCR for collagen-1 from mRNA isolated from whole lung lysate. RPL19 was used for normalization. Comparisons between groups were made using unpaired, two-tailed Student's t-test (A and B) or one way ANOVA with Tukey's post-hoc test (C and D). *= $p < 0.05$ compared to HIF1/2^{fl/fl} + rep bleo, **= $p < 0.05$ compared to untreated HIF1/2^{fl/fl}.

DISCUSSION

These studies show that while epithelial HIF signaling does not affect lung fibrosis after single dose bleomycin treatment or bleomycin treatment followed by exposure to hypoxia, it appears to play an important role in progression of fibrosis after repetitive bleomycin injury in mice.

Hypoxia and/or HIF signaling have been implicated in regulating expression of pro-fibrotic mediators including collagen (122). In our work, we found that exposure to hypoxia increases the expression of several pro-fibrotic mediators (CCN1, CTGF, collagen1, PDGFB, VEGF, and TGF β) of which few (PDGFB and VEGF) are regulated by HIF in AECs. However, epithelial HIF targeting did not affect fibrosis in mice treated with a single dose of bleomycin followed by exposure to normoxia or hypoxia. Similar to this observation, we had previously found that endothelial HIF deletion reduces pulmonary hypertension but not lung fibrosis following IP bleomycin treatment in mice (164). Contrary to our observation in the bleomycin + hypoxia model, in preliminary studies with epithelial HIF targeted mice in the repetitive bleomycin model, we found that epithelial HIF deficiency leads to reduced lung fibrosis following repetitive bleomycin injury. Taken together, these findings suggest that the effect of epithelial HIF signaling on lung fibrosis is likely dependent on the nature of injury and the stage of the disease; while epithelial HIF does not affect disease phenotype in a setting of acute injury, it seems to play an important role in progression of the disease in a setting of chronic/repetitive injury. Additional investigations regarding the mechanisms by which HIF signaling regulates lung remodeling are warranted.

VI. CONCLUDING REMARKS AND FUTURE DIRECTIONS

Our studies described in this dissertation show that following persistent injury to the lungs, localized hypoxia in AECs in areas of alveolar collapse augments ER stress. The ER stress-downstream effector CHOP plays a critical role in progression of lung fibrosis, likely through increasing apoptosis of AECs and impairing re-epithelialization. While HIF, the primary mediator of cellular responses to hypoxia, does not seem important in mediating the effects of hypoxia on ER stress, it may act through independent pathways to impact lung fibrosis after repetitive bleomycin injury. At a mechanistic level, we investigated the regulation and downstream function of CHOP in AECs exposed to hypoxia. We found that in addition to the upstream UPR pathway PERK/ATF4, commonly implicated in induction of CHOP, the IRE1-XBP1 arm of the UPR also plays an important role in regulating CHOP in AECs in hypoxia. Furthermore, we identified GADD45A, ATF5, and BNIP3L as important potential downstream-mediators of CHOP-induced apoptosis of AECs in hypoxia. Based on these findings, we propose a model (**Figure 36**) showing potential mechanisms by which localized tissue hypoxia augments fibrotic remodeling in the lung. Together, these findings represent an important advance in understanding the mechanisms linking hypoxia, ER stress, epithelial dysfunction, and progressive lung fibrosis.

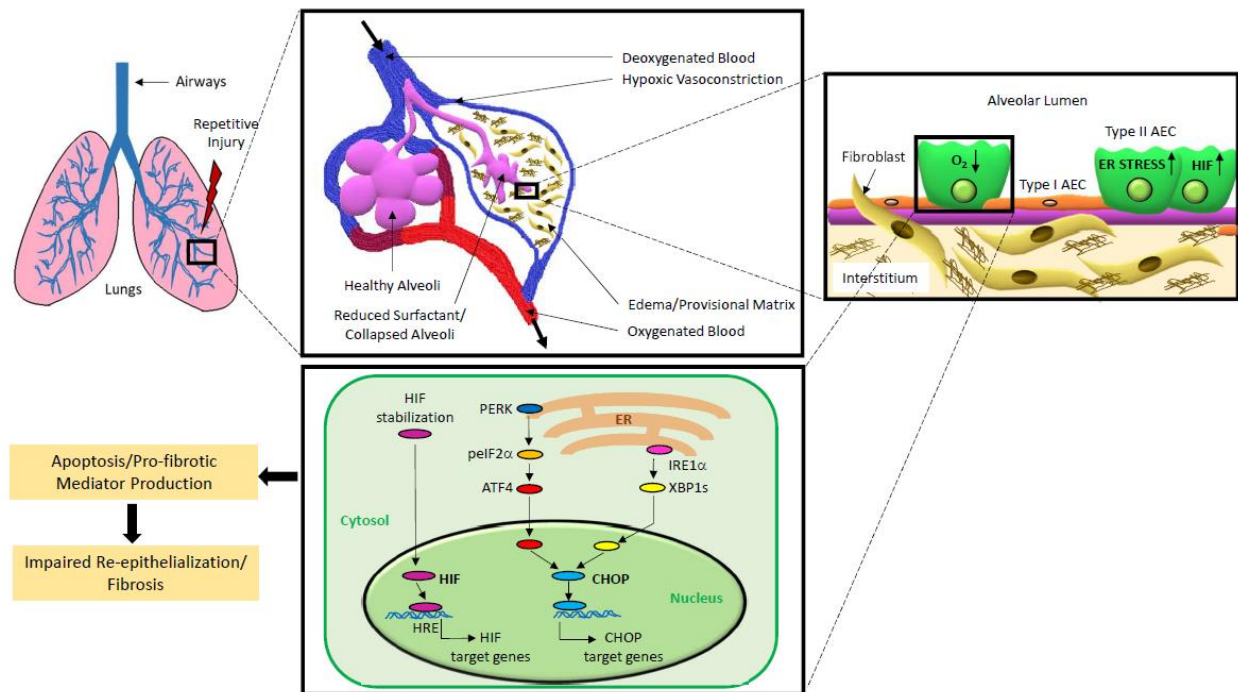


Figure 36. Model showing that tissue hypoxia leads to type II AEC dysfunction and augments lung fibrosis through ER stress and HIF signaling pathways. Exposure to repetitive injurious stimuli causes damage to the distal lung. Alveolar collapse, hypoxic vasoconstriction, and matrix deposition lead to inefficient ventilation and perfusion in localized areas giving rise to tissue hypoxia. Hypoxia causes HIF stabilization and augments ER stress in type II AECs. Specifically, ER stress-mediators PERK/ATF4 and IRE1/XBP1 contribute to induction of transcription factor CHOP. Downstream targets of HIF and CHOP favor a pro-fibrotic type II AEC phenotype. Ongoing dysfunction of type II AECs leads to impaired re-epithelialization and progressive fibrosis.

Our findings support the idea that hypoxia can develop in areas of alveolar collapse and consolidation through reduced ventilation, hypoxic vasoconstriction, and increased oxygen demand. Increased expression of a repertoire of hypoxia-inducible genes has been reported in IPF lungs and in single-cell analysis of AECs in IPF (65-67), consistent with our findings of increased expression of markers of hypoxia in lung tissue of IPF patients. In experimental models, regions of hypoxia have been observed in lungs of rats following radiation-induced injury (165) and in

injured lungs of mice following H1N1 influenza infection (67). Future studies can aim to further determine the specific contribution of localized tissue hypoxia in the injured lung parenchyma to progression of lung fibrosis.

Our data with CHOP deficient and HIF targeted mice point to an important distinction between the single dose bleomycin model, most commonly used in the IPF field, and the repetitive bleomycin model. While the effects of CHOP and HIF on lung fibrosis were not apparent in the single dose bleomycin model where localized hypoxia and ER stress in the lung parenchyma were minimal, both CHOP and HIF proved to be important in mediating lung fibrosis in the repetitive bleomycin model. Since repetitive injuries in the lung parenchyma are thought to underlie progressive fibrosis in IPF, factors identified as important in multiple-injury models may have added relevance when designing new therapeutic strategies for humans. This idea is further supported by our findings of increased expression of hypoxia markers and CHOP in hyperplastic type II AECs in IPF lungs. Based on these observations, in future studies, it would be important to pay close attention to the choice of animal models while trying to answer questions related to pathogenesis of lung fibrosis.

CHOP is a multifunctional transcription factor that regulates ER stress–induced apoptosis (151). In our studies, the effect of CHOP on fibrosis was mirrored by its effects on AEC apoptosis, thus implicating CHOP-induced AEC apoptosis as an important mechanism influencing fibrosis severity. Although we have focused on the role of CHOP in mediating ER stress–induced apoptosis, JNK and caspase-4/12 are additional ER stress–induced mediators that could affect AEC apoptosis and fibrosis (166-168). Additional studies will be needed to delineate the role of those pathways in lung fibrosis.

In addition to apoptosis, CHOP can regulate a variety of cellular processes, such as differentiation, polarization, and inflammatory signaling, through direct transcriptional regulation and interactions with other C/EBP family members (36, 39, 151, 169-171). In our studies, we found that while CHOP does not have a significant effect on inflammatory cells (except neutrophils), it has a potential role in multiple pro-fibrotic processes in AECs including epithelial differentiation, growth factor responses, and cell migration. Future investigations will be required to determine the effect of CHOP on these pro-fibrotic responses. Also, in current studies aimed at understanding the role of CHOP in AECs in lung fibrosis, we used whole body CHOP knockout mice. While our studies with L188Q SFTPC/CHOP^{-/-} mice showed that CHOP is required for mediating lung fibrosis when ER stress is induced specifically in AECs, future studies with epithelial CHOP targeted mice will be needed to more precisely define the role of epithelial CHOP in lung fibrosis.

ER stress can skew macrophages both towards the classically activated (M1) or alternatively activated (M2) phenotypes depending on the pathophysiological context. In our studies, we did not observe induction of CHOP in macrophages in WT mice on exposure of bleomycin-treated mice to hypoxia. Consistent with lack of induction of CHOP, flow cytometry experiments quantifying pulmonary macrophages in WT and CHOP^{-/-} mice in our fibrosis models showed that CHOP deficiency did not impact alveolar or interstitial macrophages (except a decrease in interstitial macrophages in mice treated with bleomycin and exposed at day 7 post-bleomycin to hypoxia for 3 days). On evaluation of the effect of CHOP on polarization of macrophages, we did not find a clear M1/M2 phenotype shift between WT and CHOP^{-/-} mice in the bleomycin + hypoxia model at either day 10 or day 21 post-bleomycin; however, we did observe a significant decrease in expression of M1 marker IL-6 and M2 marker Ym1 in CHOP^{-/-}

mice compared to WT mice at day 21 post-bleomycin and a decrease in expression of M2 marker arginase in CHOP^{-/-} mice compared to WT mice at day 10 post-bleomycin. Taken together, while we found minimal impact of CHOP on phenotype of macrophages in this body of work, further experiments are warranted to determine the effect of ER stress/CHOP in macrophages on lung fibrosis. For example, RNA sequencing analyses comparing the transcriptional signature of macrophages isolated from WT mice and mice with macrophage specific deletion of CHOP (e.g. LysMCre.CHOP^{-/-} mice) in experimental models of fibrosis will provide information on potential pro-fibrotic effects of CHOP on macrophages in the lungs.

While our studies with epithelial HIF targeted mice suggest a potential role for HIF in mediating lung fibrosis after recurrent injury to the lungs, additional investigations will be needed to precisely define the mechanisms by which HIF signaling regulates lung fibrosis. Recently, Xi et al. demonstrated that HIF1 α drives persistent Notch activity in lineage negative alveolar progenitor cells, leading to impaired epithelial regeneration in the lung parenchyma in an H1N1 influenza injury model (67). Given that impaired re-epithelialization is critical in pathogenesis of lung fibrosis, it is tempting to speculate about a potential role of the HIF1 α -Notch axis in impaired epithelial regeneration in lung fibrosis. Also, it has been suggested that HIF may interact with the UPR pathways through mammalian target of rapamycin (mTOR) signaling (39); additional studies will be needed to evaluate these potential interactions in AECs in lung injury-repair and remodeling. We used mice with epithelial deficiency of both HIF1 α and HIF2 α in our studies; however, given that HIF1 α and HIF2 α activate specific subsets of genes and can have opposing functions (172), future studies with specific HIF isoforms are warranted. Also, further work will be needed to understand the pro-fibrotic effects of HIF1 α and HIF2 α on AECs. Furthermore, the role of HIF in different cell types in lung fibrosis remains to be determined. For example,

HIF1 α has been implicated in polarization, migration and apoptosis of macrophages (**Ref**); future experiments with LysMCre.HIF1 α ^{-/-} and LysMCre.HIF2 α ^{-/-} mice will help in understanding the effect of HIF signaling in macrophages on lung fibrosis.

In summary, we have furthered knowledge in this area by discovering that ER stress is mechanistically linked to lung fibrosis through CHOP in three distinct multiple injury-induced lung fibrosis mouse models, and demonstrating that CHOP is a critical molecular mediator of ER stress-induced apoptosis and may also regulate other important profibrotic functions of AECs in lung fibrosis. Based on these findings, CHOP and its downstream targets may be attractive targets for novel therapeutic strategies in IPF. Furthermore, our work shows that localized hypoxia in areas of parenchymal damage could explain the etiology of ER stress in lung fibrosis, and suggests a potential role for epithelial HIF signaling in lung fibrosis. Taken together, this body of work advances our understanding of the role of localized hypoxia and ER stress in the pathophysiology of lung fibrosis.

REFERENCES

1. Mora AL, Rojas M, Pardo A, Selman M. Emerging therapies for idiopathic pulmonary fibrosis, a progressive age-related disease. *Nat Rev Drug Discov.* 2017;16(11):755-72.
2. Raghu G, Collard HR, Egan JJ, Martinez FJ, Behr J, Brown KK, et al. An official ATS/ERS/JRS/ALAT statement: idiopathic pulmonary fibrosis: evidence-based guidelines for diagnosis and management. *Am J Respir Crit Care Med.* 2011;183(6):788-824.
3. Zoz DF, Lawson WE, Blackwell TS. Idiopathic pulmonary fibrosis: a disorder of epithelial cell dysfunction. *Am J Med Sci.* 2011;341(6):435-8.
4. Selman M, Pardo A. Role of epithelial cells in idiopathic pulmonary fibrosis: from innocent targets to serial killers. *Proc Am Thorac Soc.* 2006;3(4):364-72.
5. Byrne AJ, Maher TM, Lloyd CM. Pulmonary Macrophages: A New Therapeutic Pathway in Fibrosing Lung Disease? *Trends Mol Med.* 2016;22(4):303-16.
6. Byrne AJ, Mathie SA, Gregory LG, Lloyd CM. Pulmonary macrophages: key players in the innate defence of the airways. *Thorax.* 2015;70(12):1189-96.
7. Cottin V, Schmidt A, Catella L, Porte F, Fernandez-Montoya C, Le Lay K, et al. Burden of Idiopathic Pulmonary Fibrosis Progression: A 5-Year Longitudinal Follow-Up Study. *PLoS One.* 2017;12(1):e0166462.
8. Nalysnyk L, Cid-Ruzafa J, Rotella P, Esser D. Incidence and prevalence of idiopathic pulmonary fibrosis: review of the literature. *Eur Respir Rev.* 2012;21(126):355-61.
9. Bors M, Tomic R, Perlman DM, Kim HJ, Whelan TP. Cognitive function in idiopathic pulmonary fibrosis. *Chron Respir Dis.* 2015;12(4):365-72.
10. Collard HR. The age of idiopathic pulmonary fibrosis. *Am J Respir Crit Care Med.* 2010;181(8):771-2.

11. Meltzer EB, Noble PW. Idiopathic pulmonary fibrosis. *Orphanet J Rare Dis.* 2008;3:8.
12. Flaherty KR, Fell CD, Huggins JT, Nunes H, Sussman R, Valenzuela C, et al. Safety of nintedanib added to pirfenidone treatment for idiopathic pulmonary fibrosis. *Eur Respir J.* 2018;52(2).
13. Vock DM, Durheim MT, Tsuang WM, Finlen Copeland CA, Tsiatis AA, Davidian M, et al. Survival Benefit of Lung Transplantation in the Modern Era of Lung Allocation. *Ann Am Thorac Soc.* 2017;14(2):172-81.
14. Collard HR, Ward AJ, Lanes S, Courtney Hayflinger D, Rosenberg DM, Hunsche E. Burden of illness in idiopathic pulmonary fibrosis. *J Med Econ.* 2012;15(5):829-35.
15. Selman M, Pardo A. Role of epithelial cells in idiopathic pulmonary fibrosis: from innocent targets to serial killers. *Proc Am Thorac Soc.* 2006;3(4):364-72.
16. Thannickal VJ, Horowitz JC. Evolving concepts of apoptosis in idiopathic pulmonary fibrosis. *Proc Am Thorac Soc.* 2006;3(4):350-6.
17. Yang J, Velikoff M, Canalis E, Horowitz JC, Kim KK. Activated alveolar epithelial cells initiate fibrosis through autocrine and paracrine secretion of connective tissue growth factor. *Am J Physiol Lung Cell Mol Physiol.* 2014;306(8):L786-96.
18. Kropski JA, Blackwell TS, Loyd JE. The genetic basis of idiopathic pulmonary fibrosis. *Eur Respir J.* 2015;45(6):1717-27.
19. Kropski JA, Lawson WE, Young LR, Blackwell TS. Genetic studies provide clues on the pathogenesis of idiopathic pulmonary fibrosis. *Dis Model Mech.* 2013;6(1):9-17.
20. Tanjore H, Blackwell TS, Lawson WE. Emerging evidence for endoplasmic reticulum stress in the pathogenesis of idiopathic pulmonary fibrosis. *Am J Physiol Lung Cell Mol Physiol.* 2012;302(8):L721-L9.

21. Tanjore H, Lawson WE, Blackwell TS. Endoplasmic reticulum stress as a pro-fibrotic stimulus. *Biochim Biophys Acta*. 2013;1832(7):940-7.
22. Kropski JA, Blackwell TS. Endoplasmic reticulum stress in the pathogenesis of fibrotic disease. *J Clin Invest*. 2018;128(1):64-73.
23. Wang S, Kaufman RJ. The impact of the unfolded protein response on human disease. *J Cell Biol*. 2012;197(7):857-67.
24. Maitra M, Wang Y, Gerard RD, Mendelson CR, Garcia CK. Surfactant protein A2 mutations associated with pulmonary fibrosis lead to protein instability and endoplasmic reticulum stress. *J Biol Chem*. 2010;285(29):22103-13.
25. Nogee LM, Dunbar AE, III, Wert SE, Askin F, Hamvas A, Whitsett JA. A mutation in the surfactant protein C gene associated with familial interstitial lung disease. *N Engl J Med*. 2001;344(8):573-9.
26. Thomas AQ, Lane K, Phillips J, III, Prince M, Markin C, Speer M, et al. Heterozygosity for a surfactant protein C gene mutation associated with usual interstitial pneumonitis and cellular nonspecific interstitial pneumonitis in one kindred. *Am J Respir Crit Care Med*. 2002;165(9):1322-8.
27. Lawson WE, Crossno PF, Polosukhin VV, Roldan J, Cheng DS, Lane KB, et al. Endoplasmic reticulum stress in alveolar epithelial cells is prominent in IPF: association with altered surfactant protein processing and herpesvirus infection. *Am J Physiol Lung Cell Mol Physiol*. 2008;294(6):L1119-L26.
28. Maguire JA, Mulugeta S, Beers MF. Endoplasmic Reticulum Stress Induced by Surfactant Protein C BRICHOS Mutants Promotes Proinflammatory Signaling by Epithelial Cells. *Am J Respir Cell Mol Biol*. 2011;44(3):404-14.

29. Mulugeta S, Nguyen V, Russo SJ, Muniswamy M, Beers MF. A surfactant protein C precursor protein BRICHOS domain mutation causes endoplasmic reticulum stress, proteasome dysfunction, and caspase 3 activation. *Am J Respir Cell Mol Biol.* 2005;32(6):521-30.
30. Mulugeta S, Maguire JA, Newitt JL, Russo SJ, Kotorashvili A, Beers MF. Misfolded BRICHOS SP-C mutant proteins induce apoptosis via caspase-4- and cytochrome c-related mechanisms. *Am J Physiol Lung Cell Mol Physiol.* 2007;293(3):L720-L9.
31. Tanjore H, Cheng DS, Degryse AL, Zoz DF, Abdolrasulnia R, Lawson WE, et al. Alveolar epithelial cells undergo epithelial-to-mesenchymal transition in response to endoplasmic reticulum stress. *J Biol Chem.* 2011;286(35):30972-80.
32. Zhong Q, Zhou B, Ann DK, Mino P, Liu Y, Banfalvi A, et al. Role of Endoplasmic Reticulum Stress in Epithelial-Mesenchymal Transition of Alveolar Epithelial Cells: Effects of Misfolded Surfactant Protein. *Am J Respir Cell Mol Biol.* 2011;45(3):498-509.
33. Korfei M, Ruppert C, Mahavadi P, Henneke I, Markart P, Koch M, et al. Epithelial endoplasmic reticulum stress and apoptosis in sporadic idiopathic pulmonary fibrosis. *Am J Respir Crit Care Med.* 2008;178(8):838-46.
34. Princiotta MF, Finzi D, Qian SB, Gibbs J, Schuchmann S, Buttgerit F, et al. Quantitating protein synthesis, degradation, and endogenous antigen processing. *Immunity.* 2003;18(3):343-54.
35. Guerriero CJ, Brodsky JL. The delicate balance between secreted protein folding and endoplasmic reticulum-associated degradation in human physiology. *Physiol Rev.* 2012;92(2):537-76.
36. Frakes AE, Dillin A. The UPR(ER): Sensor and Coordinator of Organismal Homeostasis. *Mol Cell.* 2017;66(6):761-71.

37. Hetz C, Saxena S. ER stress and the unfolded protein response in neurodegeneration. *Nat Rev Neurol.* 2017;13(8):477-91.
38. Oyadomari S, Mori M. Roles of CHOP//GADD153 in endoplasmic reticulum stress. *Cell Death Differ.* 2003;11(4):381-9.
39. Wouters BG, Koritzinsky M. Hypoxia signalling through mTOR and the unfolded protein response in cancer. *Nat Rev Cancer.* 2008;8(11):851-64.
40. Osowski CM, Urano F. Measuring ER stress and the unfolded protein response using mammalian tissue culture system. *Methods Enzymol.* 2011;490:71-92.
41. Mandl J, Meszaros T, Banhegyi G, Csala M. Minireview: endoplasmic reticulum stress: control in protein, lipid, and signal homeostasis. *Mol Endocrinol.* 2013;27(3):384-93.
42. Fu S, Watkins SM, Hotamisligil GS. The role of endoplasmic reticulum in hepatic lipid homeostasis and stress signaling. *Cell Metab.* 2012;15(5):623-34.
43. Ma Y, Hendershot LM. ER chaperone functions during normal and stress conditions. *J Chem Neuroanat.* 2004;28(1-2):51-65.
44. Bertolotti A, Zhang Y, Hendershot LM, Harding HP, Ron D. Dynamic interaction of BiP and ER stress transducers in the unfolded-protein response. *Nat Cell Biol.* 2000;2(6):326-32.
45. Schroder M, Kaufman RJ. The mammalian unfolded protein response. *Annu Rev Biochem.* 2005;74:739-89.
46. Liu CY, Schroder M, Kaufman RJ. Ligand-independent dimerization activates the stress response kinases IRE1 and PERK in the lumen of the endoplasmic reticulum. *J Biol Chem.* 2000;275(32):24881-5.
47. Krishnamoorthy T, Pavitt GD, Zhang F, Dever TE, Hinnebusch AG. Tight binding of the phosphorylated alpha subunit of initiation factor 2 (eIF2alpha) to the regulatory subunits of

guanine nucleotide exchange factor eIF2B is required for inhibition of translation initiation. *Mol Cell Biol.* 2001;21(15):5018-30.

48. Brush MH, Weiser DC, Shenolikar S. Growth arrest and DNA damage-inducible protein GADD34 targets protein phosphatase 1 alpha to the endoplasmic reticulum and promotes dephosphorylation of the alpha subunit of eukaryotic translation initiation factor 2. *Mol Cell Biol.* 2003;23(4):1292-303.

49. Harding HP, Zhang Y, Bertolotti A, Zeng H, Ron D. Perk is essential for translational regulation and cell survival during the unfolded protein response. *Mol Cell.* 2000;5(5):897-904.

50. Harding HP, Zhang Y, Zeng H, Novoa I, Lu PD, Calton M, et al. An integrated stress response regulates amino acid metabolism and resistance to oxidative stress. *Mol Cell.* 2003;11(3):619-33.

51. Ma Y, Hendershot LM. Delineation of a negative feedback regulatory loop that controls protein translation during endoplasmic reticulum stress. *J Biol Chem.* 2003;278(37):34864-73.

52. Novoa I, Zeng H, Harding HP, Ron D. Feedback Inhibition of the Unfolded Protein Response by GADD34-Mediated Dephosphorylation of eIF2a. *J Cell Biol.* 2001;153(5):1011-22.

53. Fawcett TW, Martindale JL, Guyton KZ, Hai T, Holbrook NJ. Complexes containing activating transcription factor (ATF)/cAMP-responsive-element-binding protein (CREB) interact with the CCAAT/enhancer-binding protein (C/EBP)-ATF composite site to regulate Gadd153 expression during the stress response. *Biochem J.* 1999;339 (Pt 1):135-41.

54. Harding HP, Novoa I, Zhang Y, Zeng H, Wek R, Schapira M, et al. Regulated Translation Initiation Controls Stress-Induced Gene Expression in Mammalian Cells. *Molecular Cell.* 2000;6(5):1099-108.

55. Ye J, Rawson RB, Komuro R, Chen X, Dave UP, Prywes R, et al. ER stress induces cleavage of membrane-bound ATF6 by the same proteases that process SREBPs. *Mol Cell.* 2000;6(6):1355-64.
56. Shen J, Prywes R. Dependence of site-2 protease cleavage of ATF6 on prior site-1 protease digestion is determined by the size of the luminal domain of ATF6. *J Biol Chem.* 2004;279(41):43046-51.
57. Vekich JA, Belmont PJ, Thuerauf DJ, Glembotski CC. Protein disulfide isomerase-associated 6 is an ATF6-inducible ER stress response protein that protects cardiac myocytes from ischemia/reperfusion-mediated cell death. *J Mol Cell Cardiol.* 2012;53(2):259-67.
58. Lee K, Tirasophon W, Shen X, Michalak M, Prywes R, Okada T, et al. IRE1-mediated unconventional mRNA splicing and S2P-mediated ATF6 cleavage merge to regulate XBP1 in signaling the unfolded protein response. *Genes Dev.* 2002;16(4):452-66.
59. Yoshida H, Matsui T, Yamamoto A, Okada T, Mori K. XBP1 mRNA is induced by ATF6 and spliced by IRE1 in response to ER stress to produce a highly active transcription factor. *Cell.* 2001;107(7):881-91.
60. Back SH, Lee K, Vink E, Kaufman RJ. Cytoplasmic IRE1alpha-mediated XBP1 mRNA splicing in the absence of nuclear processing and endoplasmic reticulum stress. *J Biol Chem.* 2006;281(27):18691-706.
61. Hollien J, Weissman JS. Decay of endoplasmic reticulum-localized mRNAs during the unfolded protein response. *Science.* 2006;313(5783):104-7.
62. Hollien J, Lin JH, Li H, Stevens N, Walter P, Weissman JS. Regulated Ire1-dependent decay of messenger RNAs in mammalian cells. *J Cell Biol.* 2009;186(3):323-31.

63. Moore BB, Moore TA. Viruses in Idiopathic Pulmonary Fibrosis. Etiology and Exacerbation. *Ann Am Thorac Soc.* 2015;12 Suppl 2:S186-92.
64. Kropski JA, Pritchett JM, Zoz DF, Crossno PF, Markin C, Garnett ET, et al. Extensive phenotyping of individuals at risk for familial interstitial pneumonia reveals clues to the pathogenesis of interstitial lung disease. *Am J Respir Crit Care Med.* 2015;191(4):417-26.
65. Tzouvelekis A, Harokopos V, Paparountas T, Oikonomou N, Chatziioannou A, Vilaras G, et al. Comparative expression profiling in pulmonary fibrosis suggests a role of hypoxia-inducible factor-1alpha in disease pathogenesis. *Am J Respir Crit Care Med.* 2007;176(11):1108-19.
66. Kusko RL, Brothers JF, 2nd, Tedrow J, Pandit K, Huleihel L, Perdomo C, et al. Integrated Genomics Reveals Convergent Transcriptomic Networks Underlying Chronic Obstructive Pulmonary Disease and Idiopathic Pulmonary Fibrosis. *Am J Respir Crit Care Med.* 2016;194(8):948-60.
67. Xi Y, Kim T, Brumwell AN, Driver IH, Wei Y, Tan V, et al. Local lung hypoxia determines epithelial fate decisions during alveolar regeneration. *Nat Cell Biol.* 2017;19(8):904-14.
68. Fels DR, Koumenis C. The PERK/eIF2alpha/ATF4 module of the UPR in hypoxia resistance and tumor growth. *Cancer Biol Ther.* 2006;5(7):723-8.
69. Ley B, Collard HR, King TE, Jr. Clinical course and prediction of survival in idiopathic pulmonary fibrosis. *Am J Respir Crit Care Med.* 2011;183(4):431-40.
70. Martínez G, Duran G, Aniotz C, Cabral G, Miranda F, Vivar JP, Hetz C. Endoplasmic reticulum proteostasis impairment in aging. *Aging Cell.* 2017;16(4):615-23.
71. Bratic A, Larsson NG. The role of mitochondria in aging. *J Clin Invest.* 2013;123(3):951-7.

72. Bueno M, Lai YC, Romero Y, Brands J, St.Croix CM, Kamga C, et al. PINK1 deficiency impairs mitochondrial homeostasis and promotes lung fibrosis. *J Clin Invest.* 2015;125(2):521-38.
73. Saez I, Vilchez D. The Mechanistic Links Between Proteasome Activity, Aging and Age-related Diseases. *Curr Genomics.* 2014;15(1):38-51.
74. Torres-González E, Bueno M, Tanaka A, Krug LT, Cheng DS, Polosukhin VV, et al. Role of Endoplasmic Reticulum Stress in Age-Related Susceptibility to Lung Fibrosis. *Am J Respir Cell Mol Biol.* 2012;46(6):748-56.
75. Ruggiano A, Foresti O, Carvalho P. Quality control: ER-associated degradation: protein quality control and beyond. *J Cell Biol.* 2014;204(6):869-79.
76. Araya J, Kojima J, Takasaka N, Ito S, Fujii S, Hara H, et al. Insufficient autophagy in idiopathic pulmonary fibrosis. *Am J Physiol Lung Cell Mol Physiol.* 2013;304(1):L56-69.
77. Zhang L, Wang Y, Pandupuspitasari NS, Wu G, Xiang X, Gong Q, et al. Endoplasmic reticulum stress, a new wrestler, in the pathogenesis of idiopathic pulmonary fibrosis. *Am J Transl Res.* 2017;9(2):722-35.
78. Cassel TN, Nord M. C/EBP transcription factors in the lung epithelium. *American Journal of Physiology - Lung Cellular and Molecular Physiology.* 2003;285(4):L773-L81.
79. Lekstrom-Himes J, Xanthopoulos KG. Biological Role of the CCAAT/Enhancer-binding Protein Family of Transcription Factors. *Journal of Biological Chemistry.* 1998;273(44):28545-8.
80. McCullough KD, Martindale JL, Klotz LO, Aw TY, Holbrook NJ. Gadd153 sensitizes cells to endoplasmic reticulum stress by down-regulating Bcl2 and perturbing the cellular redox state. *Mol Cell Biol.* 2001;21(4):1249-59.

81. Ma Y, Brewer JW, Diehl JA, Hendershot LM. Two distinct stress signaling pathways converge upon the CHOP promoter during the mammalian unfolded protein response. *J Mol Biol.* 2002;318(5):1351-65.
82. Scorrano L, Oakes SA, Opferman JT, Cheng EH, Sorcinelli MD, Pozzan T, et al. BAX and BAK regulation of endoplasmic reticulum Ca²⁺: a control point for apoptosis. *Science.* 2003;300(5616):135-9.
83. Reimold AM, Iwakoshi NN, Manis J, Vallabhajosyula P, Szomolanyi-Tsuda E, Gravallesse EM, et al. Plasma cell differentiation requires the transcription factor XBP-1. *Nature.* 2001;412(6844):300-7.
84. Baek HA, Kim DS, Park HS, Jang KY, Kang MJ, Lee DG, et al. Involvement of endoplasmic reticulum stress in myofibroblastic differentiation of lung fibroblasts. *Am J Respir Cell Mol Biol.* 2011:2011-0121OC.
85. Ghavami S, Yeganeh B, Zeki AA, Shojaei S, Kenyon NJ, Ott S, et al. Autophagy and the Unfolded Protein Response Promote Pro-fibrotic Effects of TGFbeta1 in Human Lung Fibroblasts. *Am J Physiol Lung Cell Mol Physiol.* 2017:ajplung.
86. McMorrow T, Gaffney MM, Slattery C, Campbell E, Ryan MP. Cyclosporine A induced epithelial-mesenchymal transition in human renal proximal tubular epithelial cells. *Nephrol Dial Transplant.* 2005;20(10):2215-25.
87. Pallet N, Bouvier N, Bendjallabah A, Rabant M, Flinois JP, Hertig A, et al. Cyclosporine-induced endoplasmic reticulum stress triggers tubular phenotypic changes and death. *Am J Transplant.* 2008;8(11):2283-96.
88. Hotamisligil GS. Endoplasmic reticulum stress and the inflammatory basis of metabolic disease. *Cell.* 2010;140(6):900-17.

89. Kaser A, Lee AH, Franke A, Glickman JN, Zeissig S, Tilg H, et al. XBP1 links ER stress to intestinal inflammation and confers genetic risk for human inflammatory bowel disease. *Cell*. 2008;134(5):743-56.
90. Heazlewood CK, Cook MC, Eri R, Price GR, Tauro SB, Taupin D, et al. Aberrant mucin assembly in mice causes endoplasmic reticulum stress and spontaneous inflammation resembling ulcerative colitis. *PLoS Med*. 2008;5(3):e54.
91. Shenderov K, Riteau N, Yip R, Mayer-Barber KD, Oland S, Hieny S, et al. Cutting edge: Endoplasmic reticulum stress licenses macrophages to produce mature IL-1beta in response to TLR4 stimulation through a caspase-8- and TRIF-dependent pathway. *J Immunol*. 2014;192(5):2029-33.
92. Braga TT, Agudelo JS, Camara NO. Macrophages During the Fibrotic Process: M2 as Friend and Foe. *Front Immunol*. 2015;6:602.
93. Shan B, Wang X, Wu Y, Xu C, Xia Z, Dai J, et al. The metabolic ER stress sensor IRE1alpha suppresses alternative activation of macrophages and impairs energy expenditure in obesity. *Nat Immunol*. 2017;18(5):519-29.
94. Grant R, Nguyen KY, Ravussin A, Albarado D, Youm YH, Dixit VD. Inactivation of C/ebp homologous protein-driven immune-metabolic interactions exacerbate obesity and adipose tissue leukocytosis. *J Biol Chem*. 2014;289(20):14045-55.
95. Oh J, Riek AE, Weng S, Petty M, Kim D, Colonna M, et al. Endoplasmic reticulum stress controls M2 macrophage differentiation and foam cell formation. *J Biol Chem*. 2012;287(15):11629-41.

96. Yao Y, Wang Y, Zhang Z, He L, Zhu J, Zhang M, et al. Chop Deficiency Protects Mice Against Bleomycin-induced Pulmonary Fibrosis by Attenuating M2 Macrophage Production. *Mol Ther.* 2016;24(5):915-25.
97. Wang Y, Zhu J, Zhang L, Zhang Z, He L, Mou Y, et al. Role of C/EBP homologous protein and endoplasmic reticulum stress in asthma exacerbation by regulating the IL-4/signal transducer and activator of transcription 6/transcription factor EC/IL-4 receptor alpha positive feedback loop in M2 macrophages. *J Allergy Clin Immunol.* 2017;140(6):1550-61 e8.
98. Bridges JP, Wert SE, Noguee LM, Weaver TE. Expression of a human surfactant protein C mutation associated with interstitial lung disease disrupts lung development in transgenic mice. *J Biol Chem.* 2003;278(52):52739-46.
99. Lawson WE, Cheng DS, Degryse AL, Tanjore H, Polosukhin VV, Xu XC, et al. Endoplasmic reticulum stress enhances fibrotic remodeling in the lungs. *Proc Natl Acad Sci U S A.* 2011;108(26):10562-7.
100. Tanaka Y, Ishitsuka Y, Hayasaka M, Yamada Y, Miyata K, Endo M, et al. The exacerbating roles of CCAAT/enhancer-binding protein homologous protein (CHOP) in the development of bleomycin-induced pulmonary fibrosis and the preventive effects of tauroursodeoxycholic acid (TUDCA) against pulmonary fibrosis in mice. *Pharmacological Research.* 2015;99(Supplement C):52-62.
101. Ayaub EA, Kolb PS, Mohammed-Ali Z, Tat V, Murphy J, Bellaye PS, et al. GRP78 and CHOP modulate macrophage apoptosis and the development of bleomycin-induced pulmonary fibrosis. *J Pathol.* 2016;239(4):411-25.
102. Winters CJ, Koval O, Murthy S, Allamargot C, Sebag SC, Paschke JD, et al. CaMKII inhibition in type II pneumocytes protects from bleomycin-induced pulmonary fibrosis by

preventing Ca(2+)-dependent apoptosis. *Am J Physiol Lung Cell Mol Physiol*. 2016;310(1):L86-L94.

103. Celardo I, Costa AC, Lehmann S, Jones C, Wood N, Mencacci NE, et al. Mitofusin-mediated ER stress triggers neurodegeneration in pink1/parkin models of Parkinson's disease. *Cell Death Dis*. 2016;7(6):e2271.

104. Nakajima F, Aratani S, Fujita H, Yagishita N, Ichinose S, Makita K, et al. Synoviolin inhibitor LS-102 reduces endoplasmic reticulum stress-induced collagen secretion in an in vitro model of stress-related interstitial pneumonia. *Int J Mol Med*. 2015;35(1):110-6.

105. Klingberg F, Hinz B, White ES. The myofibroblast matrix: implications for tissue repair and fibrosis. *J Pathol*. 2013;229(2):298-309.

106. Zimmerman KA, Graham LV, Pallerio MA, Murphy-Ullrich JE. Calreticulin Regulates Transforming Growth Factor- β -stimulated Extracellular Matrix Production. *Journal of Biological Chemistry*. 2013;288(20):14584-98.

107. Hsu HS, Liu CC, Lin JH, Hsu TW, Hsu JW, Su K, et al. Involvement of ER stress, PI3K/AKT activation, and lung fibroblast proliferation in bleomycin-induced pulmonary fibrosis. *PLoS One*. 2017;12(1):e0161117. doi:10.1371/journal.pone.0161117. 7 ed2017 12/1/2017.

108. Young LR, Gulleman PM, Short CW, Tanjore H, Sherrill T, Qi A, et al. Epithelial-macrophage interactions determine pulmonary fibrosis susceptibility in Hermansky-Pudlak syndrome. *JCI Insight*. 2016;1(17):e88947.

109. Young LR, Borchers MT, Allen HL, Gibbons RS, McCormack FX. Lung-restricted macrophage activation in the pearl mouse model of Hermansky-Pudlak syndrome. *J Immunol*. 2006;176(7):4361-8.

110. Ryan AJ, Larson-Casey JL, He C, Murthy S, Carter AB. Asbestos-induced Disruption of Calcium Homeostasis Induces Endoplasmic Reticulum Stress in Macrophages. *J Biol Chem.* 2014;289(48):33391-403.
111. Xiu F, Diao L, Qi P, Catapano M, Jeschke MG. Palmitate differentially regulates the polarization of differentiating and differentiated macrophages. *Immunology.* 2016;147(1):82-96.
112. Hu YB, Wu X, Qin XF, Wang L, Pan PH. Role of Endoplasmic Reticulum Stress in Silica-induced Apoptosis in RAW264.7 Cells. *Biomed Environ Sci.* 2017;30(8):591-600.
113. Oyadomari S, Mori M. Roles of CHOP/GADD153 in endoplasmic reticulum stress. *Cell Death Differ.* 2004;11(4):381-9.
114. Li Y, Guo Y, Tang J, Jiang J, Chen Z. New insights into the roles of CHOP-induced apoptosis in ER stress. *Acta Biochim Biophys Sin (Shanghai).* 2015;47(2):146-7.
115. Darby IA, Hewitson TD. Hypoxia in tissue repair and fibrosis. *Cell Tissue Res.* 2016;365(3):553-62.
116. Haase VH. Hypoxia-inducible factor signaling in the development of kidney fibrosis. *Fibrogenesis Tissue Repair.* 2012;5 Suppl 1:S16.
117. Roth KJ, Coppole BL. Role of Hypoxia-Inducible Factors in the Development of Liver Fibrosis. *Cell Mol Gastroenterol Hepatol.* 2015;1(6):589-97.
118. Gao Y, Chu M, Hong J, Shang J, Xu D. Hypoxia induces cardiac fibroblast proliferation and phenotypic switch: a role for caveolae and caveolin-1/PTEN mediated pathway. *J Thorac Dis.* 2014;6(10):1458-68.
119. Shimoda LA, Semenza GL. HIF and the lung: role of hypoxia-inducible factors in pulmonary development and disease. *Am J Respir Crit Care Med.* 2011;183(2):152-6.

120. Bartels K, Grenz A, Eltzschig HK. Hypoxia and inflammation are two sides of the same coin. *Proc Natl Acad Sci U S A*. 2013;110(46):18351-2.
121. Higgins DF, Biju MP, Akai Y, Wutz A, Johnson RS, Haase VH. Hypoxic induction of Ctgf is directly mediated by Hif-1. *Am J Physiol Renal Physiol*. 2004;287(6):F1223-32.
122. Copple BL, Bai S, Burgoon LD, Moon JO. Hypoxia-inducible factor-1alpha regulates the expression of genes in hypoxic hepatic stellate cells important for collagen deposition and angiogenesis. *Liver Int*. 2011;31(2):230-44.
123. Pialoux V, Mounier R, Brown AD, Steinback CD, Rawling JM, Poulin MJ. Relationship between oxidative stress and HIF-1 alpha mRNA during sustained hypoxia in humans. *Free Radic Biol Med*. 2009;46(2):321-6.
124. Rosa DP, Martinez D, Picada JN, Semedo JG, Marroni NP. Hepatic oxidative stress in an animal model of sleep apnoea: effects of different duration of exposure. *Comp Hepatol*. 2011;10(1):1.
125. Xu W, Chi L, Row BW, Xu R, Ke Y, Xu B, et al. Increased oxidative stress is associated with chronic intermittent hypoxia-mediated brain cortical neuronal cell apoptosis in a mouse model of sleep apnea. *Neuroscience*. 2004;126(2):313-23.
126. Joseph JP, Harishankar MK, Pillai AA, Devi A. Hypoxia induced EMT: A review on the mechanism of tumor progression and metastasis in OSCC. *Oral Oncol*. 2018;80:23-32.
127. Tal R. The role of hypoxia and hypoxia-inducible factor-1alpha in preeclampsia pathogenesis. *Biol Reprod*. 2012;87(6):134.
128. Higgins DF, Kimura K, Bernhardt WM, Shrimanker N, Akai Y, Hohenstein B, et al. Hypoxia promotes fibrogenesis in vivo via HIF-1 stimulation of epithelial-to-mesenchymal transition. *J Clin Invest*. 2007;117(12):3810-20.

129. Moon JO, Welch TP, Gonzalez FJ, Copple BL. Reduced liver fibrosis in hypoxia-inducible factor-1alpha-deficient mice. *Am J Physiol Gastrointest Liver Physiol.* 2009;296(3):G582-92.
130. Qu A, Taylor M, Xue X, Matsubara T, Metzger D, Chambon P, et al. Hypoxia-inducible transcription factor 2alpha promotes steatohepatitis through augmenting lipid accumulation, inflammation, and fibrosis. *Hepatology.* 2011;54(2):472-83.
131. Takikawa A, Mahmood A, Nawaz A, Kado T, Okabe K, Yamamoto S, et al. HIF-1alpha in Myeloid Cells Promotes Adipose Tissue Remodeling Toward Insulin Resistance. *Diabetes.* 2016;65(12):3649-59.
132. Hu CJ, Wang LY, Chodosh LA, Keith B, Simon MC. Differential roles of hypoxia-inducible factor 1alpha (HIF-1alpha) and HIF-2alpha in hypoxic gene regulation. *Mol Cell Biol.* 2003;23(24):9361-74.
133. Burman A, Kropski JA, Calvi CL, Serezani AP, Pascoalino BD, Han W, et al. Localized hypoxia links ER stress to lung fibrosis through induction of C/EBP homologous protein. *JCI Insight.* 2018;3(16).
134. Kapitsinou PP, Liu Q, Unger TL, Rha J, Davidoff O, Keith B, et al. Hepatic HIF-2 regulates erythropoietic responses to hypoxia in renal anemia. *Blood.* 2010;116(16):3039-48.
135. Degryse AL, Tanjore H, Xu XC, Polosukhin VV, Jones BR, McMahon FB, et al. Repetitive intratracheal bleomycin models several features of idiopathic pulmonary fibrosis. *Am J Physiol Lung Cell Mol Physiol.* 2010;299(4):L442-L52.
136. Degryse AL, Tanjore H, Xu XC, Polosukhin VV, Jones BR, Boomershine CS, et al. TGFbeta signaling in lung epithelium regulates bleomycin-induced alveolar injury and fibroblast recruitment. *Am J Physiol Lung Cell Mol Physiol.* 2011;300(6):L887-L97.

137. Tanjore H, Xu XC, Polosukhin VV, Degryse AL, Li B, Han W, et al. Contribution of epithelial-derived fibroblasts to bleomycin-induced lung fibrosis. *Am J Respir Crit Care Med.* 2009;180(7):657-65.
138. Lawson WE, Polosukhin VV, Stathopoulos GT, Zoia O, Han W, Lane KB, et al. Increased and prolonged pulmonary fibrosis in surfactant protein C-deficient mice following intratracheal bleomycin. *Am J Pathol.* 2005;167(5):1267-77.
139. Lawson WE, Polosukhin VV, Zoia O, Stathopoulos GT, Han W, Plieth D, et al. Characterization of fibroblast-specific protein 1 in pulmonary fibrosis. *Am J Respir Crit Care Med.* 2005;171(8):899-907.
140. Tanjore H, Degryse AL, Crossno PF, Xu XC, McConaha ME, Jones BR, et al. beta-catenin in the alveolar epithelium protects from lung fibrosis after intratracheal bleomycin. *Am J Respir Crit Care Med.* 2013;187(6):630-9.
141. Young LR, Gulleman PM, Bridges JP, Weaver TE, Deutsch GH, Blackwell TS, et al. The Alveolar Epithelium Determines Susceptibility to Lung Fibrosis in Hermansky-Pudlak Syndrome. *American Journal of Respiratory and Critical Care Medicine*; 11/15/2012: American Thoracic Society - AJRCCM; 2012. p. 1014-24.
142. Han W, Zaynagetdinov R, Yull FE, Polosukhin VV, Gleaves LA, Tanjore H, et al. Molecular Imaging of Folate Receptor Positive Macrophages during Acute Lung Inflammation. *Am J Respir Cell Mol Biol.* 2015;53(1):50-9.
143. Koumenis C, Naczki C, Koritzinsky M, Rastani S, Diehl A, Sonenberg N, et al. Regulation of protein synthesis by hypoxia via activation of the endoplasmic reticulum kinase PERK and phosphorylation of the translation initiation factor eIF2alpha. *Mol Cell Biol.* 2002;22(21):7405-16.

144. Varia MA, Calkins-Adams DP, Rinker LH, Kennedy AS, Novotny DB, Fowler J, et al. Pimonidazole: A Novel Hypoxia Marker for Complementary Study of Tumor Hypoxia and Cell Proliferation in Cervical Carcinoma. *Gynecologic Oncology*. 1998;71(2):270-7.
145. Polosukhin VV, Degryse AL, Newcomb DC, Jones BR, Ware LB, Lee JW, et al. Intratracheal bleomycin causes airway remodeling and airflow obstruction in mice. *Exp Lung Res*. 2012;38(3):135-46.
146. Wojtan P, Mierzejewski M, Osinska I, Domagala-Kulawik J. Macrophage polarization in interstitial lung diseases. *Cent Eur J Immunol*. 2016;41(2):159-64.
147. Gordon S, Martinez FO. Alternative activation of macrophages: mechanism and functions. *Immunity*. 2010;32(5):593-604.
148. Nair MG, Du Y, Perrigoue JG, Zaph C, Taylor JJ, Goldschmidt M, et al. Alternatively activated macrophage-derived RELM- α is a negative regulator of type 2 inflammation in the lung. *J Exp Med*. 2009;206(4):937-52.
149. Oyadomari S, Araki E, Mori M. Endoplasmic reticulum stress-mediated apoptosis in pancreatic beta-cells. *Apoptosis*. 2002;7(4):335-45.
150. Oyadomari S, Koizumi A, Takeda K, Gotoh T, Akira S, Araki E, et al. Targeted disruption of the Chop gene delays endoplasmic reticulum stress-mediated diabetes. *J Clin Invest*. 2002;109(4):525-32.
151. Yang Y, Liu L, Naik I, Braunstein Z, Zhong J, Ren B. Transcription Factor C/EBP Homologous Protein in Health and Diseases. *Front Immunol*. 2017;8:1612.
152. Nishitoh H. CHOP is a multifunctional transcription factor in the ER stress response. *J Biochem*. 2012;151(3):217-9.

153. Mimura N, Fulciniti M, Gorgun G, Tai YT, Cirstea D, Santo L, et al. Blockade of XBP1 splicing by inhibition of IRE1alpha is a promising therapeutic option in multiple myeloma. *Blood*. 2012;119(24):5772-81.
154. Sanches M, Duffy NM, Talukdar M, Thevakumaran N, Chiovitti D, Canny MD, et al. Structure and mechanism of action of the hydroxy-aryl-aldehyde class of IRE1 endoribonuclease inhibitors. *Nat Commun*. 2014;5:4202.
155. Volkmann K, Lucas JL, Vuga D, Wang X, Brumm D, Stiles C, et al. Potent and selective inhibitors of the inositol-requiring enzyme 1 endoribonuclease. *J Biol Chem*. 2011;286(14):12743-55.
156. Koo JH, Lee HJ, Kim W, Kim SG. Endoplasmic Reticulum Stress in Hepatic Stellate Cells Promotes Liver Fibrosis via PERK-Mediated Degradation of HNRNPA1 and Up-regulation of SMAD2. *Gastroenterology*. 2016;150(1):181-93 e8.
157. Hassler J, Cao SS, Kaufman RJ. IRE1, a double-edged sword in pre-miRNA slicing and cell death. *Dev Cell*. 2012;23(5):921-3.
158. Heindryckx F, Binet Fo, Ponticos M, Rombouts K, Lau J, Kreuger J, et al. Endoplasmic reticulum stress enhances fibrosis through IRE1+IGCÉmediated degradation of miRGÇÉ150 and XBPGÇÉ1 splicing. *EMBO Mol Med*. 2016;8(7):729-44.
159. Maurel M, Chevet E, Tavernier J, Gerlo S. Getting RIDD of RNA: IRE1 in cell fate regulation. *Trends Biochem Sci*. 2014;39(5):245-54.
160. Salvador JsM, Brown-Clay JD, Fornace AJ. Gadd45 in Stress Signaling, Cell Cycle Control, and Apoptosis. In: Liebermann DA, Hoffman B, editors. *Gadd45 Stress Sensor Genes*. New York, NY: Springer New York; 2013. p. 1-19.

161. Steele MP, Luna LG, Coldren CD, Murphy E, Hennessy CE, Heinz D, et al. Relationship between gene expression and lung function in Idiopathic Interstitial Pneumonias. *BMC Genomics*. 2015;16:869.
162. Teske BF, Fusakio ME, Zhou D, Shan J, McClintick JN, Kilberg MS, et al. CHOP induces activating transcription factor 5 (ATF5) to trigger apoptosis in response to perturbations in protein homeostasis. *Mol Biol Cell*. 2013;24(15):2477-90.
163. Ney PA. Mitochondrial autophagy: Origins, significance, and role of BNIP3 and NIX. *Biochim Biophys Acta*. 2015;1853(10 Pt B):2775-83.
164. Bryant AJ, Carrick RP, McConaha ME, Jones BR, Shay SD, Moore CS, et al. Endothelial HIF signaling regulates pulmonary fibrosis-associated pulmonary hypertension. *Am J Physiol Lung Cell Mol Physiol*. 2016;310(3):L249-62.
165. Vujaskovic Z, Anscher MS, Feng QF, Rabbani ZN, Amin K, Samulski TS, et al. Radiation-induced hypoxia may perpetuate late normal tissue injury. *International Journal of Radiation Oncology*Biography*Physics*. 2001;50(4):851-5.
166. Casson CN, Yu J, Reyes VM, Taschuk FO, Yadav A, Copenhaver AM, et al. Human caspase-4 mediates noncanonical inflammasome activation against gram-negative bacterial pathogens. *Proc Natl Acad Sci U S A*. 2015;112(21):6688-93.
167. Morishima N, Nakanishi K, Takenouchi H, Shibata T, Yasuhiko Y. An endoplasmic reticulum stress-specific caspase cascade in apoptosis. Cytochrome c-independent activation of caspase-9 by caspase-12. *J Biol Chem*. 2002;277(37):34287-94.
168. Nakagawa T, Zhu H, Morishima N, Li E, Xu J, Yankner BA, et al. Caspase-12 mediates endoplasmic-reticulum-specific apoptosis and cytotoxicity by amyloid-beta. *Nature*. 2000;403(6765):98-103.

169. Endo M, Mori M, Akira S, Gotoh T. C/EBP homologous protein (CHOP) is crucial for the induction of caspase-11 and the pathogenesis of lipopolysaccharide-induced inflammation. *J Immunol.* 2006;176(10):6245-53.
170. Han J, Kaufman RJ. Physiological/pathological ramifications of transcription factors in the unfolded protein response. *Genes Dev.* 2017;31(14):1417-38.
171. Willy JA, Young SK, Stevens JL, Masuoka HC, Wek RC. CHOP links endoplasmic reticulum stress to NF-kappaB activation in the pathogenesis of nonalcoholic steatohepatitis. *Mol Biol Cell.* 2015;26(12):2190-204.
172. Raval RR, Lau KW, Tran MG, Sowter HM, Mandriota SJ, Li JL, et al. Contrasting properties of hypoxia-inducible factor 1 (HIF-1) and HIF-2 in von Hippel-Lindau-associated renal cell carcinoma. *Mol Cell Biol.* 2005;25(13):5675-86.